

NEDO-20566-1-A  
REVISION 1  
77NED304  
CLASS I  
OCTOBER 1982

LICENSING TOPICAL REPORT

**GENERAL ELECTRIC COMPANY ANALYTICAL  
MODEL FOR LOSS-OF-COOLANT ANALYSIS  
IN ACCORDANCE WITH 10CFR50 APPENDIX K  
AMENDMENT NO. 1 —  
CALCULATION OF LOW FLOW FILM BOILING  
HEAT TRANSFER FOR BWR LOCA ANALYSIS**

J. E. LEONARD  
K. H. SUN  
J. G. MUNTHE ANDERSEN  
G. E. DIX  
T. YUOH  
Edited by B. S. SHIRALKAR

8303160236 830224  
PDR TOPRP EMVGENE  
B PDR

GENERAL  ELECTRIC

NEDO-20566-1-A  
Revision 1  
77NED304  
Class I  
October 1982

LICENSING TOPICAL REPORT

GENERAL ELECTRIC COMPANY ANALYTICAL MODEL FOR  
LOSS-OF-COOLANT ANALYSIS IN ACCORDANCE WITH  
10CFR50 APPENDIX K AMENDMENT NO. 1 - CALCULATION  
OF LOW FLOW FILM BOILING HEAT TRANSFER FOR EWR  
LOCA ANALYSIS


This amendment is also applicable to NEDE-20566-P

J. E. Leonard  
K. H. Sun  
J. G. Munthe Andersen\*  
G. E. Dix  
T. Yuoh

Edited by B. S. Shiralkar

\*Danish Atomic Energy Commission, Consultant to General Electric Co.

Approved:

  
H. H. Klepfer, General Manager  
Nuclear Fuel Engineering Department

---

NUCLEAR ENERGY BUSINESS OPERATIONS • GENERAL ELECTRIC COMPANY  
SAN JOSE, CALIFORNIA 95125

---

GENERAL  ELECTRIC

### DISCLAIMER OF RESPONSIBILITY

*This document was prepared by or for the General Electric Company. Neither the General Electric Company nor any of the contributors to this document:*

- A. Makes any warranty or representation, express or implied, with respect to the accuracy, completeness, or usefulness of the information contained in this document, or that the use of any information disclosed in this document may not infringe privately owned rights; or*
- B. Assumes any responsibility for liability or damage of any kind which may result from the use of any information disclosed in this document.*



UNITED STATES  
NUCLEAR REGULATORY COMMISSION  
WASHINGTON, D. C. 20555

MFN 022-81

RAB

FEB 4 1981

RECEIVED  
FEB 11 1981  
H. H. BUCHHEIT

General Electric Company  
ATTN: Dr. G. G. Sherwood, Manager  
Safety and Licensing  
175 Curtner Avenue  
San Jose, California 95114

Dear Dr. Sherwood:

SUBJECT: ACCEPTANCE FOR REFERENCING OF TOPICAL REPORT NEDE-20566P,  
NEDE-20566-1 REVISION 1 AND NEDE-20566-4 REVISION 4

The Nuclear Regulatory Commission has completed its review of the General Electric Company Licensing Topical Report NEDE-20566 entitled "General Electric Company Analytical Model for Loss of Coolant Analysis in Accordance with 10 CFR 50 Appendix K, Volumes I and II" dated November 1975; its revision NEDE-20566-1 entitled "General Electric Company Analytical Model for Loss of Coolant Analysis in Accordance with 10 CFR Appendix K, Amendment No. 1-Calculation of Low Flow Film Boiling Heat Transfer for BWR LOCA Analysis" dated January 1978; and NEDE-20566-4 entitled "General Electric Company Analytical Model for Loss of Coolant Analyses in Accordance with 10 CFR 50 Appendix K, Amendment No. 4-Saturated Counter Flow Characteristics of a BWR Upper Tie Plate."

Topical Report NEDE-20566 documents the General Electrical Company analytical models for prediction of Boiling Water Reactor response to loss-of-coolant accidents. The report is organized into three sections namely Section I. Required and Acceptable Features of Evaluation Models-Conformance to 10 CFR 50 Appendix K; Section II. Required Documentation; and Section III. General Electric Boiling Water Reactor-Conformance to 10 CFR 50.46 Acceptance Criteria. Topical Report NEDE-20566-1 provides the development of a model to calculate the heat transfer coefficient under low flow film or pool boiling conditions in the BWR geometry. The model includes the heat transferred by convection due to the boundary layer and that transferred by radiation between the high-temperature surface and the liquid. Topical Report NEDE-20566-4 provides an improved saturated liquid counter-current flow limiting (CCFL) correlation for the fuel bundle upper tieplate for use in BWR loss-of-coolant accident analysis has been developed. It is shown that when the spray water that is introduced evenly into and constrained within, the region above the test bundle, all steam condensation occurs above the upper tieplate.

Dr. G. G. Sherwood

-2-

FEB 4 1981

The summaries of our evaluations are enclosed.

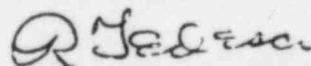
As a result of our reviews, we find the Licensing Topical Report NEDE-20566P (proprietary version) dated November 1975 and NEDO-20566 (non-proprietary version) dated January 1976; Licensing Topical Report Amendment NEDO-20566-1 (non-proprietary) dated January 1978; and Licensing Topical Report Amendment NEDE-20566-4P (proprietary version) dated July 1978 and NEDO-20566-4 (non-proprietary version) dated July 1978 are all acceptable for referencing in relevant operating license applications to the extent specified and under the limitations stipulated in the three corresponding attached topical report evaluations.

We do not intend to repeat the review of the safety features described in the topical reports and found acceptable in the attachments. Our acceptance applies only to the use of features described in the topical report and as discussed in the attachments. Acceptance of the reports identified in the above paragraph is in no way to be construed as a blanket approval of other amendments of NEDE-20566P.

In accordance with established procedure, it is requested that General Electric Company publish an approved version of these reports, proprietary and non-proprietary, within three months of receipt of this letter. The revisions are to incorporate this letter and the enclosed topical report evaluation following the title page and thus just in front of the abstract as well as appropriately incorporate responses to NRC requests for additional information. The report identifications of the approved reports are to have a -A suffix.

Should Nuclear Regulatory Commission criteria or regulations change such that our conclusions as to the acceptability of the report are invalidated, General Electric Company and/or the applicants referencing the topical report will be expected to revise and resubmit their respective documentation or submit justification for the continued effective applicability of the topical report without revision of their respective documentation.

Sincerely,



Robert L. Tedesco, Assistant Director  
for Licensing  
Division of Licensing

Enclosures:  
As Stated

## APPENDIX I

### TOPICAL REPORT EVALUATION

Report No.: NEDO-20566-1, Revision 1

Report Title: General Electric Company Analytical Model for Loss-of-Coolant Analysis in Accordance with 10 CFR 50 Appendix K  
Amendment No. 1 - Calculation of Low Flow Film Boiling Heat Transfer for BWR LOCA Analysis

Report Date: January, 1978

Originating Organization: General Electric Company

Reviewed By: Reactor Systems Branch, DSI

#### SUMMARY OF TOPICAL REPORT

The subject topical report describes the development and verification of a model to calculate the heat transfer coefficient under low flow film boiling or pool boiling conditions. General Electric's intent is to use the proposed model in four applications in the CHASTE code. The CHASTE code is a core heatup code which simulates the BWR fuel bundle and considers heat conduction, heat convection, thermal radiation and exothermic chemical reactions to predict the peak clad temperature and percent cladding oxidation. The proposed model would be applied to:

1. Flow window period prior to lower plenum flashing and following boiling transition;
2. Post lower plenum flashing period;
3. Channel wall during reflooding of bypass and core regions; and
4. Rod bundle during reflooding.

In the proposed model, the Bromley correlation (Reference 1) is modified by the addition of a radiation component to the zero-flow convective heat transfer relation and takes the form

$$h = h_{FB} + h_R$$

where  $h_{FB}$  is the film boiling correlation developed by Bromley and  $h_R$  is the radiation heat transfer component. The resulting expression is designated as the modified Bromley correlation.

General Electric has provided a discussion of the results of experimental verification studies in the range of applicability of the modified Bromley correlation. These are separated into quenching/reflood experiments and blowdown phase experiments. Single rod quench tests conducted by GE consisted of an 18-inch long heated tube dropped vertically into volumes of saturated and subcooled water at atmospheric pressure. The data range for wall superheat ( $T_{wall} - T_{sat}$ ) was 300 to 900 °F. Bundle reflood tests discussed were from the Westinghouse PWR-FLECHT program and tests conducted at KWU. These were full scale bundles tested under transient reflooding conditions. The data range was

    wall superheat   0 to 1500 °F  
    pressure           15 to 90 psia.

Blowdown phase experiments discussed were full-scale TLTA bundle data under transient flow conditions. The results of four 7x7 rod bundle TLTA tests were presented. The range of superheats for the tests was

<u>Test No.</u>	<u><math>T_w - T_{sat}</math> (°F)</u>
4910	300 to 750
4907	390 to 750
4914	390 to 750
4904	300 to 700

The tests were conducted under time-varying pressure conditions (700 to 1000 psia). At the request of the staff, data for an 8x8 rod bundle

tests were presented to supplement the 7x7 rod bundle tests. General Electric provided comparisons of test data with predictions from the modified Bromley correlation for the window period and the post lower plenum flashing period. Similar comparisons were made with predictions from the Ellion correlation (Reference 2). (The currently accepted GE evaluation model uses the pool film boiling correlation by Ellion for the time periods immediately preceding and following lower plenum flashing.) The intent of the comparisons is to show that the modified Bromley correlation provides a lower-bound estimate of the experimental data.

Additional information provided in the topical report is a derivation of the theoretical model for film boiling on a vertical surface (Appendix A), a discussion of the applicable range of the modified Bromley correlation (Appendix B), and responses to NRC questions (Appendix C).

#### SUMMARY OF EVALUATION

The theoretical development of the modified Bromley correlation is based on established procedures and is acceptable to the staff. The general form of the film boiling portion of the correlation is

$$h_{FB} = K \left[ \frac{K_g^3 \rho_g (\rho_f - \rho_g) h_{fg} g}{\mu_g (T_{WALL} - T_{SAT}) L_H} \right]^{1/4}$$

where the value of K is dependent upon the analytical model used for film boiling heat transfer with laminar film flow. For the previously approved Ellion correlation, K = 0.714; for the Bromley correlation, K = 0.62.



The radiation component

$$h_R = \frac{\epsilon \sigma (T_w^4 - T_{SAT}^4)}{(T_w - T_{SAT})}$$

is also based on established theoretical procedures and is acceptable to the staff.

Comparisons of the predicted film boiling coefficient with the reported experimental data indicate that the data are predicted or conservatively bounded. Values of the coefficient predicted by the modified Bromley correlation were generally in the range 100-150 Btu/hr-ft<sup>2</sup>-°F. The Ellion correlation predicted 50 Btu/hr-ft<sup>2</sup>-°F or less. For the time periods of interest in the transient, the experimental data resulted in heat transfer coefficients in the range 100-300 Btu/hr-ft<sup>2</sup>-°F. For the TLTA test data reported, a small number of data points were 10% below the prediction with modified Bromley. These data were at the beginning or end of the post-lower-plenum-flashing period. The staff concludes that the modified Bromley correlation is adequately based on appropriate experimental data and is acceptable.

For the four applications intended for the proposed model, the staff concludes that the modified Bromley correlation is an acceptable replacement for the Ellion correlation for the flow window period prior to lower plenum flashing and following boiling transition. Specifically, in the selection of the heat transfer coefficient for this region, the higher of the modified Bromley correlation and the "pool film/transition boiling" heat transfer coefficient lower bound value of 30 Btu/hr-ft<sup>2</sup>-°F will be used.

The modified Bromley correlation is also an acceptable replacement for the Ellion correlation for the post-lower-plenum-flashing period. Specifically, the higher predicted coefficient of the modified Bromley correlation and the Dougall-Rohsenow correlation will be used before uncovering.

For the remaining applications, i.e., outside channel wall during reflooding of bypass and inside channel wall during core reflooding, and rod bundle during reflooding, the applicable data from the single rod quench tests resulted in experimental heat transfer coefficients generally larger than  $25 \text{ Btu/hr-ft}^2\text{-}^\circ\text{F}$ . The modified Bromley correlation predicted coefficients between 28 and  $33 \text{ Btu/hr-ft}^2\text{-}^\circ\text{F}$ . The staff concludes that the proposed model adequately represents the available data.

#### REGULATORY POSITION

The staff concludes that the modified Bromley correlation is conservatively based on appropriate experimental data and is acceptable as a replacement for the Ellion correlation in the prediction of the heat transfer coefficient for (1) the fuel rods during the window period immediately prior to lower plenum flashing and (2) the flooded portion of the fuel rods following lower plenum flashing.

The GE proposal to use the modified Bromley correlation to replace (1) the currently used value of  $5 \text{ Btu/hr-ft}^2\text{-}^\circ\text{F}$  on the outer channel wall during reflooding of bypass and inner channel wall during core reflooding and (2) the currently used value of  $25 \text{ Btu/hr-ft}^2\text{-}^\circ\text{F}$  for the rod bundle during reflooding is acceptable based on comparisons with available experimental data.

REFERENCES

1. L. A. Bromley, "Heat Transfer in Stable Film Boiling", Chem. Eng. Progr., B46, 221-227 (1950).
2. M. E. Ellion, A Study of the Mechanism of Boiling Heat Transfer, Jet Propulsion Laboratory, Memo 20-88, C.I.T. (1954).

TABLE OF CONTENTS

	<u>Page</u>
ABSTRACT	ix
1 INTRODUCTION	1
2 THEORETICAL MODEL	5
3 EXPERIMENTAL VERIFICATION	11
3.1 Quenching/Reflood Experiments	11
3.2 Blowdown Phase Experiments	16
4 CONCLUSION	55
5 NOMENCLATURE	57
6 REFERENCES	59
APPENDIX A - THEORETICAL MODEL FOR FILM BOILING ON A VERTICAL SURFACE	A-1
APPENDIX B - APPLICABLE RANGE OF THE MODIFIED BROMLEY CORRELATION	B-1
APPENDIX C - RESPONSE TO NRC QUESTIONS TRANSMITTED BY LETTER FROM OLAN D. PARR TO G. G. SHERWOOD DATED 5/30/79	C-1
DISTRIBUTION	

LIST OF ILLUSTRATIONS

<u>Figure</u>	<u>Title</u>	<u>Page</u>
1	Low Flow Film Boiling Condition	1
2	Flow Patterns During Reflooding	2
3	Models of Laminar Film Boiling on a Vertical Surface	6
4	Comparison of Laminar and Laminar/Turbulent Pool Film Boiling Correlations	7
5	A Comparison of Taylor and Heilmholtz Stability Criteria	9
6	Comparison of Saturated Film Boiling Data with Modified Bromley Correlation	12
7	$h$ versus $(T_W - T_{SAT})$ for Run 6	13
8	$h$ versus $(T_W - T_{SAT})$ for Run 7	14
9	$h$ versus $(T_W - T_{SAT})$ for Run 8	15
10	Heat Transfer Coefficient for Transition and Film Boiling at 15 psi	17
11	Heat Transfer Coefficient for Transition and Film Boiling at 60 psi	18
12	Heat Transfer Coefficient for Transition and Film Boiling at 90 psi	19
13	KWU Reflood Data Compared to Modified Bromley Correlation	20
14	Inlet Flow Variation for Test 4910, Run 13	23
15	Measured and Predicted Level in Bundle, Test 4910, Run 13	23
16	Comparison of Measured Heat Transfer Coefficients with Various Correlations for Test 4910, Run 13	24
17	Comparison of Measured Heat Transfer Coefficients with Various Correlations for Test 4910, Run 13	24
18	Comparison of Measured Heat Transfer Coefficients with Various Correlations for Test 4910, Run 13	25
19	Comparison of Measured Heat Transfer Coefficients with Various Correlations for Test 4910, Run 13	25
20	Comparison of Measured Heat Transfer Coefficients with Various Correlations for Test 4910, Run 13	26
21	Comparison of Measured Heat Transfer Coefficients with Various Correlations for Test 4910, Run 13	27
22	Comparison of Measured Heat Transfer Coefficients with Various Correlations for Test 4910, Run 13	27

LIST OF ILLUSTRATIONS (Cont)

<u>Figure</u>	<u>Title</u>	<u>Page</u>
23	Comparison of Heat Transfer Coefficients versus Modified Bromley Correlation as a Function of Wall Superheat, Test 4910, Run 13	28
24	Calculated Void Fractions at Three Elevations, Test 4910, Run 13	29
25	Inlet Flow Variation for Test 4907, Run 10	30
26	Two-Phase Level Measurements and Predictions in Bundle, Test 4907, Run 10	30
27	Comparison of Measured Heat Transfer Coefficients with Various Correlations for Test 4907, Run 10	31
28	Comparison of Measured Heat Transfer Coefficients with Various Correlations for Test 4907, Run 10	32
29	Comparison of Measured Heat Transfer Coefficients with Various Correlations for Test 4907, Run 10	32
30	Comparison of Measured Heat Transfer Coefficients with Various Correlations for Test 4907, Run 10	33
31	Comparison of Measured Heat Transfer Coefficients with Various Correlations for Test 4907, Run 10	33
32	Comparison of Measured Heat Transfer Coefficients with Various Correlations for Test 4907, Run 10	34
33	Comparison of Measured Heat Transfer Coefficients with Various Correlations for Test 4907, Run 10	34
34	Comparison of Measured Heat Transfer Coefficients with Various Correlations for Test 4907, Run 10	35
35	Comparison of Heat Transfer Coefficients versus Modified Bromley Correlation as a Function of Wall Superheat, Test 4907, Run 10	36
36	Calculated Void Fractions at Three Elevations, Test 4907, Run 10	37
37	Inlet Flow Variation for Test 4914, Run 8	37
38	Level Measurements and Predictions in Bundle, Test 4914, Run 8	38
39	Comparison of Measured Heat Transfer Coefficients with Various Correlations for Test 4914, Run 8	38
40	Comparison of Measured Heat Transfer Coefficients with Various Correlations for Test 4914, Run 8	39
41	Comparison of Measured Heat Transfer Coefficients with Various Correlations for Test 4914, Run 8	39

LIST OF ILLUSTRATIONS (Cont)

<u>Figure</u>	<u>Title</u>	<u>Page</u>
42	Comparison of Measured Heat Transfer Coefficients with Various Correlations for Test 4914, Run 8	40
43	Comparison of Measured Heat Transfer Coefficients with Various Correlations for Test 4914, Run 8	40
44	Comparison of Measured Heat Transfer Coefficients with Various Correlations for Test 4914, Run 3	41
45	Comparison of Measured Heat Transfer Coefficients with Various Correlations for Test 4914, Run 8	41
46	Comparison of Measured Heat Transfer Coefficients with Various Correlations for Test 4914, Run 8	42
47	Comparison of Measured Heat Transfer Coefficients with Various Correlations for Test 4914, Run 8	42
48	Comparison of Measured Heat Transfer Coefficients with Various Correlations for Test 4914, Run 8	43
49	Comparison of Measured Heat Transfer Coefficients with Various Correlations for Test 4914, Run 8	43
50	Comparison of Measured Heat Transfer Coefficients with Various Correlations for Test 4914, Run 8	44
51	Comparison of Measured Heat Transfer Coefficients versus Modified Bromley Correlation as a Function of Wall Superheat, Test 4914, Run 8	45
52	Calculated Void Fractions at Three Elevations, Test 4914, Run 8	46
53	Inlet Flow Variation for Test 4904, Run 45	47
54	Two-Phase Level Measurements and Predictions in Bundle, Test 4904, Run 45	47
55	Comparison of Measured Heat Transfer Coefficients with Various Correlations for Test 4904, Run 45	48
56	Comparison of Measured Heat Transfer Coefficients with Various Correlations for Test 4904, Run 45	48
57	Comparison of Measured Heat Transfer Coefficients with Various Correlations for Test 4904, Run 45	49
58	Comparison of Measured Heat Transfer Coefficients with Various Correlations for Test 4904, Run 45	49
59	Comparison of Measured Heat Transfer Coefficients with Various Correlations for Test 4904, Run 45	50

LIST OF ILLUSTRATIONS (Cont)

<u>Figure</u>	<u>Title</u>	<u>Page</u>
60	Comparison of Measured Heat Transfer Coefficients with Various Correlations for Test 4904, Run 45	50
61	Comparison of Measured Heat Transfer Coefficients with Various Correlations for Test 4904, Run 45	51
62	Comparison of Measured Heat Transfer Coefficients with Various Correlations for Test 4904, Run 45	51
63	Comparison of Measured Heat Transfer Coefficients versus Modified Bromley Correlation as a Function of Wall Superheat, Test 4904, Run 45	52
64	Calculated Void Fractions at Three Elevations, Test 4904, Run 45	53



ABSTRACT

*A model has been developed to calculate the heat transfer coefficient under low flow film or pool boiling conditions in the BWR geometry. The model includes the heat transferred by convection due to the vapor boundary layer and that transferred by radiation between the high-temperature surface and the liquid.*

*The model is verified against a range of single-rod and full-scale rod bundle data. These data confirm the applicability of the model for a range of conditions postulated to occur during the BWR loss-of-coolant accident.*

1. INTRODUCTION

For the Loss-of-Coolant Accident (LOCA) analysis of a BWR, there are several conditions which require that the heat transfer coefficient be specified for film boiling on a high temperature surface exposed to a low flow or stagnant two-phase mixture (see Figure 1).<sup>\*</sup> Conditions requiring such heat transfer specification include: (1) the fuel rods during the "window" period immediately prior to lower plenum flashing, (2) the flooded portion of the fuel rods following lower plenum flashing, (3) the flooded portion of the outside channel wall, and (4) the fuel rods during bundle reflooding (from ECCS action).

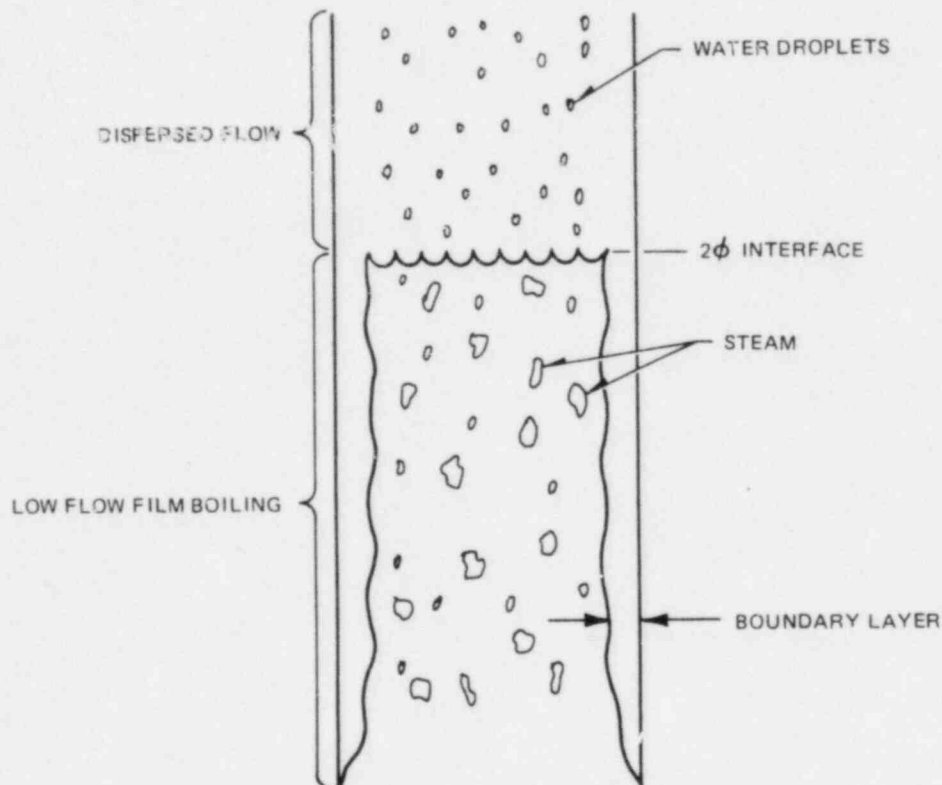


Figure 1. Low Flow Film Boiling Condition

<sup>\*</sup> As illustrated in Figure 1, this refers to regions below a two-phase "level" which separates this region with liquid as the continuous phase (low void fraction) from the dispersed flow region with vapor as the continuous phase (high void fraction).

To make realistic calculations of the heat transfer for these cases, it is necessary to have accurate predictions of the local flow and fluid conditions. Present methods are not adequate to provide these predictions for very low flow conditions. The alternative procedure of using a zero flow ("pool") film boiling correlation provides a conservative bounding result. The present report develops and verifies the appropriate zero flow film boiling correlation for BWR analysis.

There are some differences in the flow regimes between the cases 1 - 4 stated earlier. However, the basic heat transfer mechanism is similar. In situations involving flooding hot surfaces from below, in general, there will be a quench front in addition to the continuous liquid level (Figure 2). The separation between these two fronts depends on the flooding rate. At low flooding rates, these will virtually coincide and nucleate boiling is obtained below the front. At high flooding rates, there is a well defined inverted annular flow regime between the quench front and the two-phase mixture level.

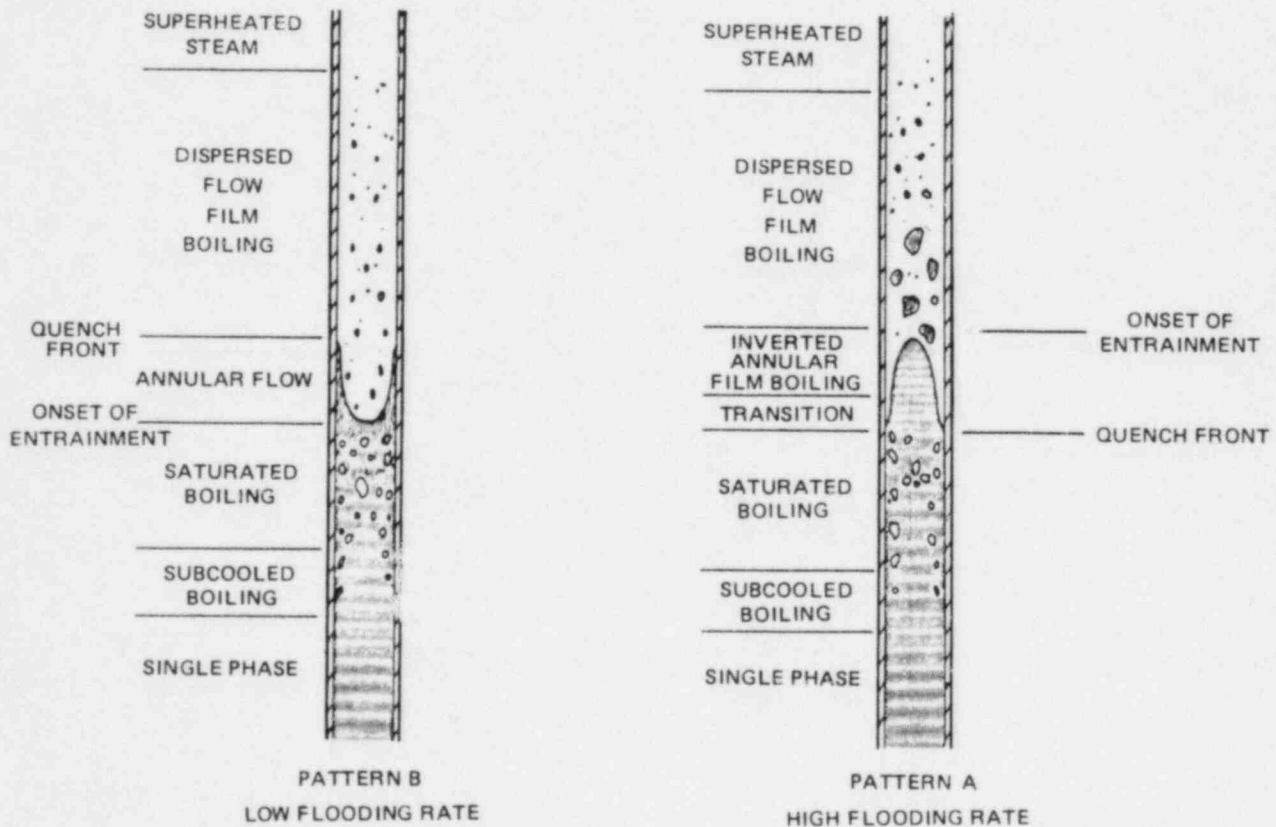


Figure 2. Flow Patterns During Reflooding

In the proximity of the quench front, the heat transfer is enhanced by axial conduction and sputtering of drops. The model to be developed in this report will, in any event, be a lower bound for predicting heat transfer in inverted annular flow.

The current General Electric models for predicting the heat transfer during the periods listed above range from a laminar pool film boiling correlation to a legislated heat transfer coefficient. For the periods immediately preceding and following lower plenum flashing the current methods apply a laminar, pool film boiling correlation by Ellion.<sup>1</sup>

The present models do not include a specific heat transfer calculation for reflooding of the external channel walls. The current model ignores this reflooding period and applies a legislated heat transfer coefficient of  $5 \text{ Btu/h-ft}^2 \text{ } ^\circ\text{F}$  on both sides of the channel until a wetting criterion<sup>2</sup> is met. Reflooding heat transfer in the bundle is assumed to become effective when the mixture, assuming 50% average void fraction, reaches a given plane. When this condition is reached, an empirically based heat transfer coefficient of  $25 \text{ Btu/h-ft}^2 \text{ } ^\circ\text{F}$  is applied. Thus, the current models include three different approaches to calculate the heat transfer for essentially the same physical situation. A single approach to the calculation of heat transfer for this common physical situation is the objective of this study. The experimental verification studies have, however, been grouped into blowdown and reflood categories for qualification in each of these regimes.

2. THEORETICAL MODEL

A calculation of the exact heat transfer below the two-phase level for the case of low flow on a high temperature vertical surface is very difficult because it requires precise knowledge of local flow and fluid conditions in the region of interest. Since such local condition information is not available from present design hydraulics models, the heat transfer for low flow situations will be conservatively approximated by pool film boiling relations.

Very similar analytical models for film boiling heat transfer with laminar film flow on a vertical surface have been developed by Ellion,<sup>1</sup> Bromley,<sup>3</sup> and Bailey.<sup>4</sup> The physical basis of these models is illustrated in Figure 3, and developed in Appendix A. The three models use slightly different assumptions for the vapor-liquid interface velocity, but the resultant heat transfer coefficient relations are quite similar. They can be expressed in the general form:

$$h = K_1 \left[ \frac{K_g^3 \rho_g (\rho_f - \rho_g) h_{fg} g}{\mu_g (T_{WALL} - T_{SAT}) L} \right]^{1/4} \quad (1)$$

where

$$K_1 = 0.714 \text{ (Ellion)}$$

$$= 0.62 \text{ (Bromley*)}$$

$$= 0.76 \text{ (Bailey)}$$

\* Bromley's theoretical analysis for a vertical surface yields a factor of 0.943 for zero vapor-liquid interface shear, and 0.667 for zero interface velocity. For film boiling on a horizontal cylinder the equivalent factors are 0.724 and 0.512, respectively. The value of 0.62 is actually an empirical result (average of the two theoretical limits) for the horizontal cylinder case; however, this empirical value has recently been suggested as applicable to vertical surfaces by Hsu.<sup>6</sup> As subsequently indicated, this represents a conservative value for use in Equation 1.

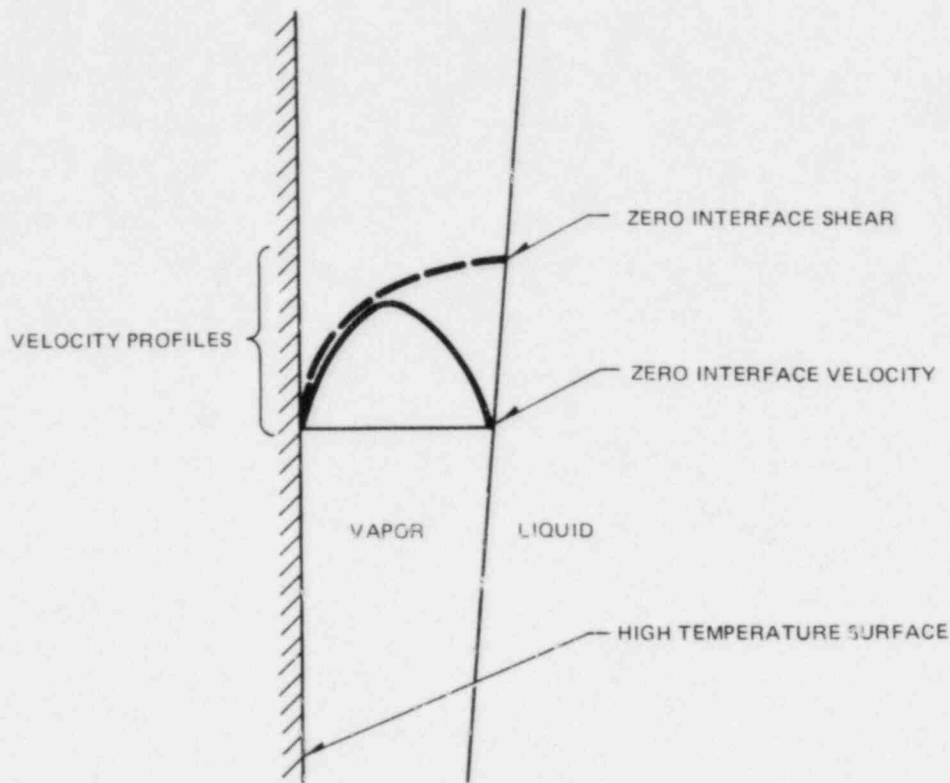


Figure 3. Models of Laminar Film Boiling on a Vertical Surface

It can be seen from Equation 1 that the heat transfer coefficient decreases monotonically with length to the  $1/4$  power. This results from the increasing laminar vapor film thickness with length assumed for this model.

In the work of Hsu and Westwater<sup>5</sup> it was indicated that the laminar boundary layer (i.e., smooth, viscous film) assumed in the derivation of Equation 1 only existed up to a Reynolds number in the film of approximately 100. At Reynolds numbers exceeding 100, Hsu and Westwater indicate the flow in the vapor film becomes turbulent. Once this turbulence develops the heat transfer coefficient would increase significantly with increasing length (Figure 4).\* In application to the BWR LOCA the plane of maximum interest is generally in the high-power region near the fuel bundle midplane, approximately 6 feet up the vertical

\* The correlation of Hsu and Westwater was checked using a data base of results from short length tests (4.0 to 5.5 inches) in liquid methanol, carbon tetrachloride, benzene, and nitrogen. The correlation was extended analytically to water.

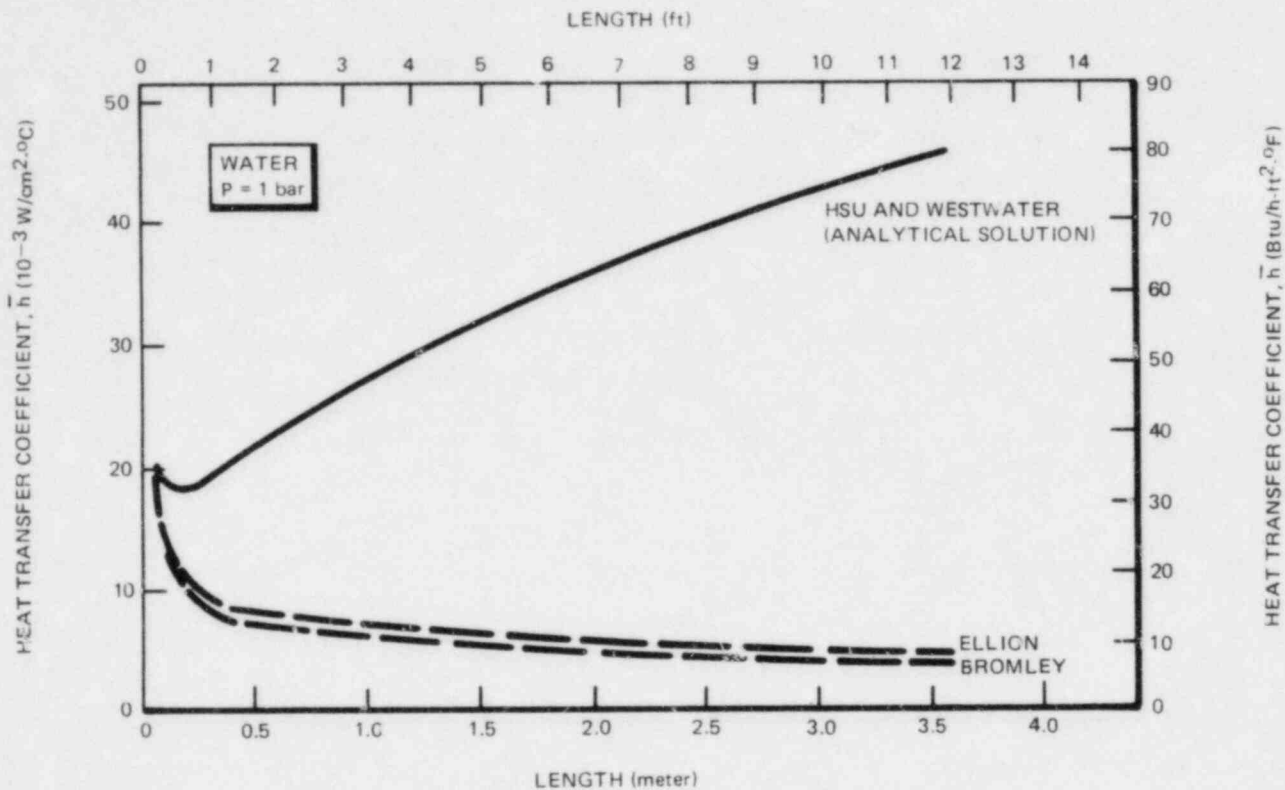


Figure 4. Comparison of Laminar and Laminar/Turbulent Pool Film Boiling Correlations

system. As shown by Figure 4, the heat transfer coefficient  $\bar{h}$  calculated for this elevation can vary by a factor of almost six depending on the boundary layer assumptions made.

Photographic studies of film boiling on vertical surfaces by Hsu and Westwater<sup>5</sup> and by Simoneau and Simon<sup>7</sup> indicate a wave character to the liquid-steam interface. Using high-speed motion pictures to study the wave phenomena, they concluded that the characteristic wavelength of the liquid-vapor interface is close to the classical Taylor instability wavelength:\*

\* Bailey<sup>4</sup> concluded that the instability of the liquid-vapor interface causes the laminar boundary layer to restart over each wavelength (i.e., all of the vapor generated over each instability wavelength leaves the surface). From Chandrasekhar's<sup>8</sup> analysis on a vertical hollow cylindrical jet of radius  $r$ , he suggested the instability criterion:  $L_B = 2\pi r/0.484$  for use in Equation 1.

$$L_T = 2\pi \left[ \frac{\sigma g_c}{g(\rho_f - \rho_g)} \right]^{1/2} \quad (2)$$

For large vertical systems a physically more reasonable approach would be to use the Helmholtz instability criteria to determine the length of the film. This approach shows that an interface with a velocity difference existing across it will be unstable for wavelengths exceeding some critical value. Using this criterion (see Appendix A for a detailed derivation) the critical film length for the cases of interest can be determined to be,

$$L_H = 16.24 \left[ \frac{\sigma^4 h_f^3 g_c^5}{\rho_g (\rho_f - \rho_g)^5 g^5 k_g^3 (T_W - T_{SAT})^3} \right]^{1/11} \quad (3)$$

Using either Equation 2 or 3 in Equation 1, the result is that the film boiling heat transfer coefficient is held approximately constant over the entire length\* of a uniform temperature vertical surface, as the vapor film instability wavelength process inhibits transition to turbulent flow. The film instability also eliminates the continuing decrease in heat transfer coefficient associated with a growing laminar film; however, this process would be arrested by a transition to turbulent flow, even in the absence of the instability wavelength.

A comparison of the results obtained using the Taylor (Equation 2) and Helmholtz (Equation 3) criteria in Equation 1 is given in Figure 5. The Helmholtz approach gives a critical length which decreases with wall temperature. As shown in Figure 5, in the temperature range of interest for the BWR the Helmholtz criterion gives slightly lower critical film lengths (i.e., larger heat transfer coefficients) than the Taylor approach. The relatively close agreement obtained with the two criteria indicates that either one could be used for BWR-LOCA calculations. Physical considerations dictate the use of the Helmholtz criterion.

\* In principle, the heat transfer coefficient would be much higher immediately above the leading edge. However, this exists only for the first few inches and is, therefore, of no particular significance for BWR-LOCA analysis.



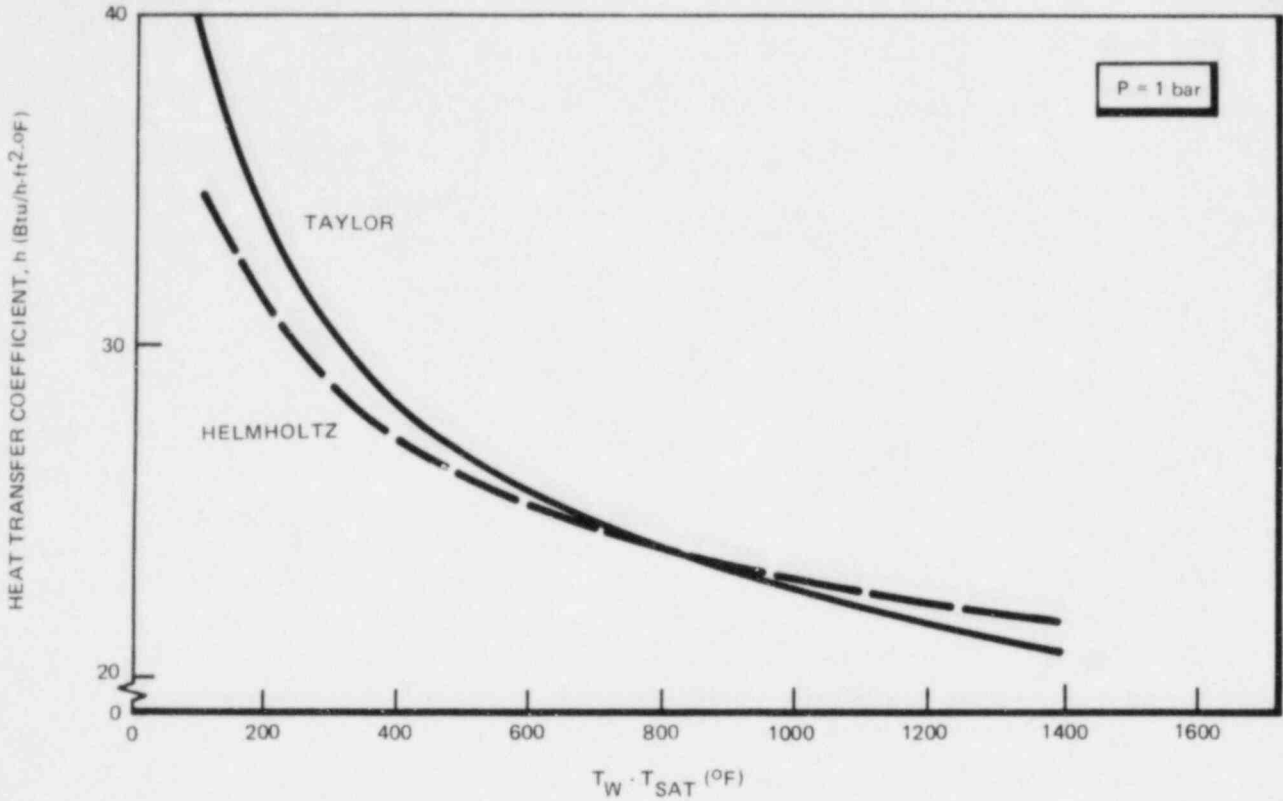


Figure 5. A Comparison of Taylor and Helmholtz Stability Criteria

Therefore, using the coefficient developed by Bromley<sup>3</sup> (slightly more conservative than other developments), the recommended zero-flow convective film boiling coefficient is:\*

$$h_{FB} = 0.62 \left[ \frac{K_g^3 (\rho_f - \rho_g) h_{fg} g}{\mu_g (T_{WALL} - T_{SAT}) L_H} \right]^{1/4} \quad (4)$$

where

$$L_H = 16.24 \left[ \frac{\sigma^4 h_{fg}^3 \mu_g^5 g_c^4}{\rho_g (\rho_f - \rho_g) g^5 K_g^3 (T_{WALL} - T_{SAT})^3} \right]^{1/11}$$

\*The recommended coefficient in Equation 4 is noted to have the same form as that derived by Berenson<sup>9</sup> for film boiling on a horizontal surface. The equivalent constant for the horizontal case is 0.673.

For the conditions of interest in the BWR LOCA analysis, surface temperatures on the fuel rod and channel surfaces can become high enough (especially in the reflood periods) for radiation heat transfer to be an important consideration. In this case, the convective heat transfer relation of Equation 4 must be supplemented by a radiation component. This can be done by directly adding a radiation component as suggested by Hsu<sup>6</sup> and by Amm and Ulrych.<sup>10</sup>

$$h = h_{FB} + h_R^* \quad (5)$$

where, for approximately parallel surface conditions between the wall and the water ( $\epsilon = 1$ ),

$$h_R = \epsilon_W \sigma_R \frac{(T_W^4 - T_{SAT}^4)}{(T_W - T_{SAT})} \quad (6)$$

The combination of Equations 4, 5, and 6 is hereafter referred to as the "modified Bromley correlation."

---

\* Bailey<sup>4</sup> recommended modifying the laminar flow model to include radiation heat transfer. This results in an implicit relation that requires an iterative solution. Comparison with the explicit approach of Equation 5 shows a maximum difference of approximately 10%. However, the direct explicit relation of Equation 5 is recommended on the basis of the resultant data correlation accuracy.

### 3. EXPERIMENTAL VERIFICATION

An extensive range of data is available to verify the applicability of the modified Bromley correlation Equations 4-6 to the low flow boiling periods of interest in the postulated BWR LOCA. These data come from several sources and include small-scale quench tests and full-scale blowdown and reflood type experiments.

These are presented separately for qualification of the correlation in the various phases of the transient.

#### 3.1 QUENCHING/REFLOOD EXPERIMENTS

Single-rod quench tests have been conducted at General Electric where a high-temperature specimen was vertically dropped into a large volume of saturated and subcooled water at atmospheric pressure. The heated tube was 18 inches long and contained five equally spaced thermocouples. The thickness of the tube was 1/32 inch. To obtain the data, the tube was heated to a prescribed temperature and then plunged into the pool. The surface temperature of the tube was then recorded as a function of time. Knowing the mass of the tube, the specific heat, and the time response of the surface temperature, the surface heat flux from the tube was calculated. Then the heat transfer coefficient was computed from the heat flux, the surface temperature (from the thermocouples), and the known pool temperature. The following data are extracted from Reference 11, which describes the experiment in greater detail.

Comparison of the data from these tests with predictions from the modified Bromley correlation show very good agreement (see Figure 6) for  $T_W - T_{SAT} \geq 350^\circ\text{F}$ . The correlation underpredicts  $h$  when the wall temperatures are close to the wetting temperature, which is about  $500^\circ\text{F}$  for saturated water at atmospheric pressure.<sup>2</sup>

The modified Bromley correlation is also compared with the subcooled film boiling data obtained from runs 6, 7, and 8 as shown in Figures 7, 8, and 9. The

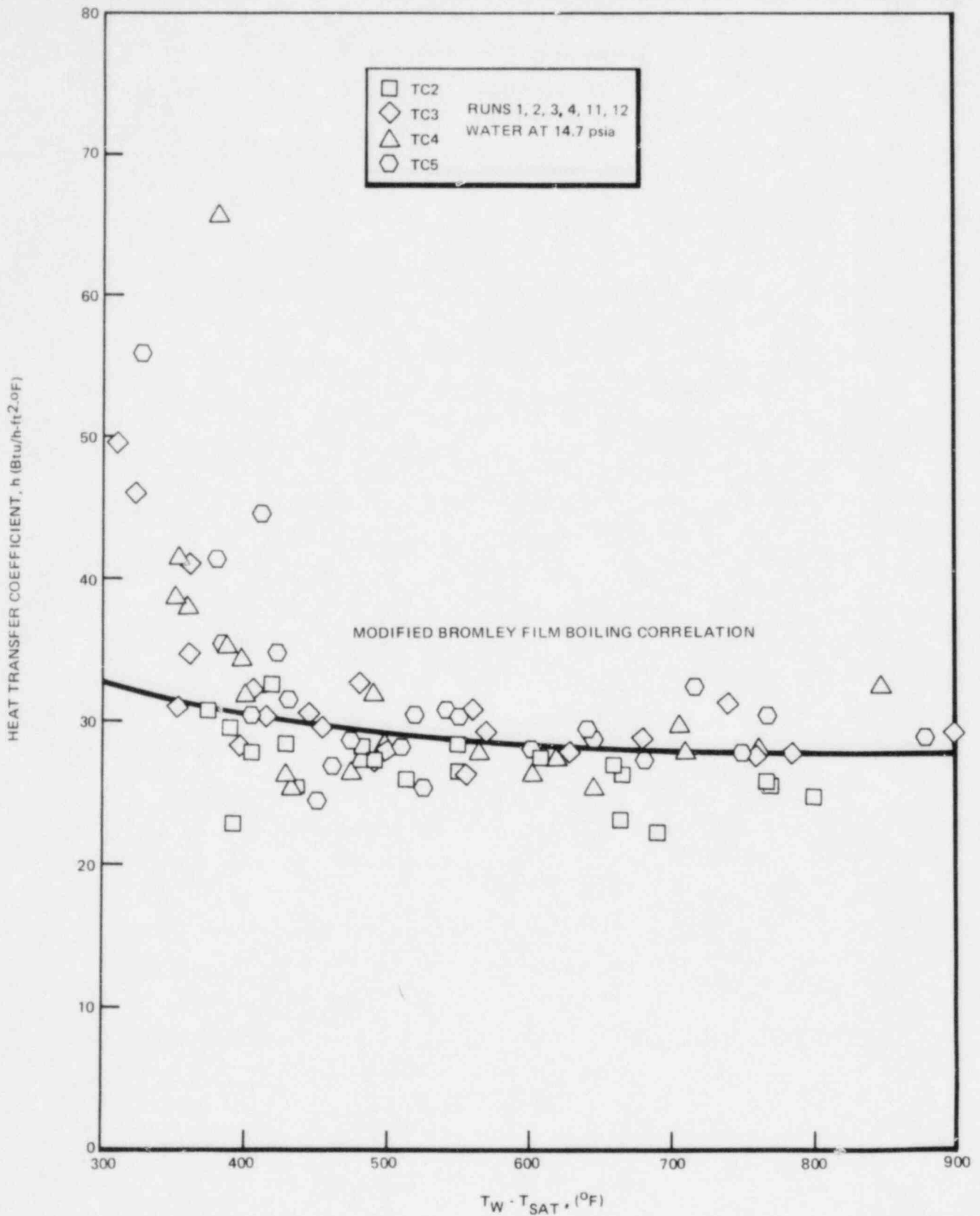


Figure 6. Comparison of Saturated Film Boiling Data with Modified Bromley Correlation

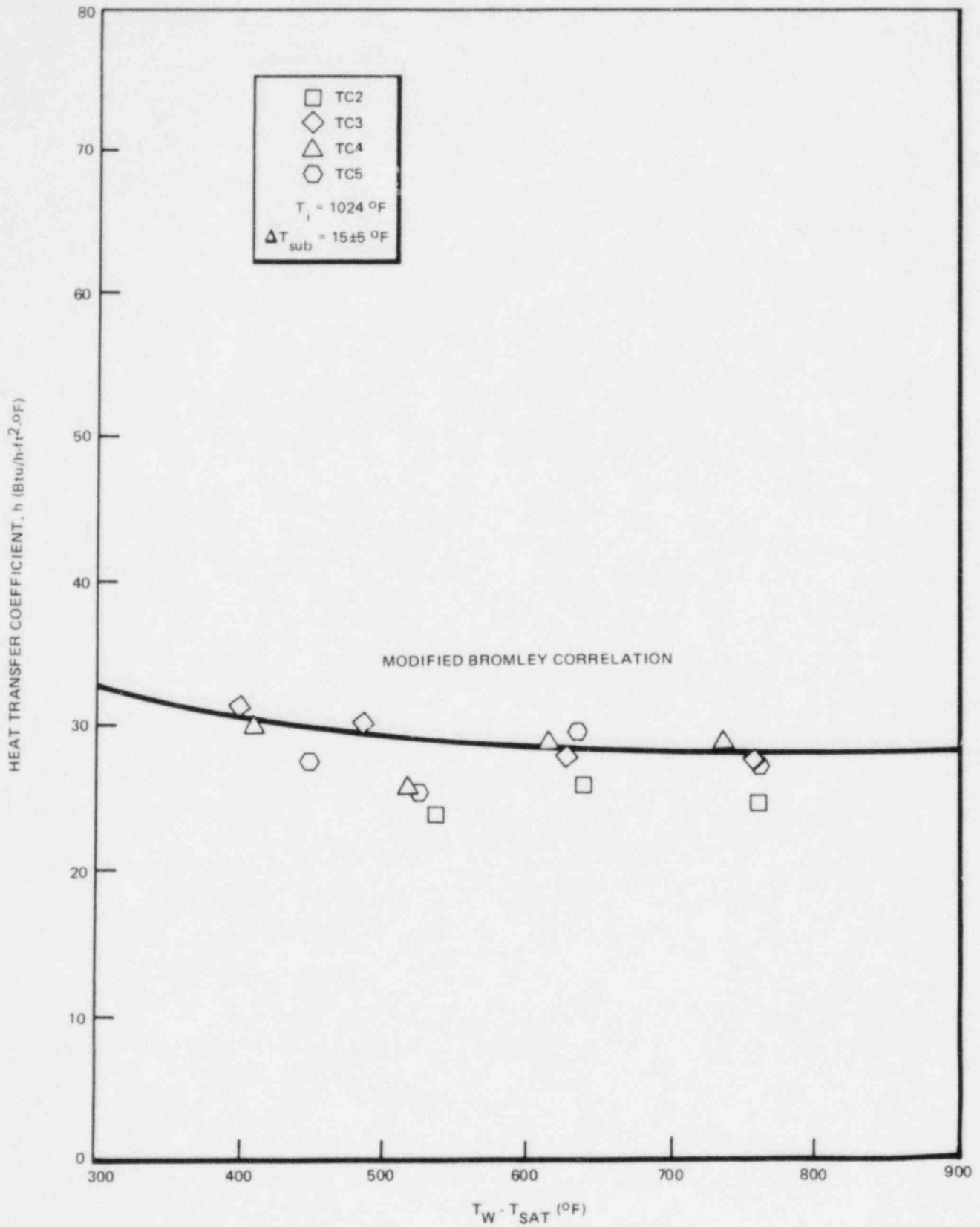


Figure 7.  $h$  versus  $(T_W - T_{SAT})$  for Run 6

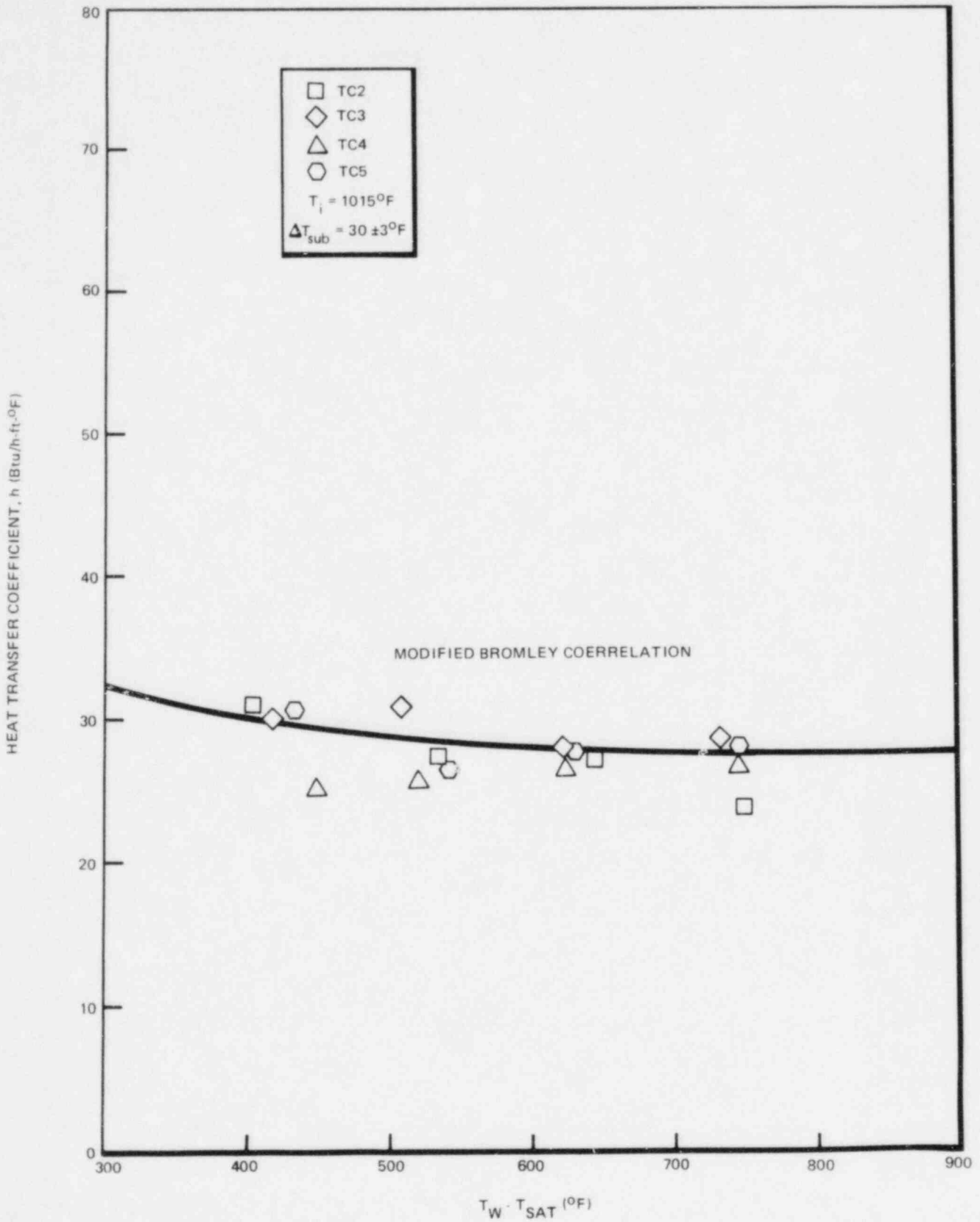


Figure 8. h versus  $(T_W - T_{\text{SAT}})$  for Run 7

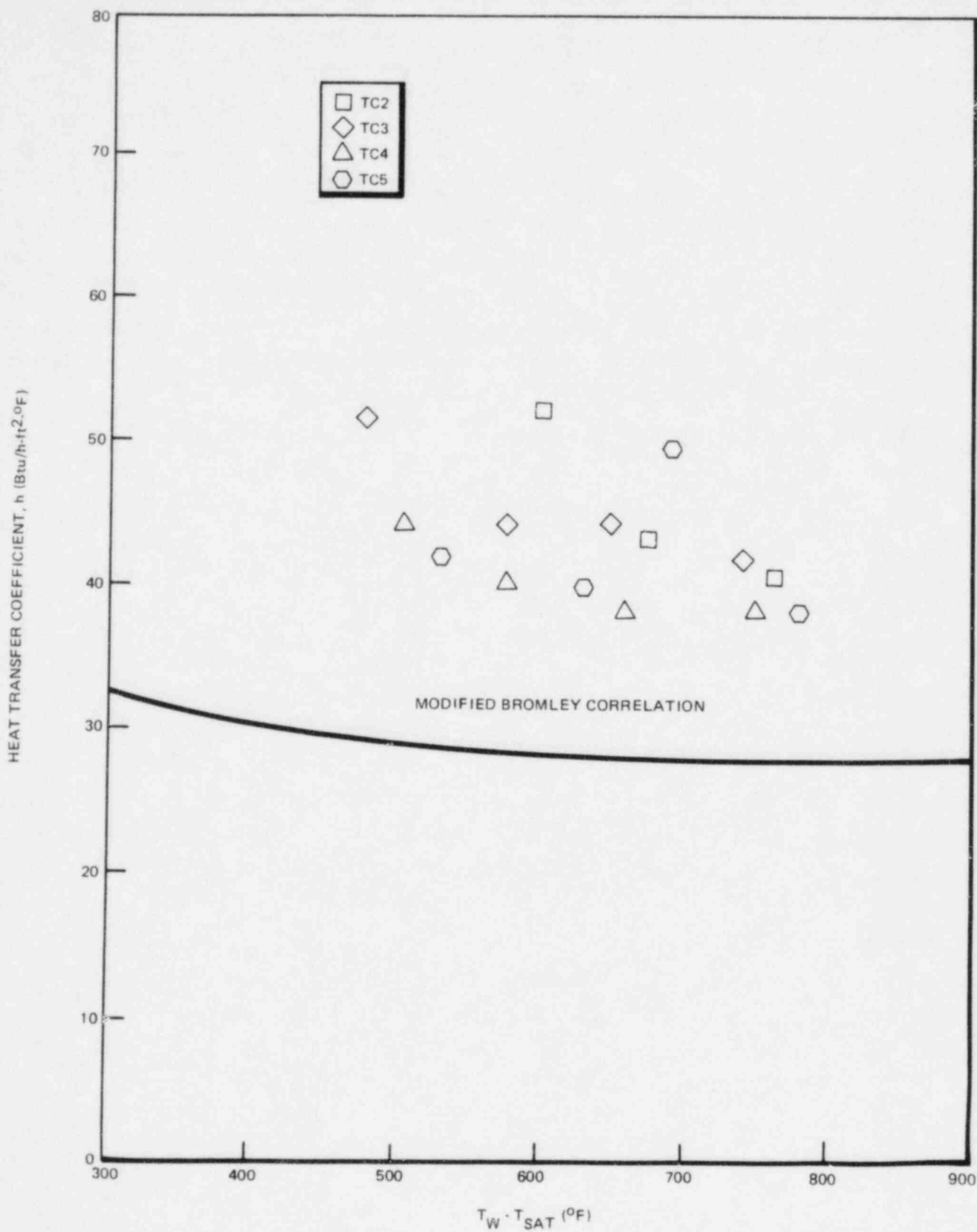


Figure 9. h versus ( $T_W - T_{SAT}$ ) for Run 8

low subcooling film boiling data are not different from the saturated ones, and hence, agree well with the modified Bromley correlation. For highly subcooled conditions (Run 8,  $\Delta T_{\text{sub}} = 62^\circ\text{F}$ ), the data are noticeably higher than the predicted values.

Bundle reflooding experiments conducted at Westinghouse<sup>6</sup> (PWR-FLECHT program) and KWU<sup>10</sup> show the modified Bromley correlation does an excellent job of predicting the experimental results for the region below the two-phase level (Figures 10 through 13). These experiments were conducted on full-scale bundles (49-rod at Westinghouse and 340-rod at KWU) under transient reflooding conditions at different system pressures. The Westinghouse data are shown in Figures 10, 11, and 12 as functions of the wall superheat during the transient. The modified Bromley correlation combined with a transition boiling correlation suggested by Hsu<sup>6</sup> predict the data very well. The modified Bromley correlation alone is seen to provide a conservative lower-bound prediction of these data. The data from the KWU experiments (Figure 13) are also in excellent agreement with the modified Bromley correlation for the film boiling portion of the transient.

### 3.2 BLOWDOWN PHASE EXPERIMENTS

Full-scale 49-rod bundle data from the two-loop test apparatus (TLTA) on the cooperative NRC/EPRI/GE BWR Blowdown Heat Transfer (BDHT) program<sup>12</sup> shows the conservatism of the recommended correlation for non-zero flow conditions. The BDHT experiments are transient tests and the local conditions in the bundle only approach a zero flow film boiling condition when the two-phase level approaches the plane in question.

A great deal of emphasis will be placed on these experiments because they provide information in a prototypical bundle geometry under representative flow and heat flux conditions.

The tests selected for this investigation were the high bundle power 7x7 BDHT tests. The tests and corresponding bundle powers are: 4904 (6.09 MW), 4907 (6.09 MW), 4910 (6.55 MW), and 4914 (6.55 MW). These tests were chosen because



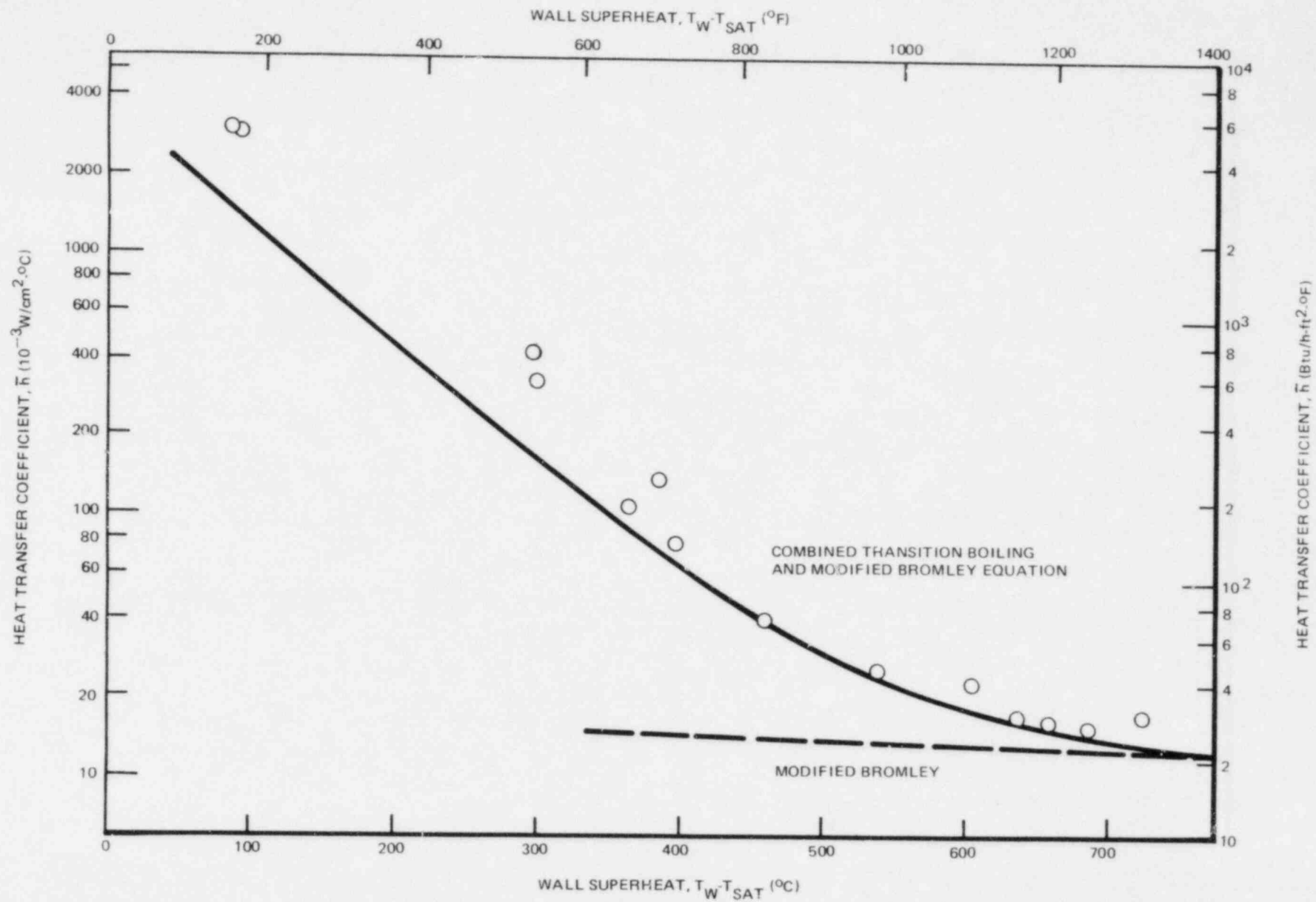


Figure 10. Heat Transfer Coefficient for Transition and Film Boiling at 15 psi

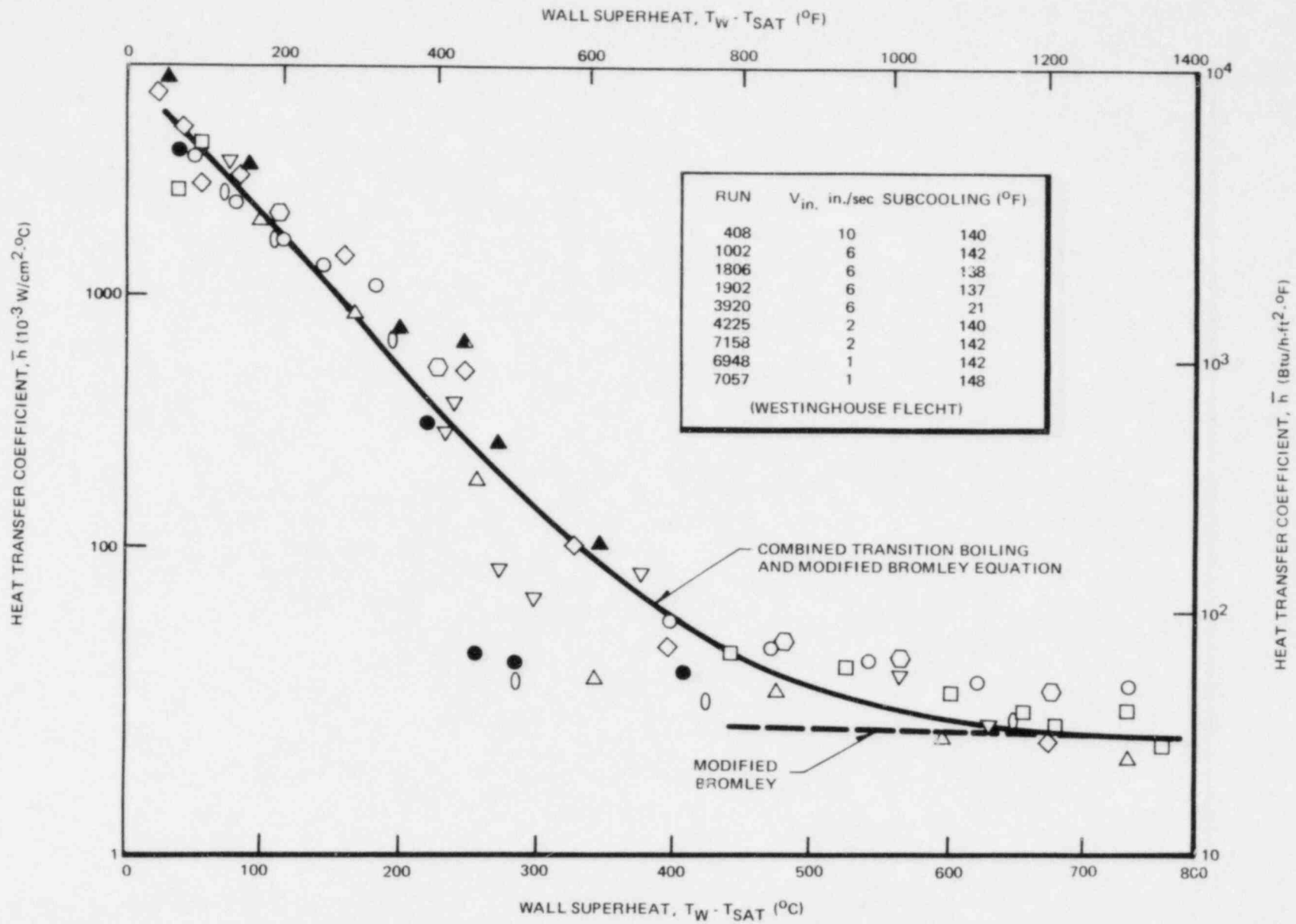


Figure 11. Heat Transfer Coefficient for Transition and Film Boiling at 60 psi

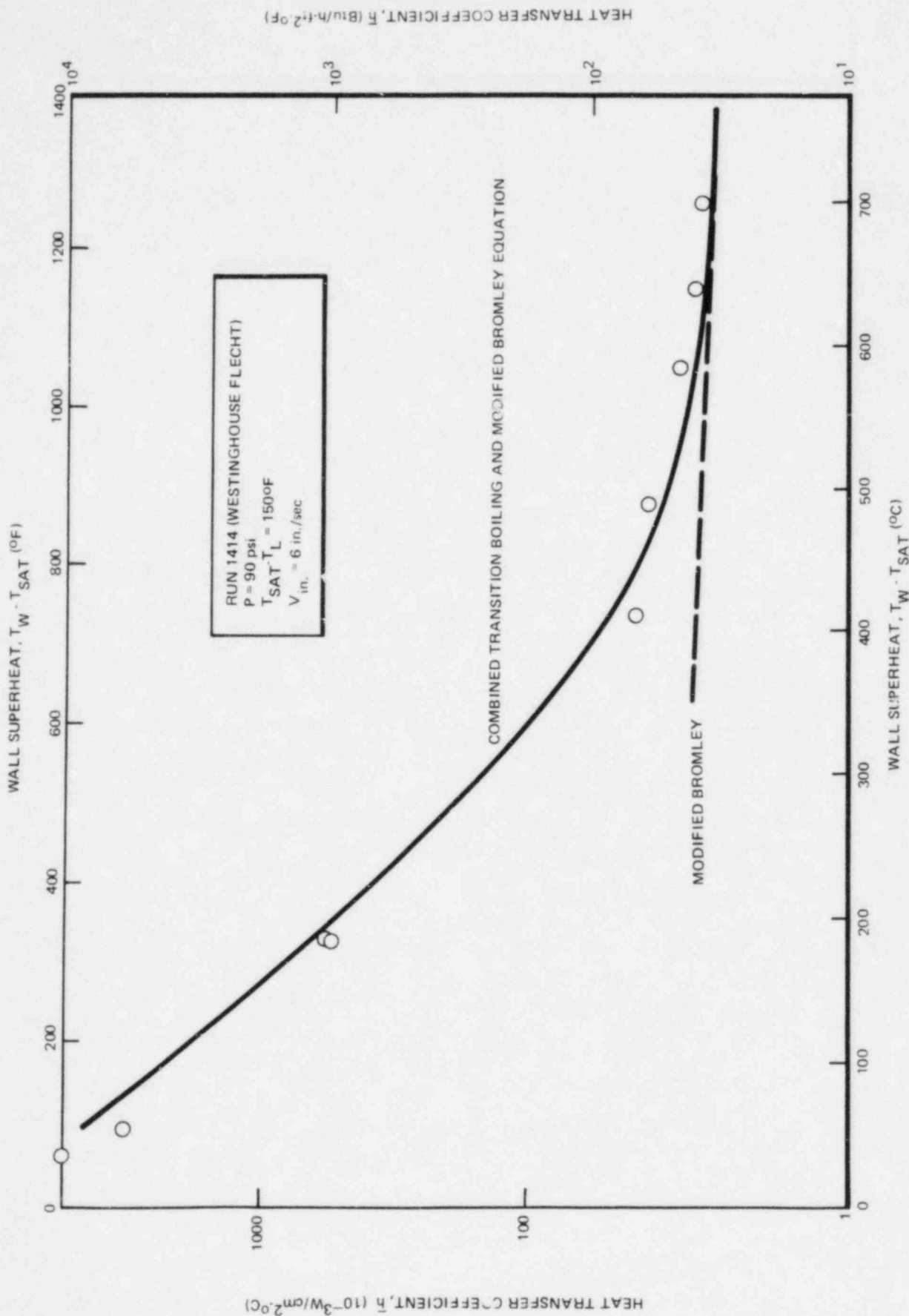


Figure 12. Heat Transfer Coefficient for Transition and Film Boiling at 90 psi

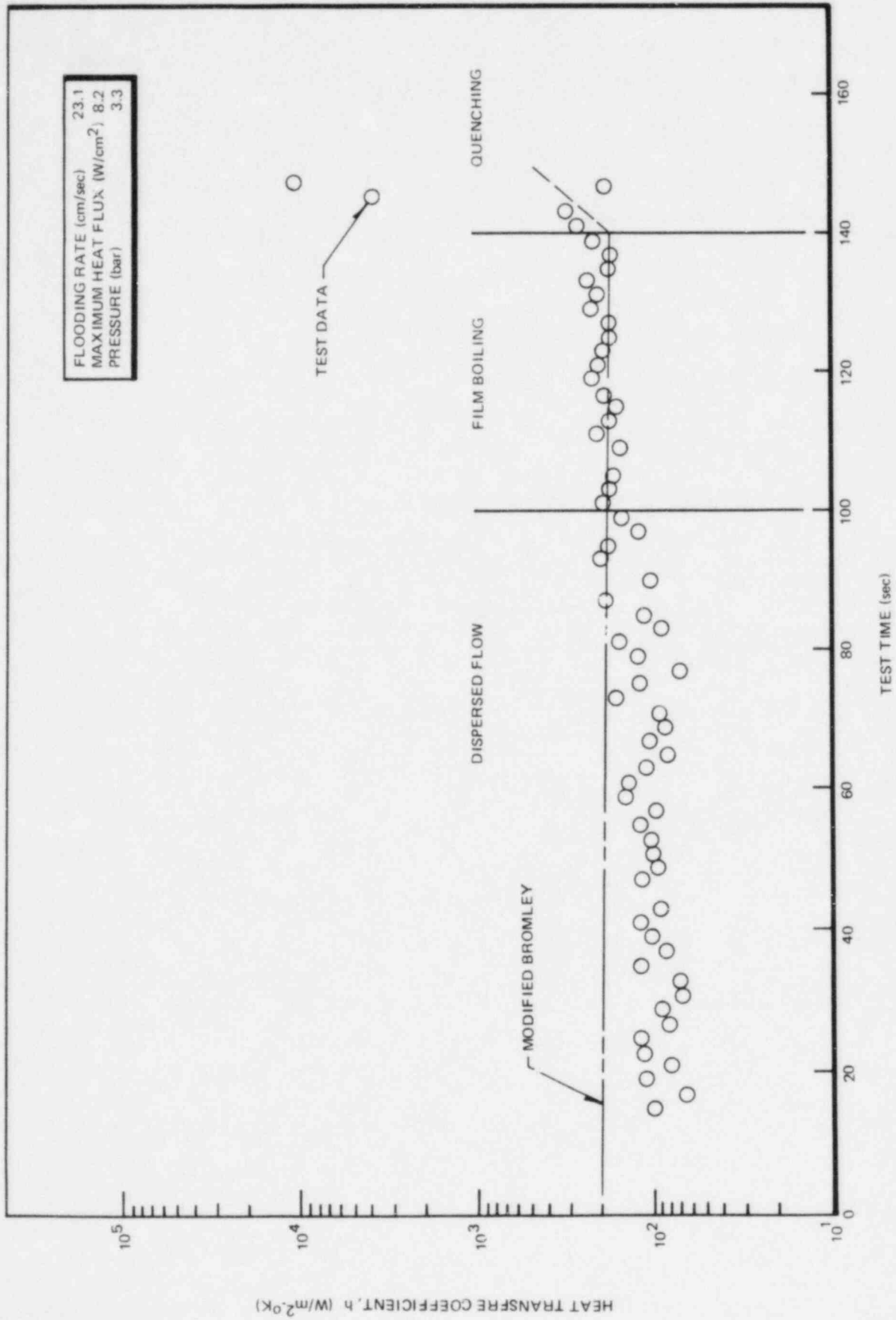


Figure 13. KWU Reflood Data Compared to Modified Bromley Correlation

they were the only tests that resulted in boiling transition (BT) with sustained dryout (film boiling) in the low flow periods or pool film boiling heat transfer regime. In the other tests, nucleate boiling was maintained throughout this period.

An important element of this qualification was to assure that the data under consideration were indeed in a pool film boiling heat transfer regime. The heater temperature data were examined during periods of low flow for various elevations for situations where some of the thermocouples indicated a departure from nucleate boiling while others at the same elevation remained in nucleate boiling. This situation indicates occurrence of a previous boiling transition (usually on the higher powered rods) below the two-phase mixture level. This low flow film boiling heat transfer regime persists until the two-phase level drops below the measurement elevation - an event which is signaled by all the remaining thermocouples indicating dryout. As further substantiation of the heat transfer regime, calculations were made using a transient thermal hydraulics code to assure that the data under consideration were below the two-phase level.\* The level calculations were driven by the measured bundle power, pressure, core inlet flow, and inlet fluid enthalpy.

The heat transfer coefficients were calculated from measured wall temperatures using an inverse heat conduction solution. Four test runs were used for qualification, and data from a number of thermocouples on rods with varying power generation and at several elevations were evaluated.

---

\* As expected, the heat transfer coefficient is lower in the dispersed flow region above the two-phase level. Current BWR analysis methods conservatively assume zero heat transfer for this region.

### 3.2.1 Discussion of Results

#### a) TEST 4910

The core inlet flow for this test is shown in Figure 14. Periods of low inlet flow during the window and post lower plenum flashing (PLPF) are indicated. Direct measurement of the two-phase mixture level or local conditions within the bundle are not made in the BDHT tests. However, using the measured flow and other test measurements as noted above, the calculated two-phase level is shown in Figure 15.\* The movement of the two-phase level is confirmed experimentally by the observation of the thermocouples at the same elevation on the other rods. These experimental values are also indicated on the figure. Thermocouple elevations are noted on the plot for future reference.

Measured heater temperatures at the 118-, 98-, and 78-in. elevations were used. Temperatures at the peak power plane (71 inches) and below generally remained well cooled during the tests. Two criteria were used in the selection of thermocouples:

1. Indication of film boiling in the low flow region,
2. Evidence of continuous liquid region (below two-phase level).

Figures 16 through 19 show calculated heat transfer coefficients obtained from measured data from four rods at the 118-in. elevation, and comparisons with three correlations — modified Bromley (Equation 5), Bromley without the radiation term, and the Ellion correlation. The inverse heat conduction method used to derive the heat transfer coefficients from the data results in numerical noise which is represented by the uncertainty bands in Figures 16 and 17. Similar uncertainties are present in other data plots but are omitted for convenience. The noise results from noise in the data together with the process of differentiation involved in the method. The uncertainty bands thus

---

\* The calculations are based on a transient hydraulics model "THRST". The hydraulics equations and solution scheme in this model are identical to those in MAYU04.<sup>13</sup>

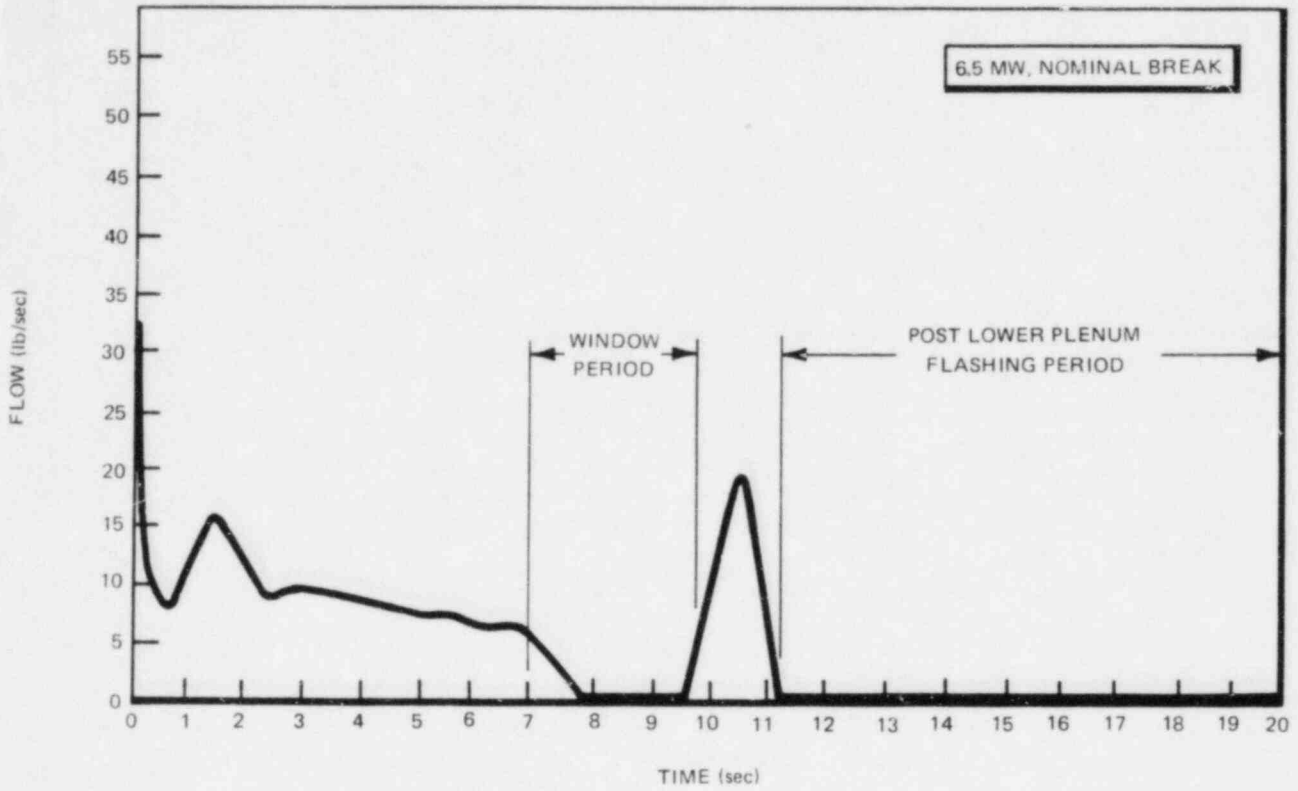


Figure 14. Inlet Flow Variation for Test 4910, Run 13

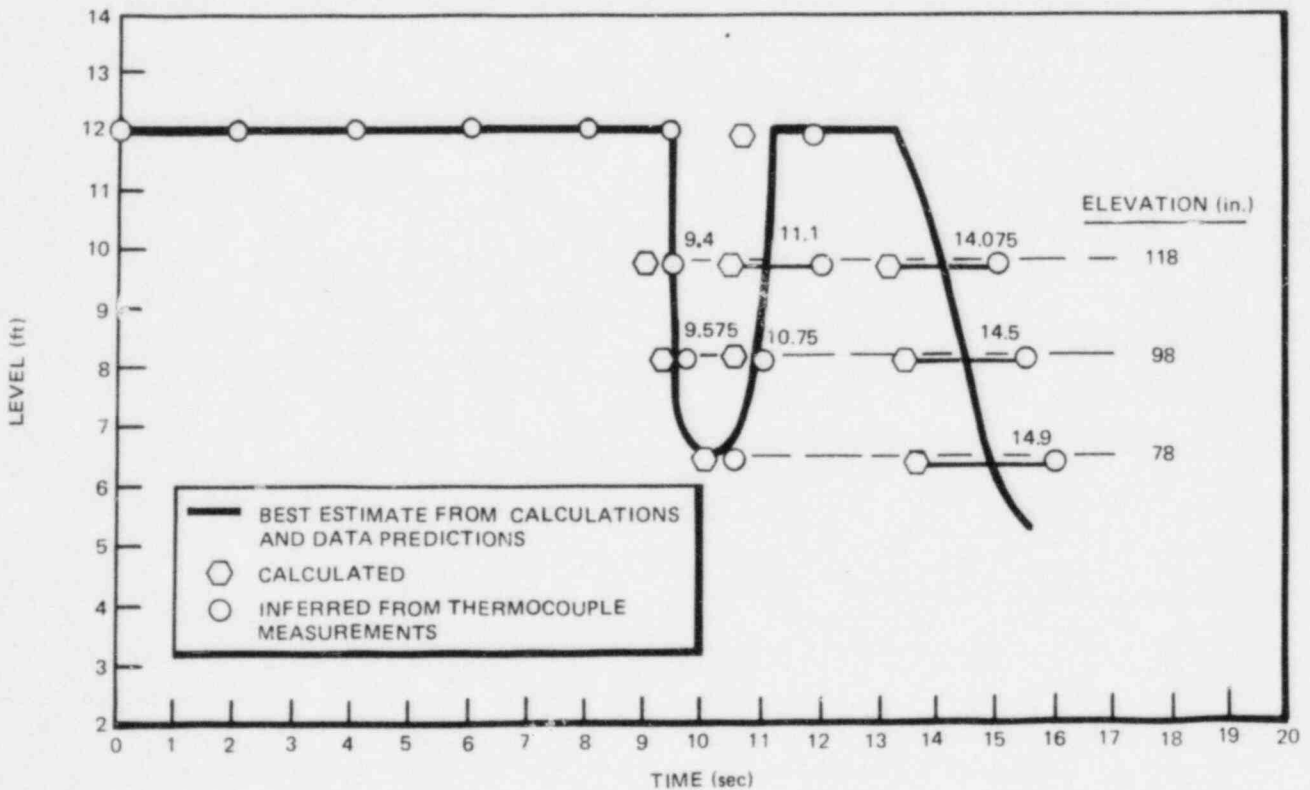


Figure 15. Measured and Predicted Level in Bundle, Test 4910, Run 13

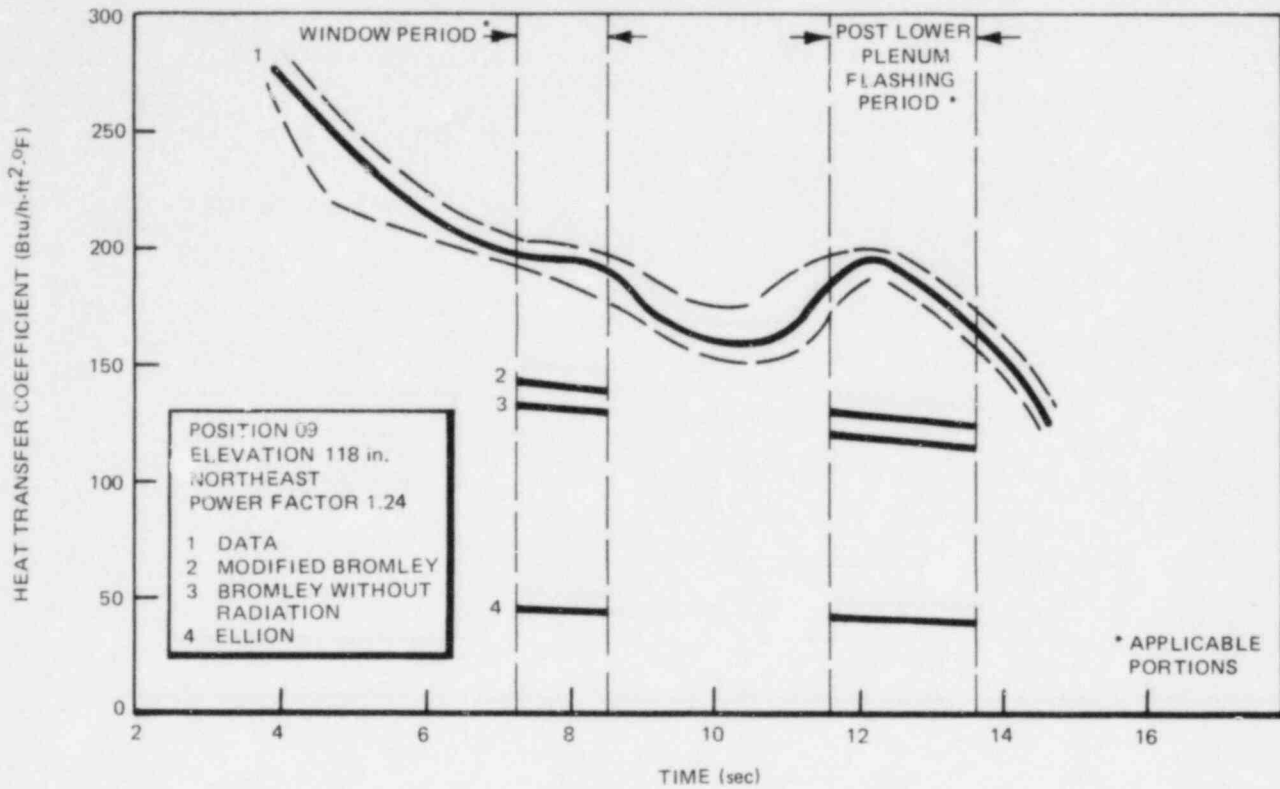


Figure 16. Comparison of Measured Heat Transfer Coefficients with Various Correlations for Test 4910, Run 13

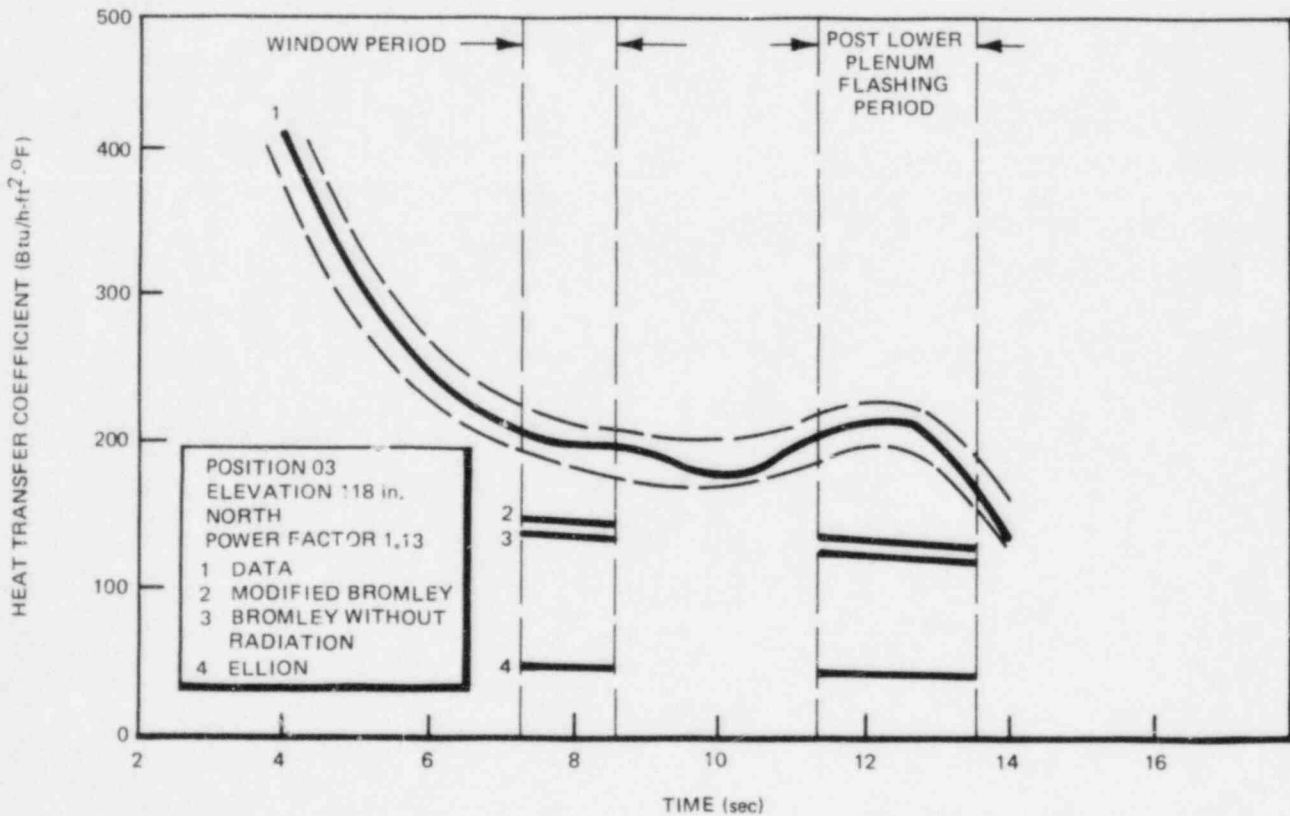


Figure 17. Comparison of Measured Heat Transfer Coefficients with Various Correlations for Test 4910, Run 13



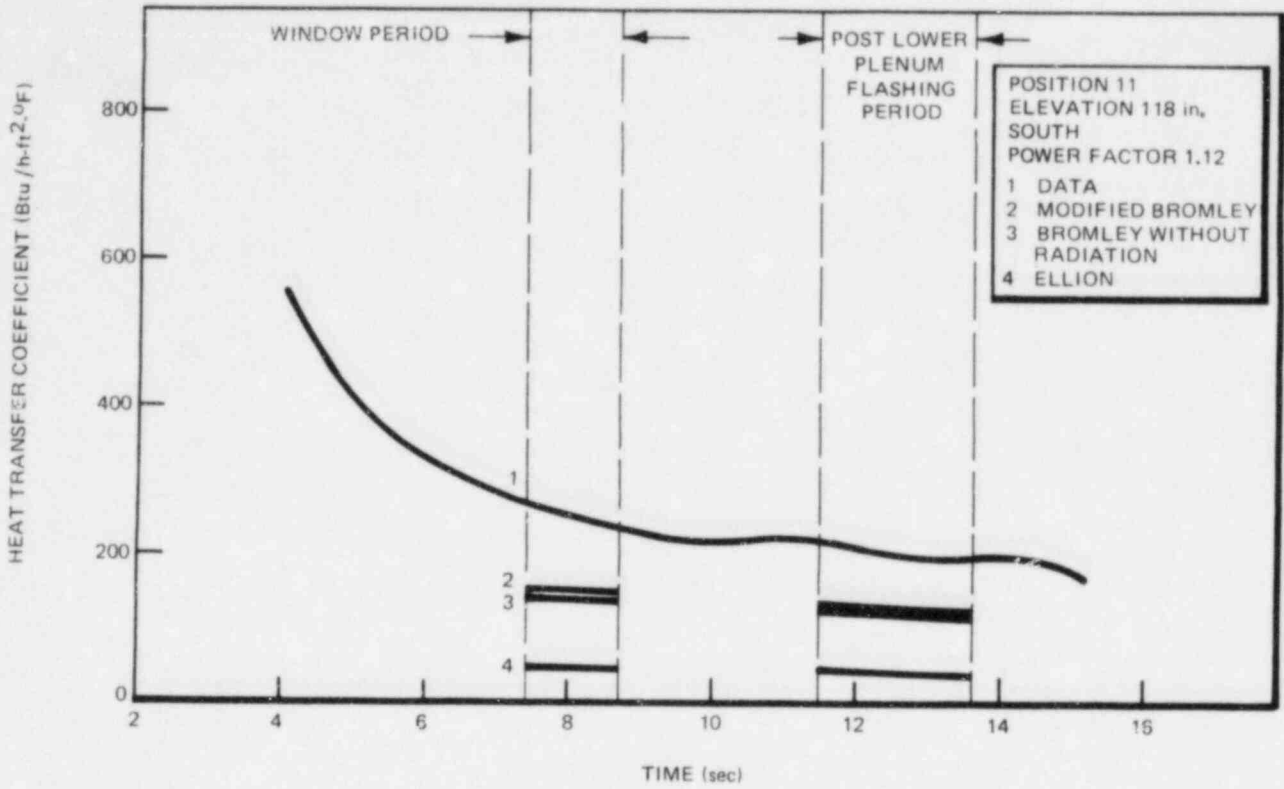


Figure 18. Comparison of Measured Heat Transfer Coefficients with Various Correlations for Test 4910, Run 13

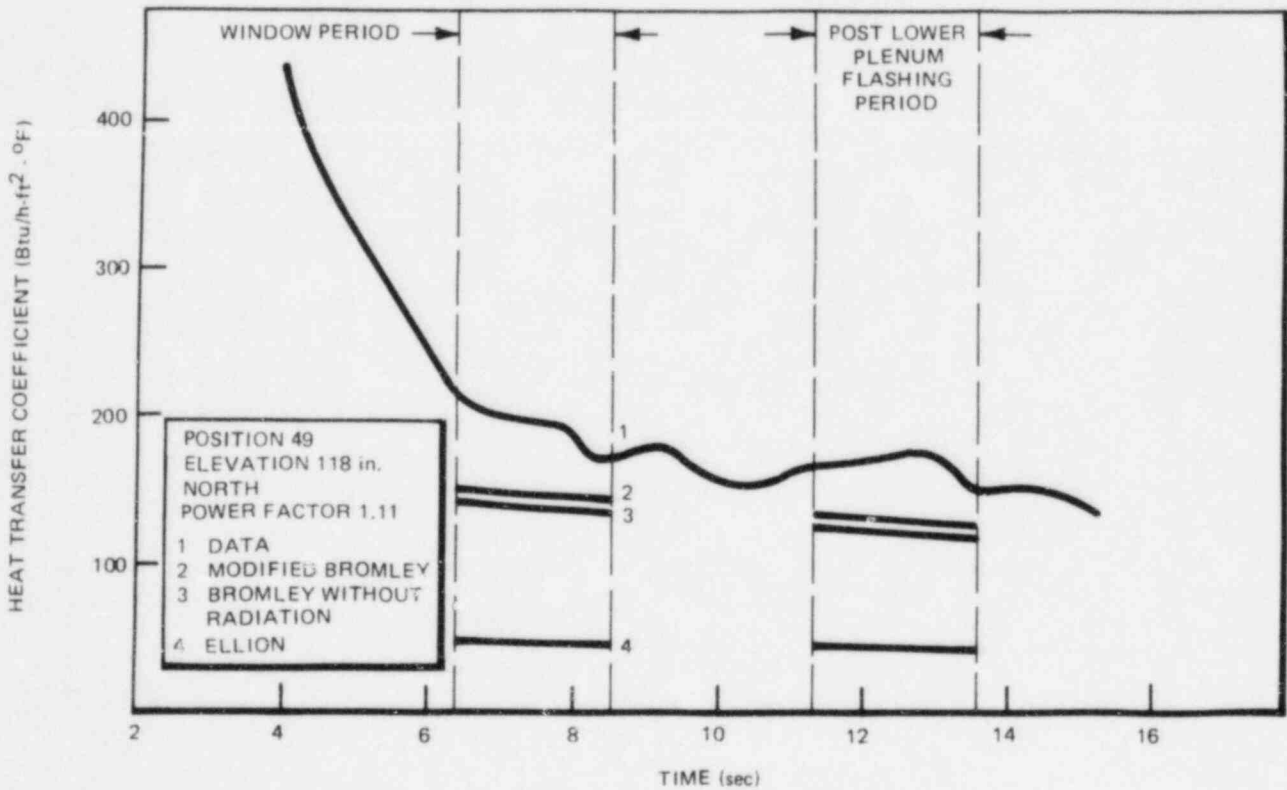


Figure 19. Comparison of Measured Heat Transfer Coefficients with Various Correlations for Test 4910, Run 13

represent the combined effects of the methodology used and the uncertainty in the measurements. In the window period, the measured heat transfer coefficients were generally greater than 200 Btu/h-ft<sup>2</sup>-°F, whereas the predicted values using the modified Bromley correlation were of the order of 150 Btu/h-ft<sup>2</sup>-°F.

Figures 20 and 21 are for the 98-in elevation and Figure 22 for the 78-in. elevation. In every case the modified Bromley correlation was found to be lower than the data and significantly so in the majority of the cases.

All the data for Test 4910 are summarized in Figure 23, which shows the variation in heat transfer coefficient as a function of wall superheat. For the purposes of this comparison, several points were picked from the plots of measured heat transfer coefficients shown in the earlier figures over the range of wall temperatures encountered. The modified Bromley correlation is a weak function of pressure in this portion of the transient and a mean prediction curve can be plotted. The maximum scatter in the predictions about this curve because of

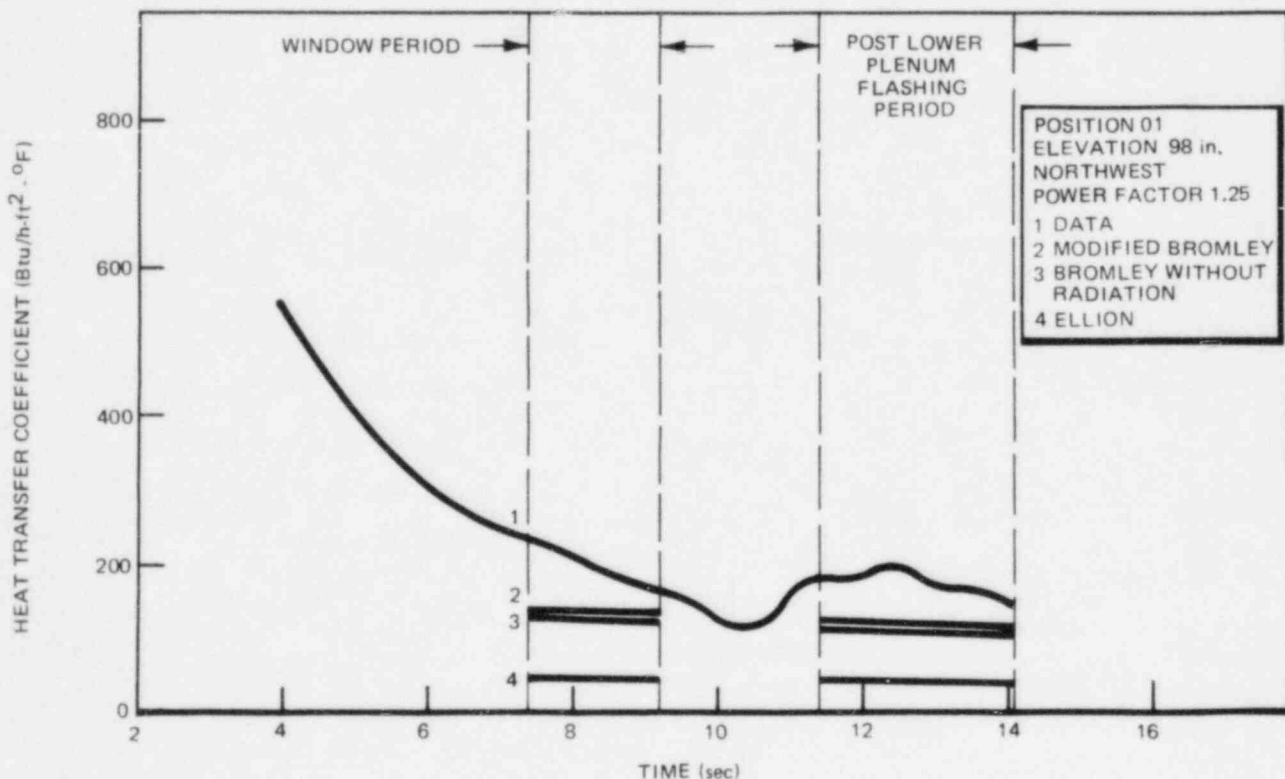


Figure 20. Comparison of Measured Heat Transfer Coefficients with Various Correlations for Test 4910, Run 13

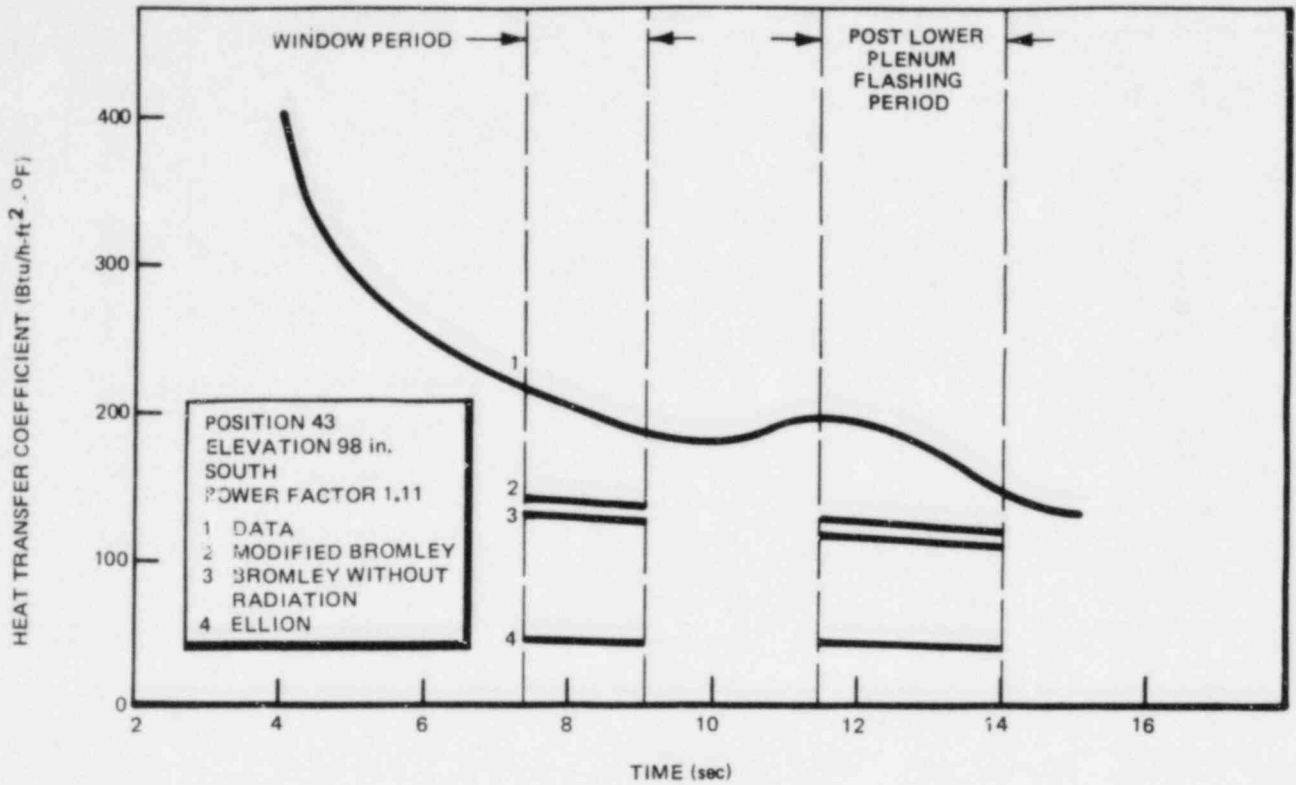


Figure 21. Comparison of Measured Heat Transfer Coefficients with Various Correlations for Test 4910, Run 13

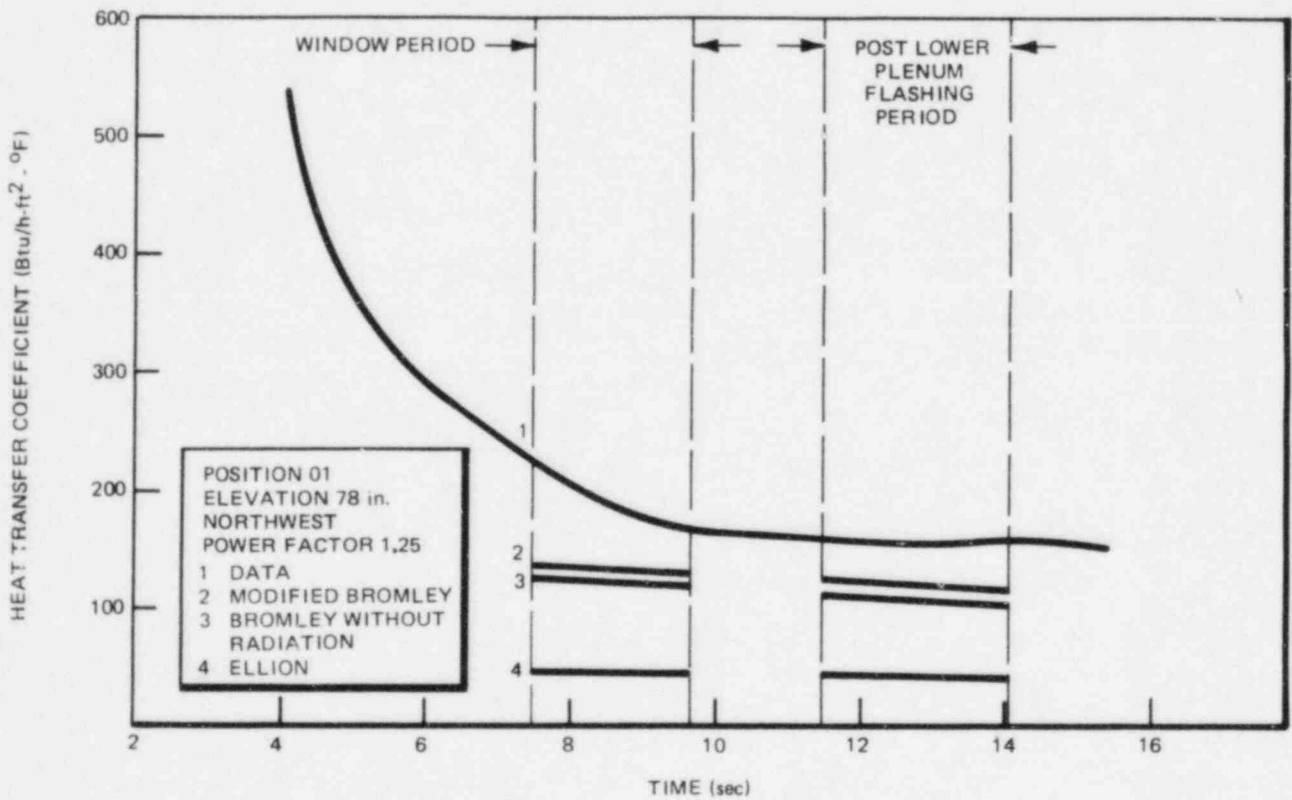


Figure 22. Comparison of Measured Heat Transfer Coefficients with Various Correlations for Test 4910, Run 13

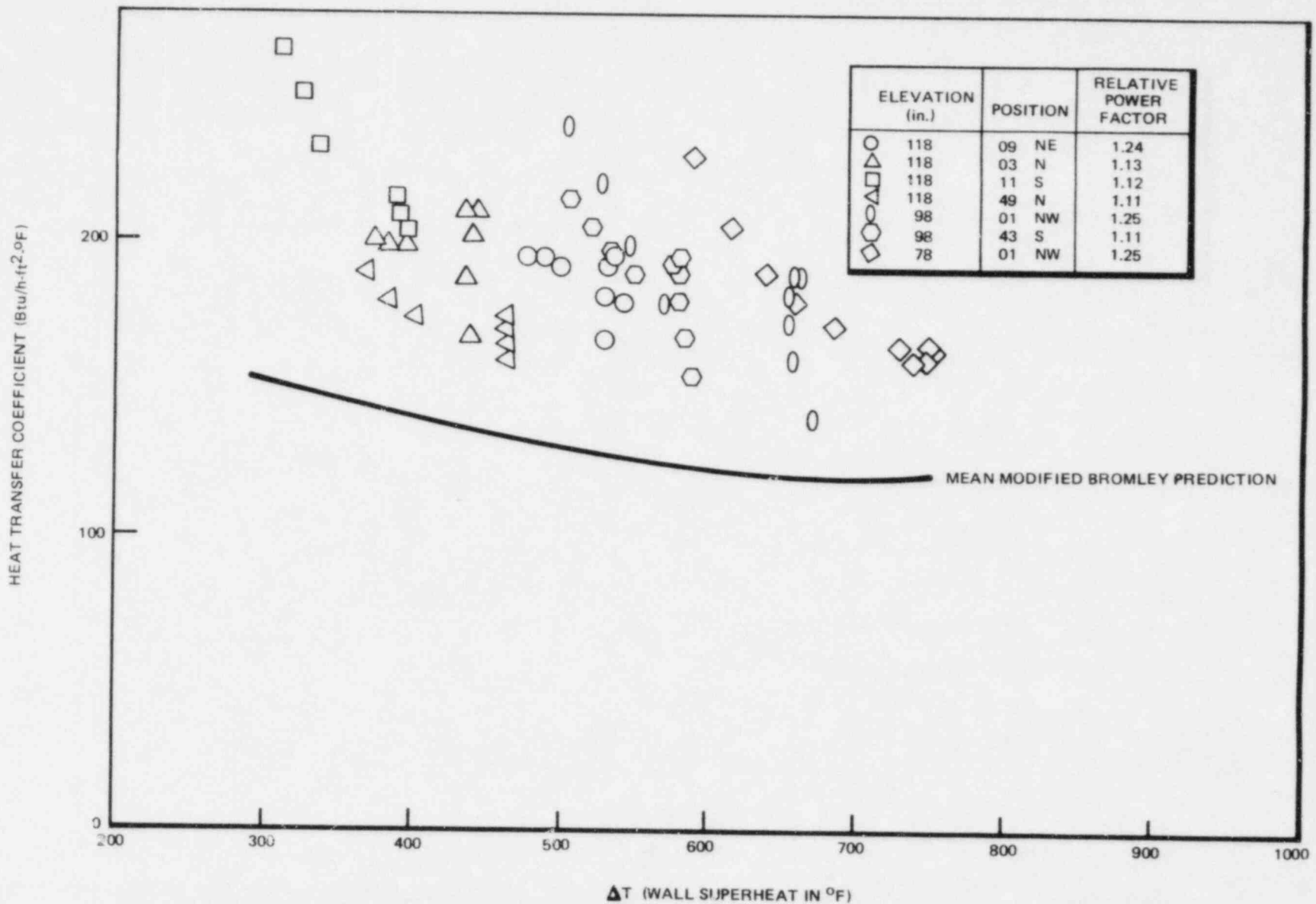


Figure 23. Comparison of Heat Transfer Coefficients versus Modified Bromley Correlation as a Function of Wall Superheat, Test 4910, Run 13

differences in the time (and, therefore, the pressure) at which different rods and elevations heated up to a given wall superheat is of the order of  $\pm 10 \text{ Btu/h-ft}^2\text{-}^\circ\text{F}$ . The data are seen to lie above the correlation over the whole range of wall superheats examined.

Of particular interest are the void fractions at the elevations under consideration. These were calculated from the mass and energy balances and the measured boundary conditions. Figure 24 shows the void fractions calculated at elevations nearest the TC measurement locations. During the low flow and PLPF period, the data lie in a high void fraction regime,  $0.80 < \alpha < 0.90$ . At low flow rates, a liquid-continuous region can exist at fairly high void fractions, and transition to the dispersed-droplet region does not occur until the void fractions are close to unity.

b) TEST 4907

Data representative of pool film boiling were obtained from three elevations, 118, 98, and 78 inches. Figure 25 shows the core inlet flow history for this test; Figure 26 shows the calculated and measured two-phase levels. At the

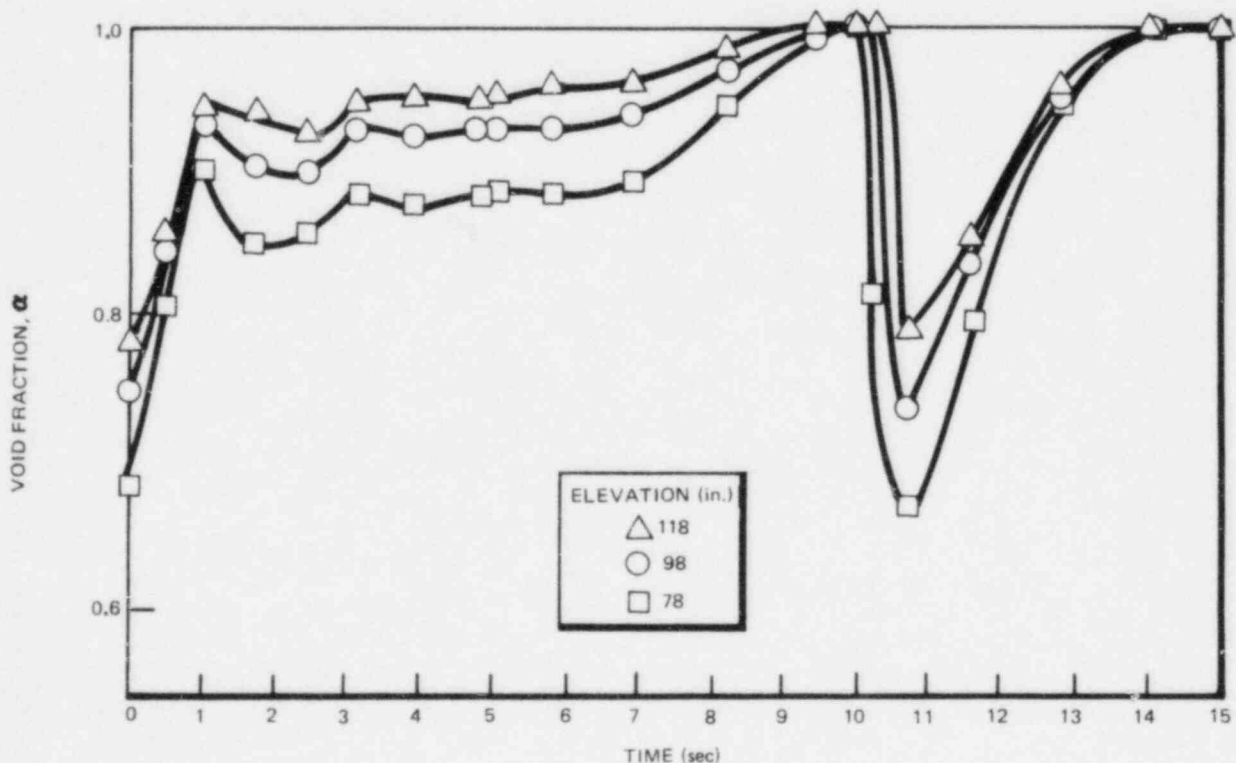


Figure 24. Calculated Void Fractions at Three Elevations, Test 4910, Run 13

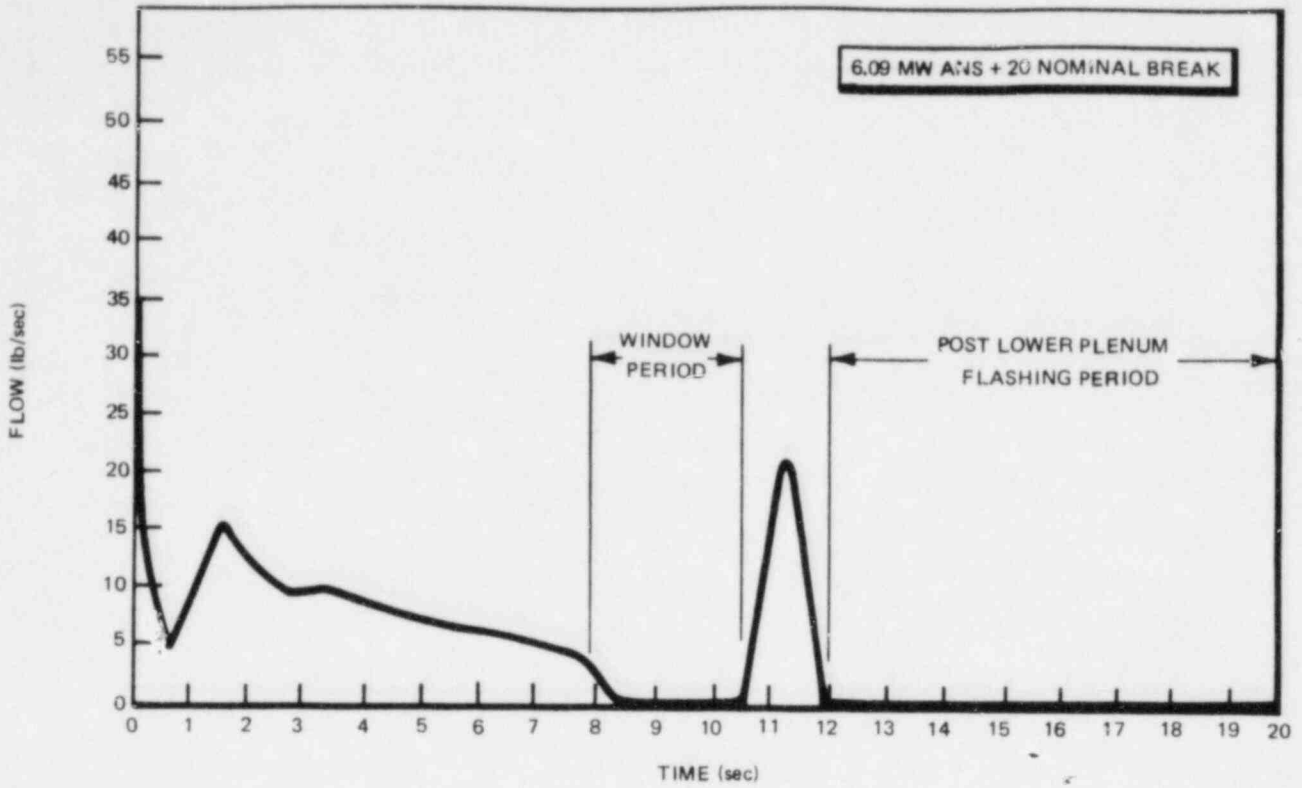


Figure 25. Inlet Flow Variation for Test 4907, Run 10

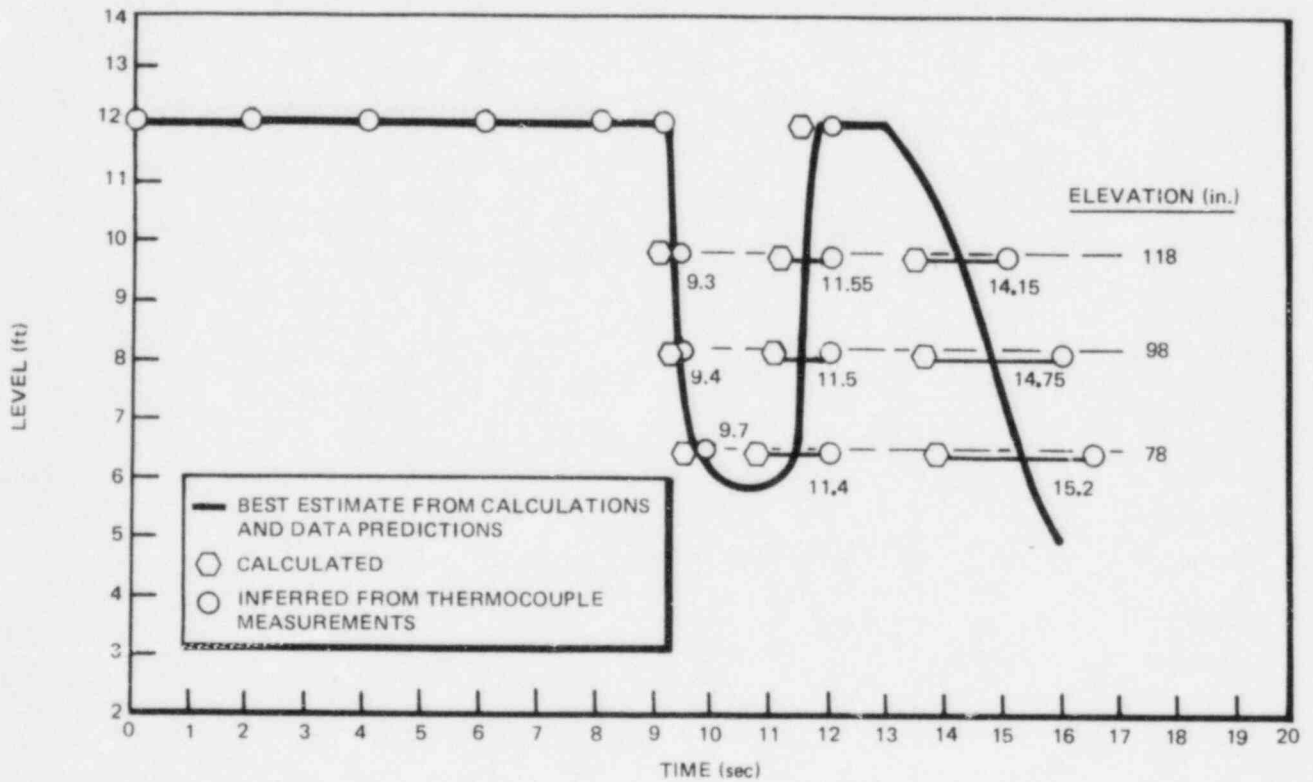


Figure 26. Two-Phase Level Measurements and Predictions in Bundle, Test 4907, Run 10

two lower elevations there were clear indications of simultaneous rewet at several rod positions following lower plenum flashing, from which it was inferred that the two-phase level had risen to these elevations. At the 118-in. elevation, some rods did rewet between 12 and 15 seconds, but there is greater uncertainty about the inferred time at which the level reached this elevation. Figures 27 through 34 show comparisons between the heat transfer coefficients derived from thermocouple data and the modified Bromley correlation. In the appropriate time periods, the correlation is seen to be a lower bound to the data except for two rods, positions 29 and 45, for brief intervals at the start of the PLPF period, with the lowest data point being 10% below the correlation. As stated earlier, there was uncertainty regarding the position of the two-phase level at that time and the data may be representative of a period of transition between the dispersed-flow and liquid-continuous regimes. The predictions with the modified Bromley correlation have been shown for the entire period for the 118-in. elevation. It should be noted that even when the two-phase level is expected to be below 118 inches, the drop in heat transfer is not very significant. The steam velocities in dispersed film flow are sufficiently large to provide substantial heat transfer.

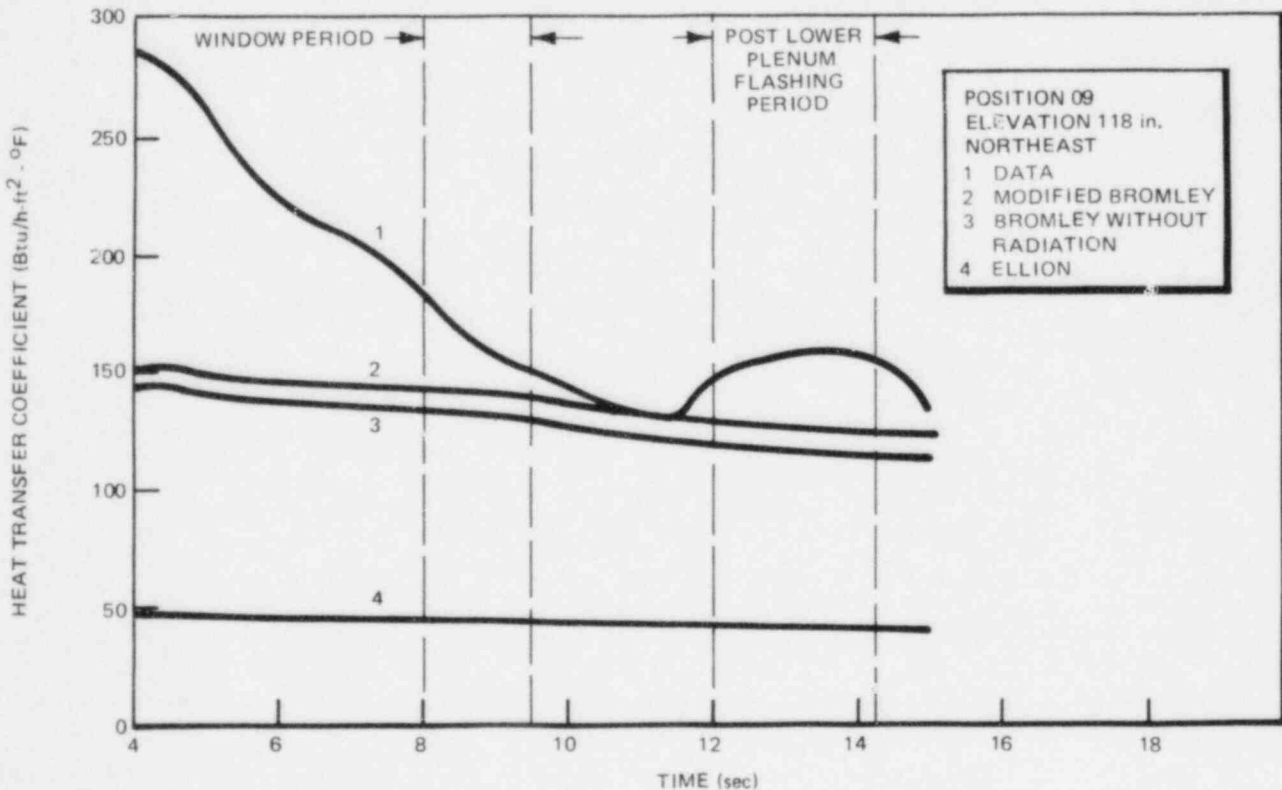


Figure 27. Comparison of Measured Heat Transfer Coefficients with Various Correlations for Test 4907, Run 10

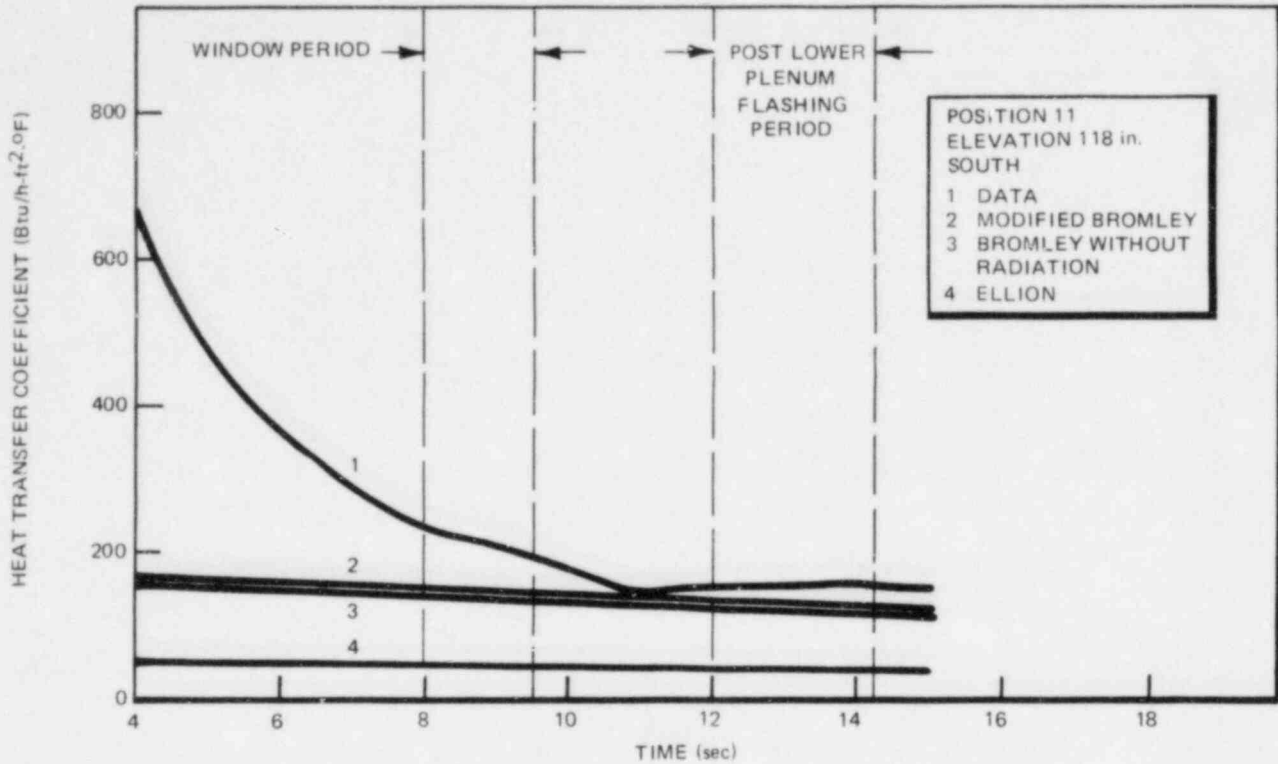


Figure 28. Comparison of Measured Heat Transfer Coefficients with Various Correlations for Test 4907, Run 10

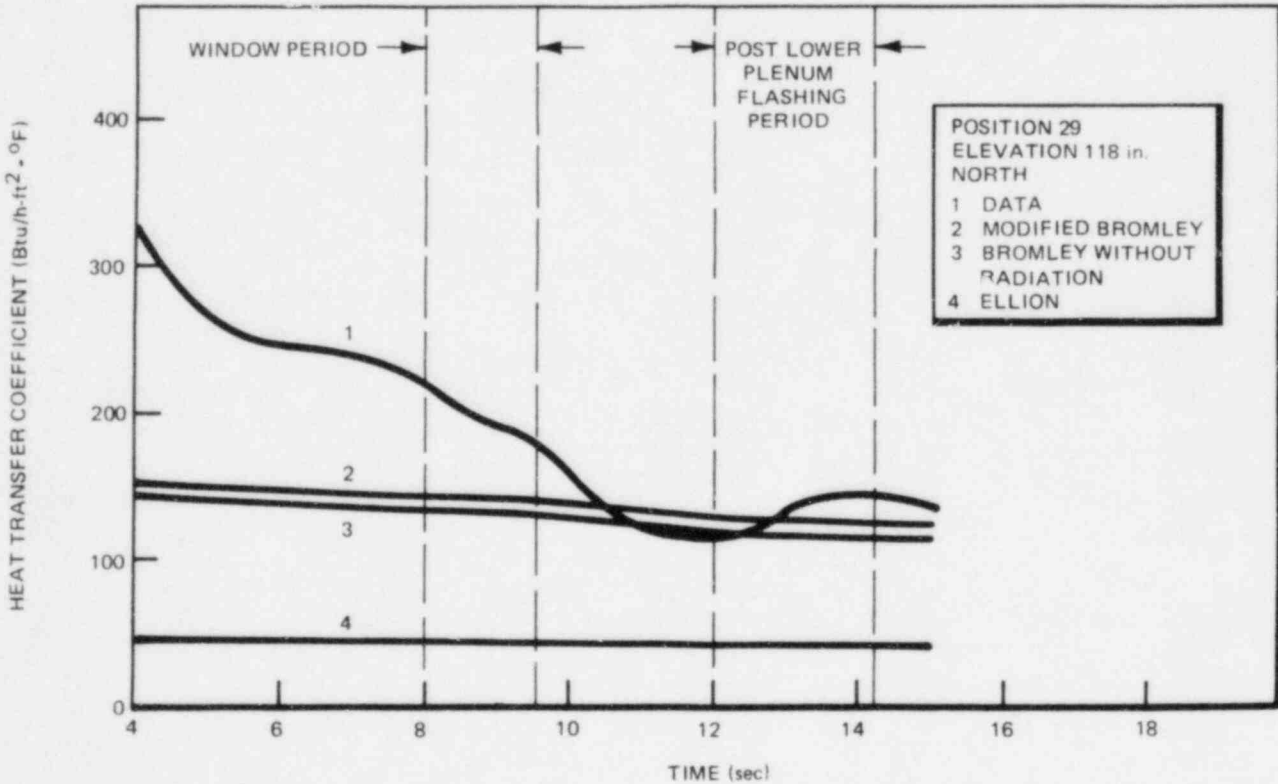


Figure 29. Comparison of Measured Heat Transfer Coefficients with Various Correlations for Test 4907, Run 10



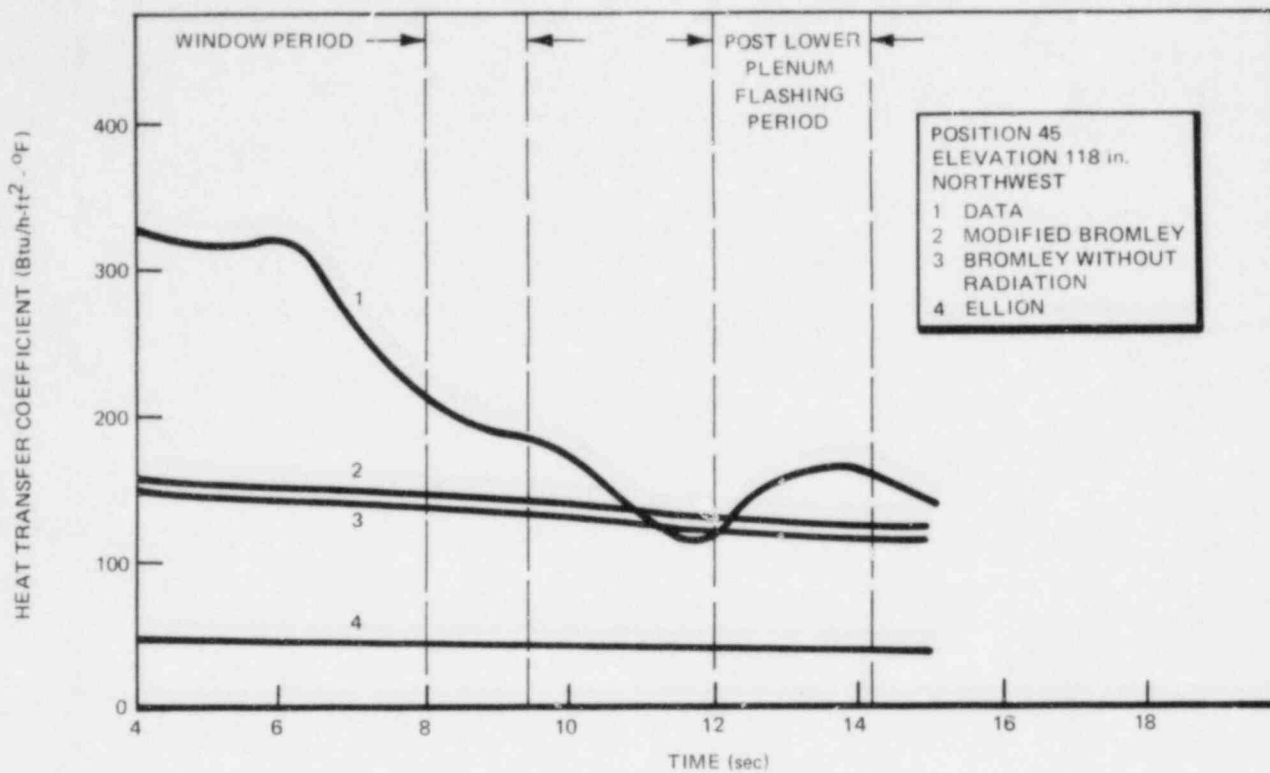


Figure 30. Comparison of Measured Heat Transfer Coefficients with Various Correlations for Test 4907, Run 10

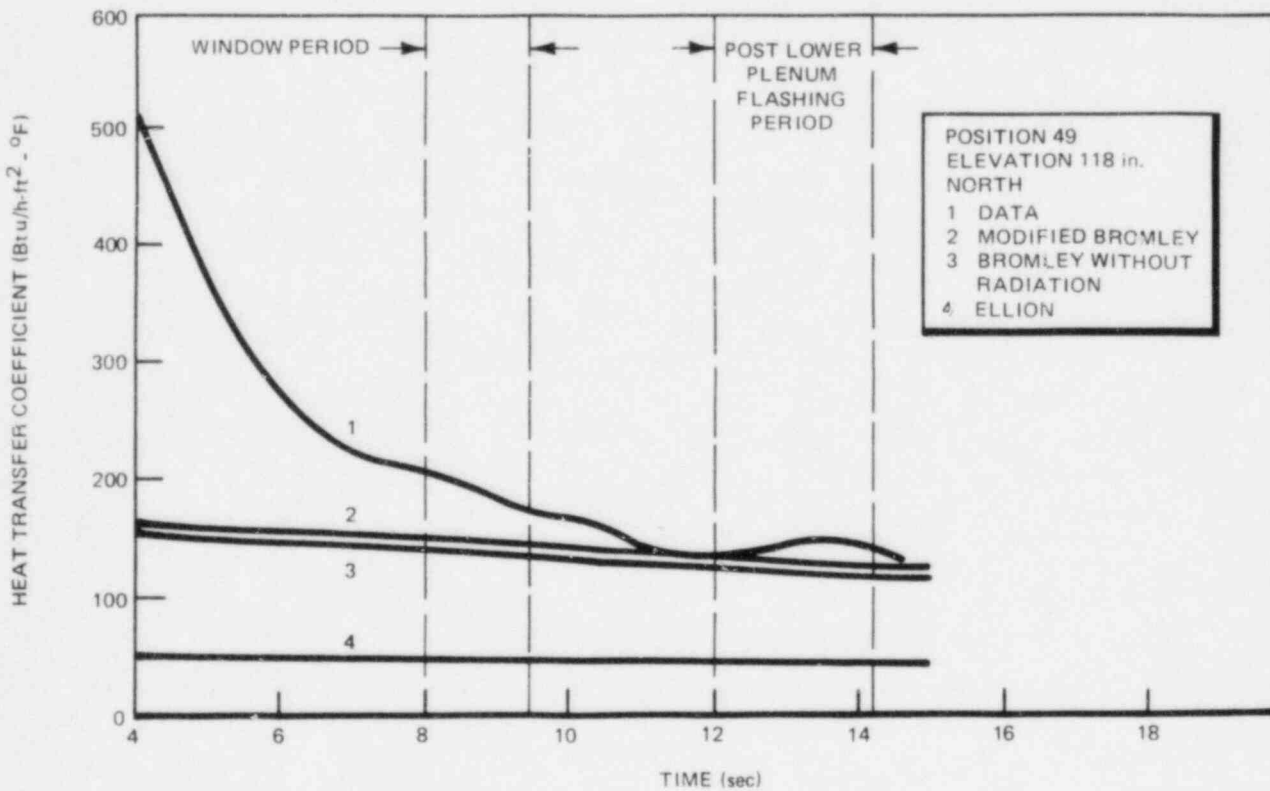


Figure 31. Comparison of Measured Heat Transfer Coefficients with Various Correlations for Test 4907, Run 10

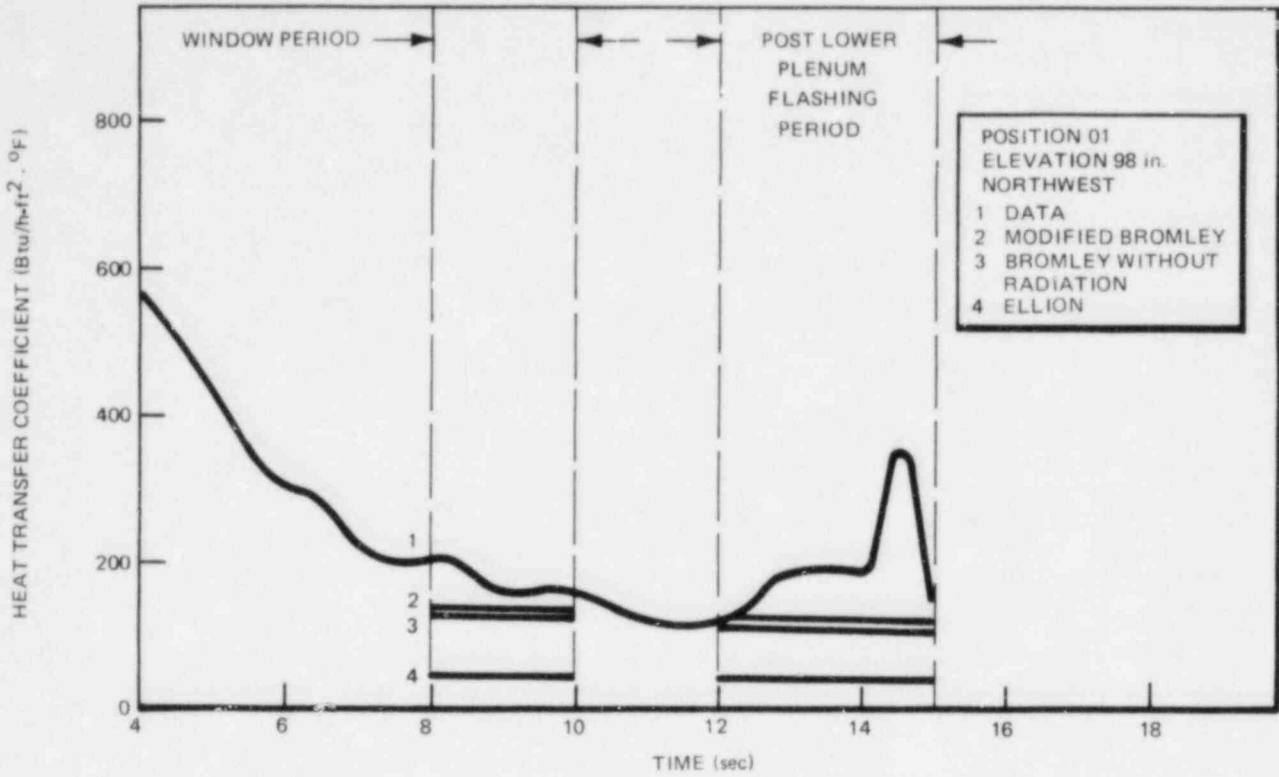


Figure 32. Comparison of Measured Heat Transfer Coefficients with Various Correlations for Test 4907, Run 10

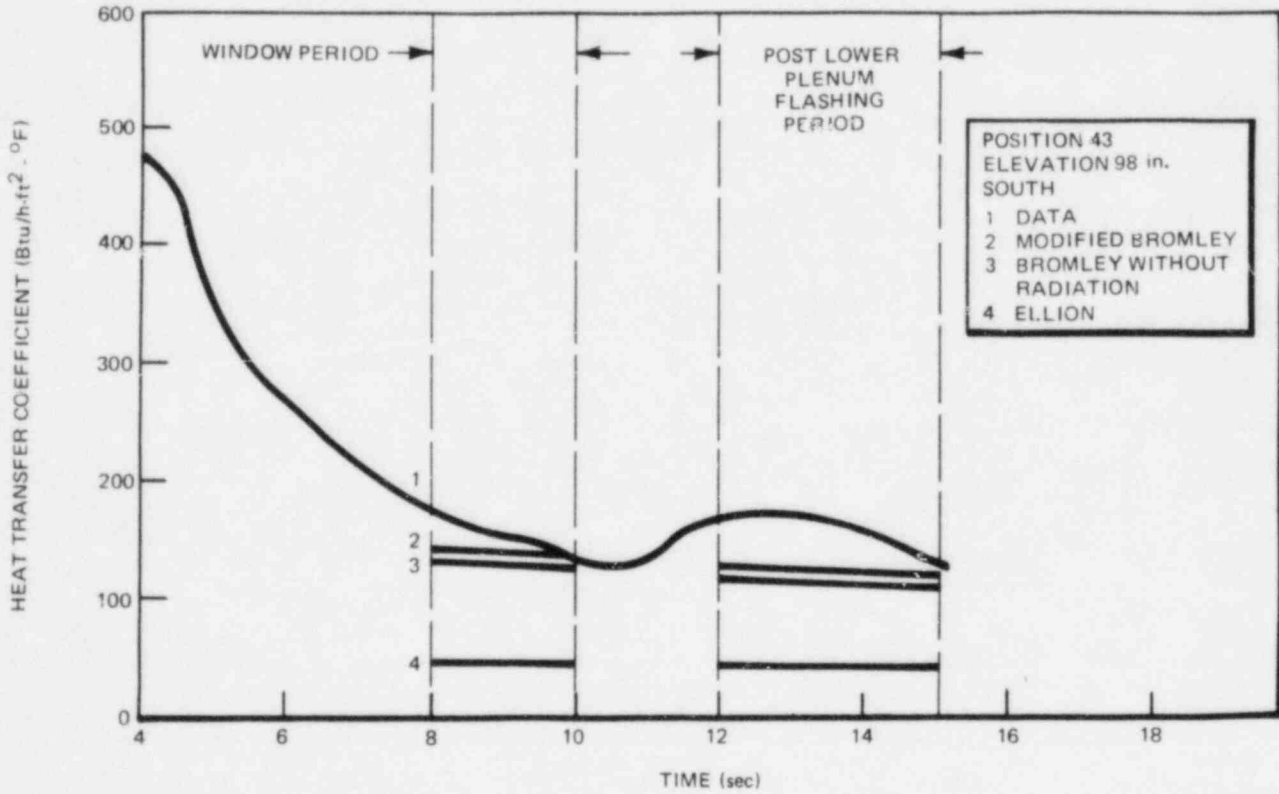


Figure 33. Comparison of Measured Heat Transfer Coefficients with Various Correlations for Test 4907, Run 10

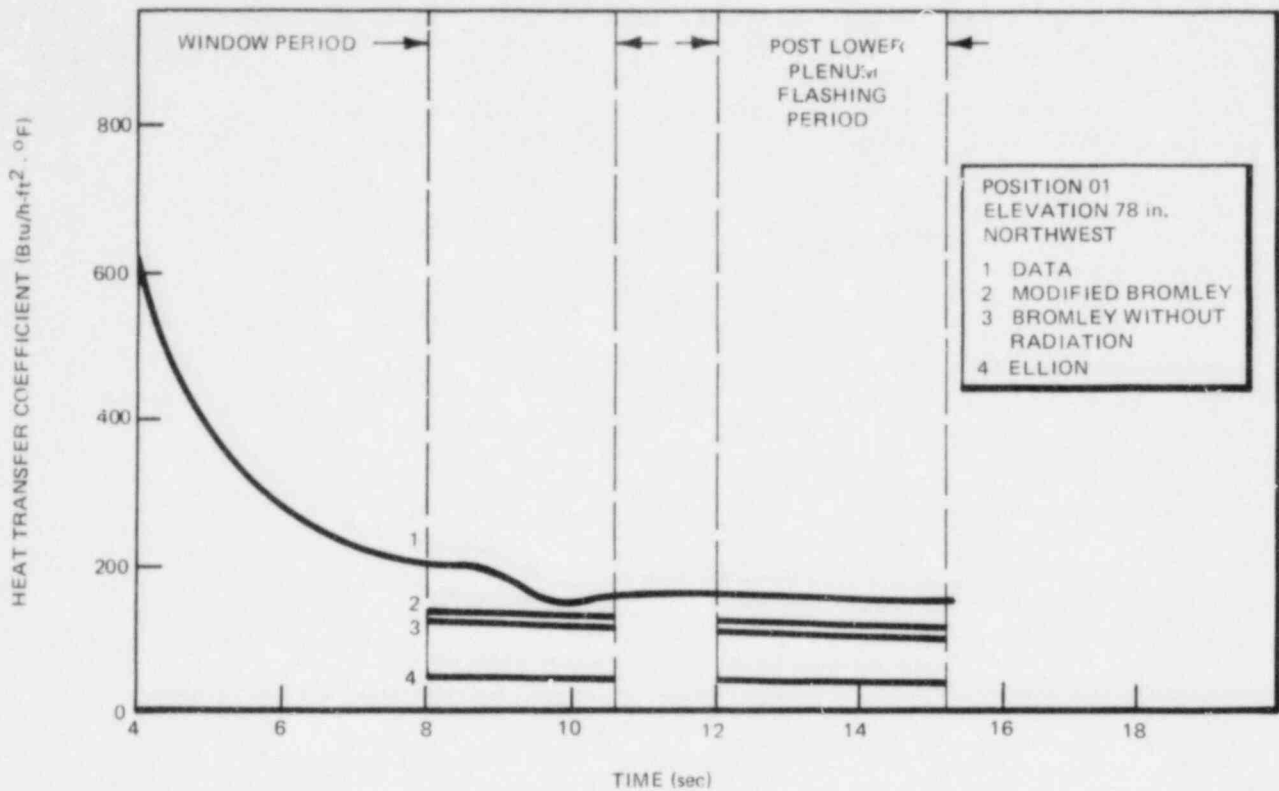


Figure 34. Comparison of Measured Heat Transfer Coefficients with Various Correlations for Test 4907, Run 10

Figure 35 summarizes all the heat transfer coefficient data for Test 4907, showing that the great majority of the data lie above the modified Bromley correlation through the entire range of wall superheats from 390 to 750°F.

Figure 36 shows the calculated void fractions at the three elevations. These are seen to be above 80% throughout the low flow period where the heat transfer coefficients are higher than predicted by the modified Bromley correlation.

#### c) TEST 4914

The inlet flow and the two-phase level variation for this test are shown in Figures 37 and 38. Heat transfer coefficients calculated from thermocouple data for this test are shown in Figures 39 through 50. The data were obtained and the representative time periods chosen in the same manner as for the other tests. The results for the test are summarized in Figure 51. It can be seen that, except for a very small number of points, the data lie well above the modified

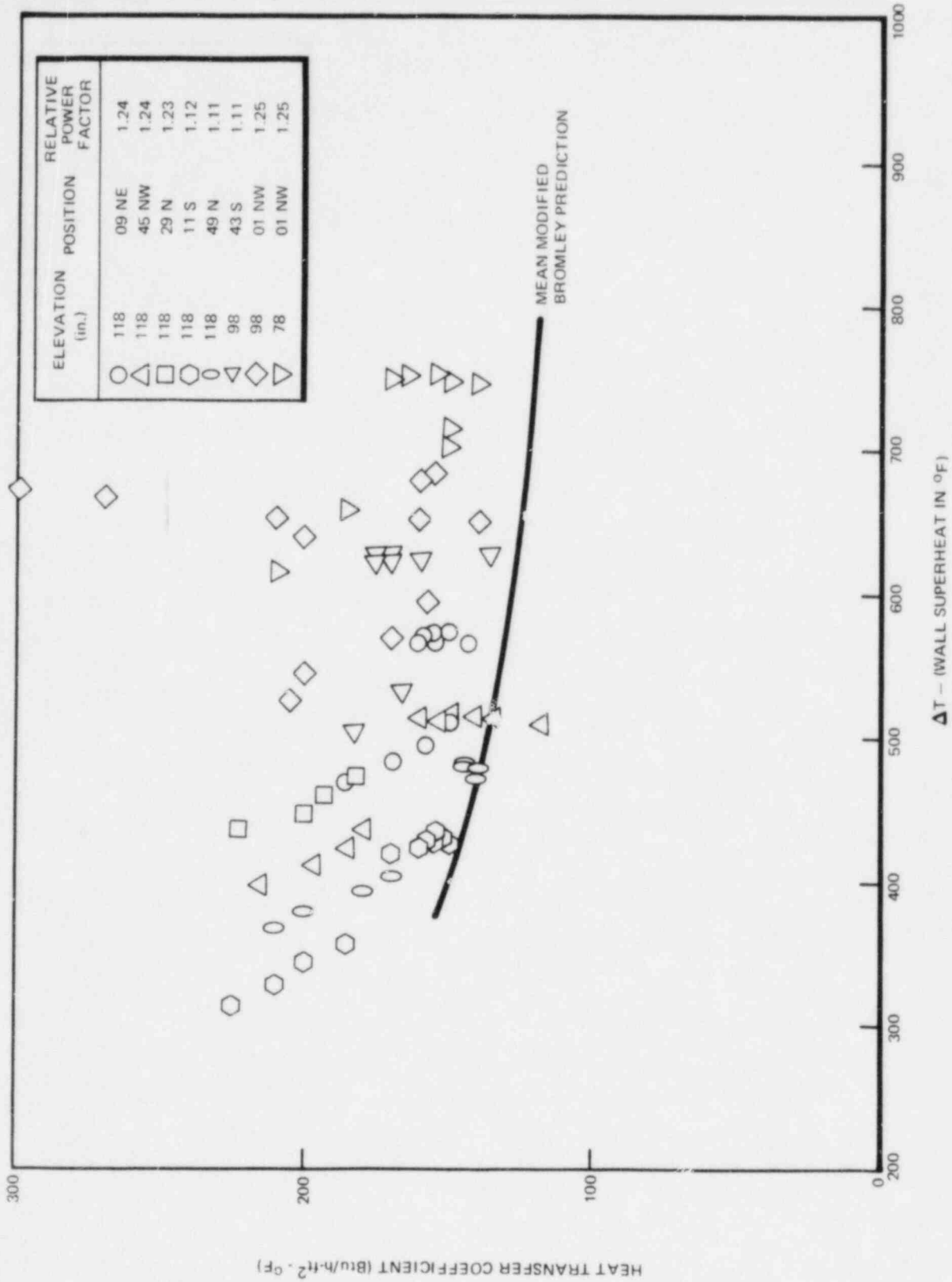


Figure 35. Comparison of Heat Transfer Coefficients versus Modified Bromley Correlation as a Function of Wall Superheat, Test 4907, Run 10

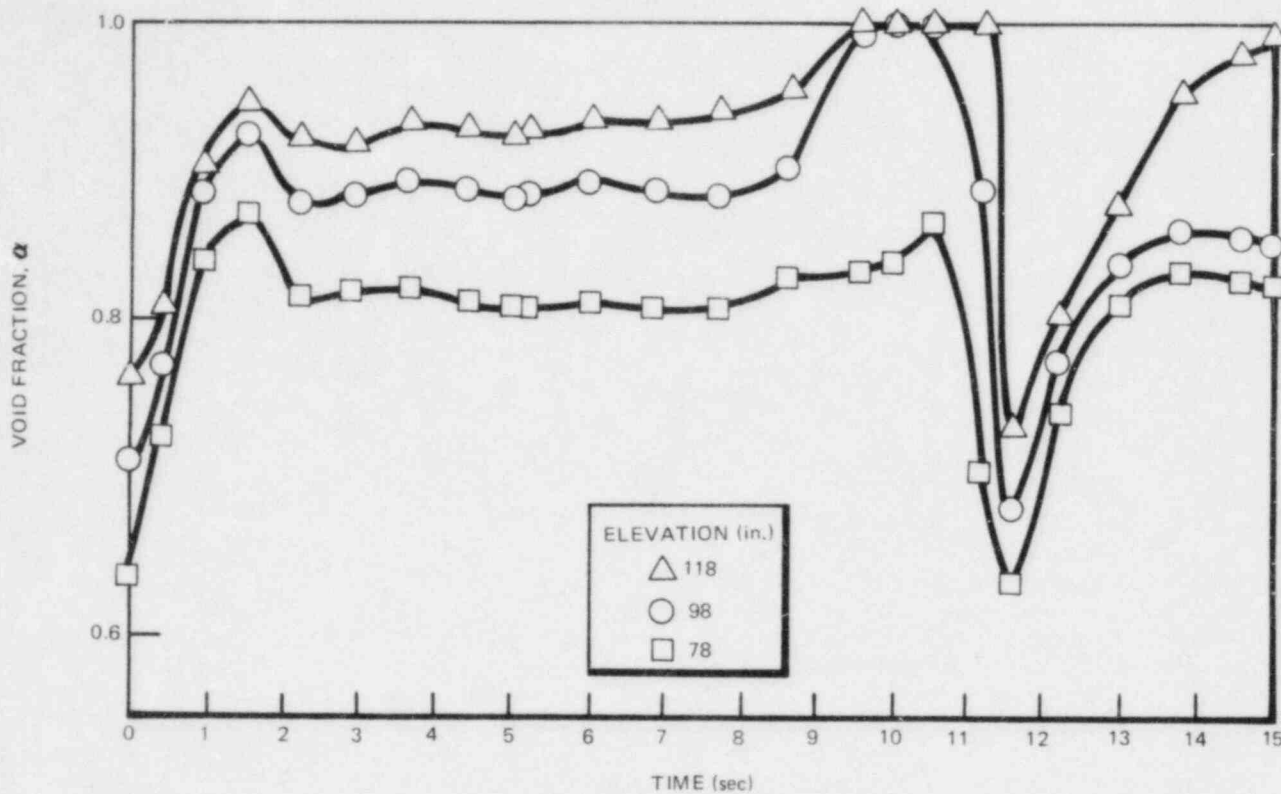


Figure 36. Calculated Void Fractions at Three Elevations, Test 4907, Run 10

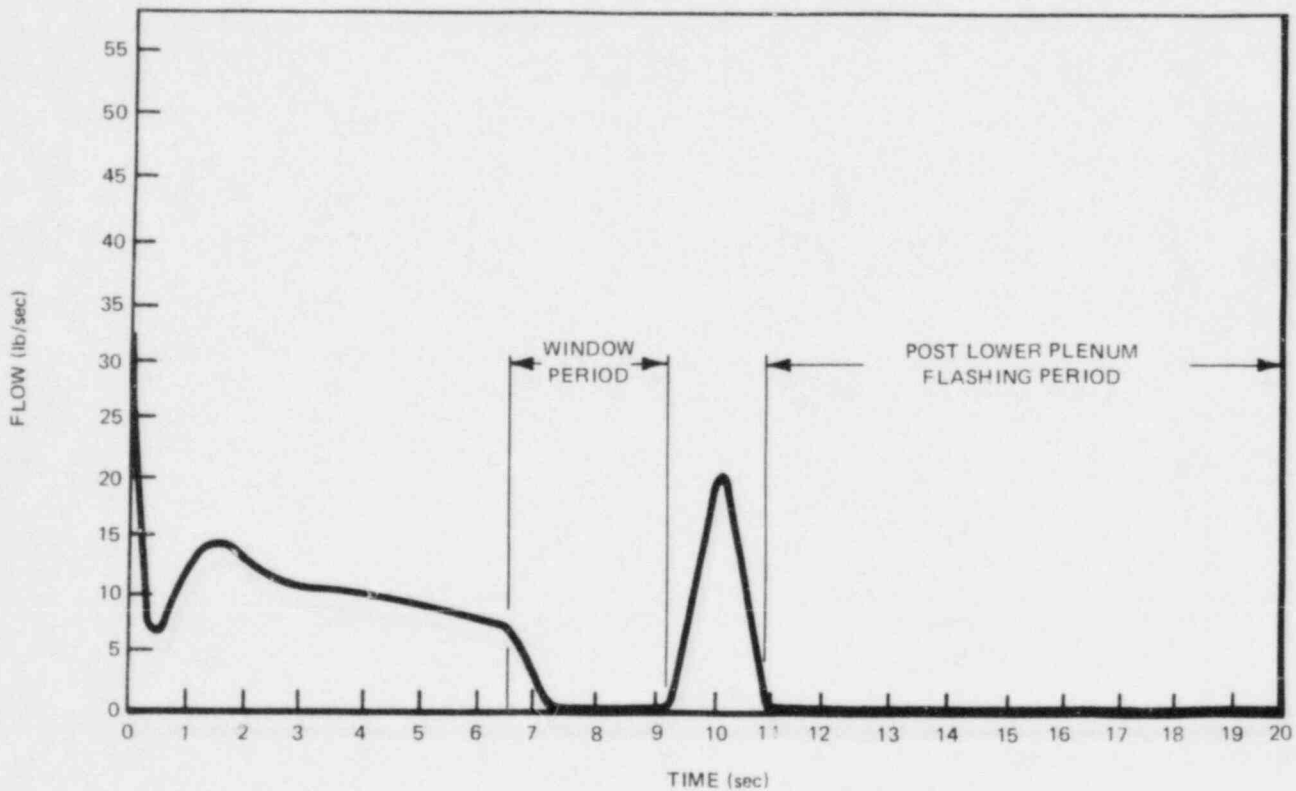


Figure 37. Inlet Flow Variation for Test 4914, Run 8

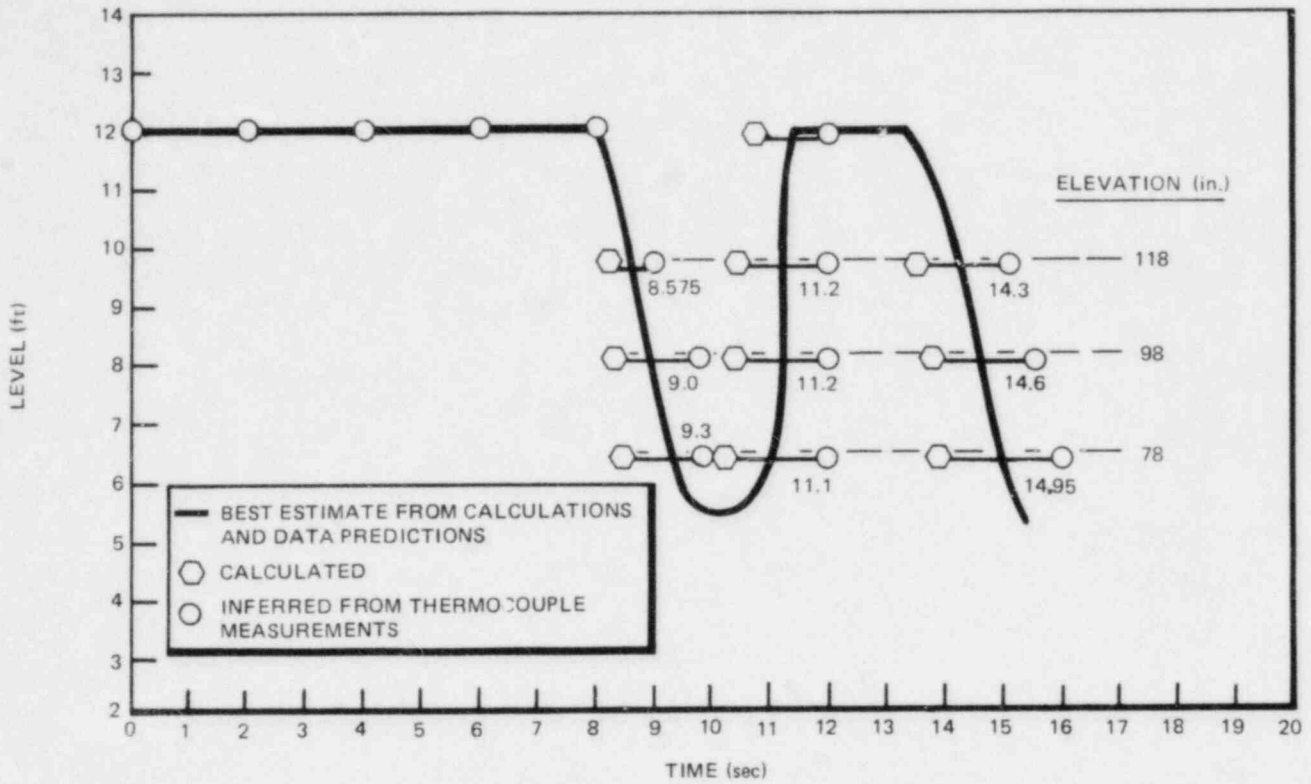


Figure 38. Level Measurements and Predictions in Bundle, Test 4914, Run 8

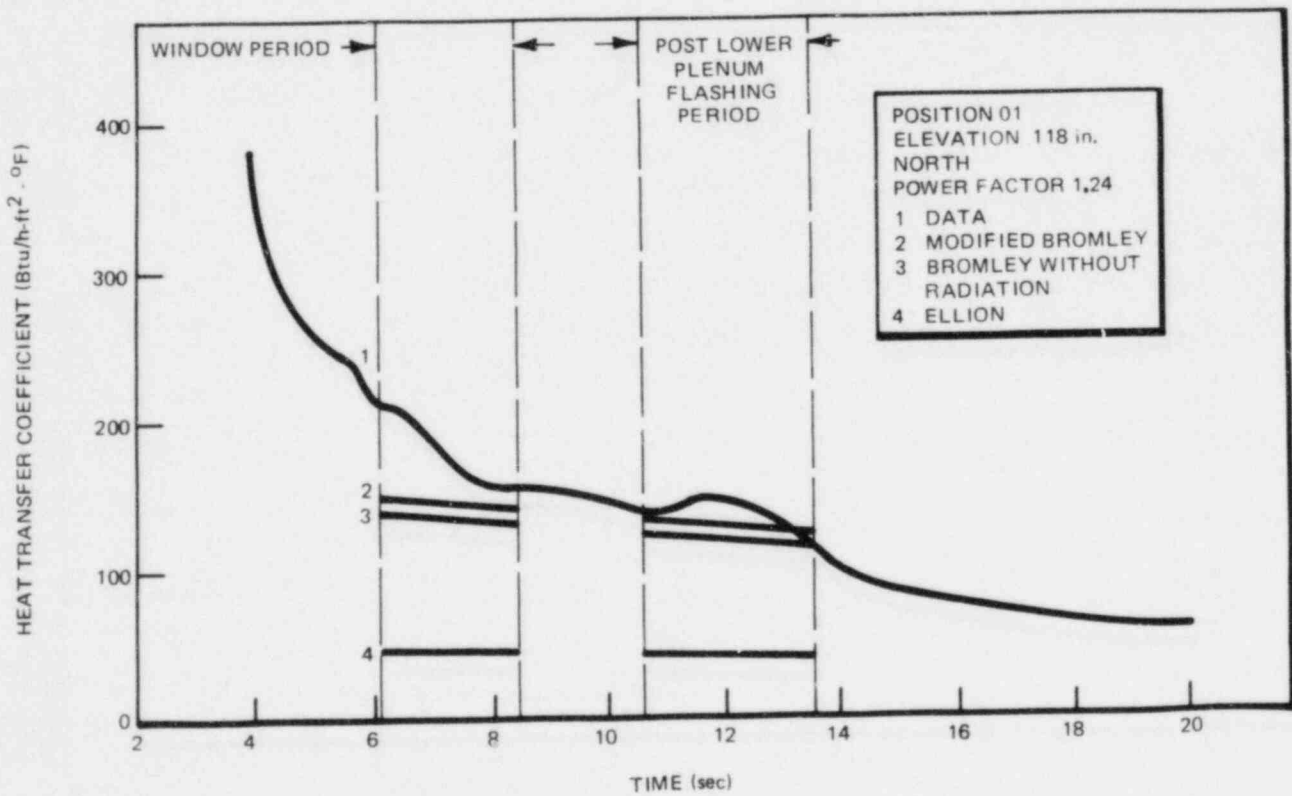


Figure 39. Comparison of Measured Heat Transfer Coefficients with Various Correlations for Test 4914, Run 8

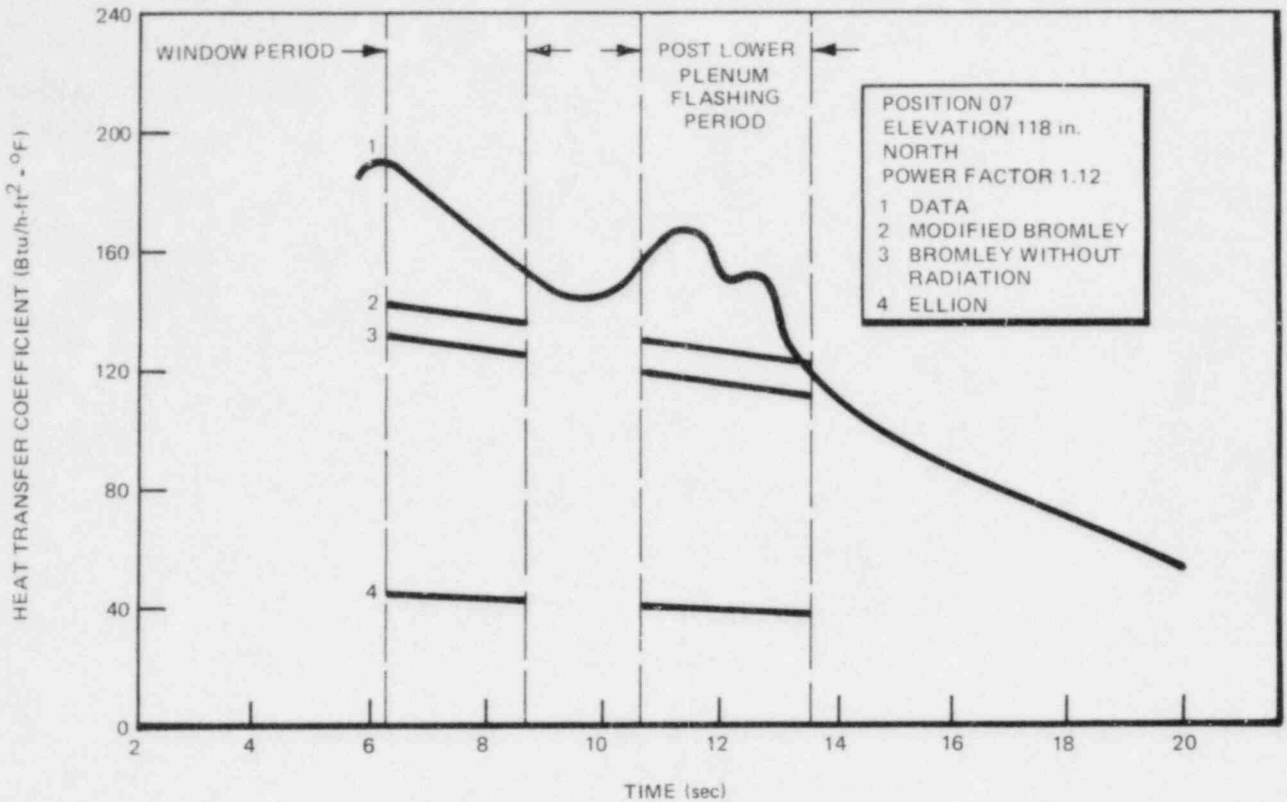


Figure 40. Comparison of Measured Heat Transfer Coefficients with Various Correlations for Test 4914, Run 8

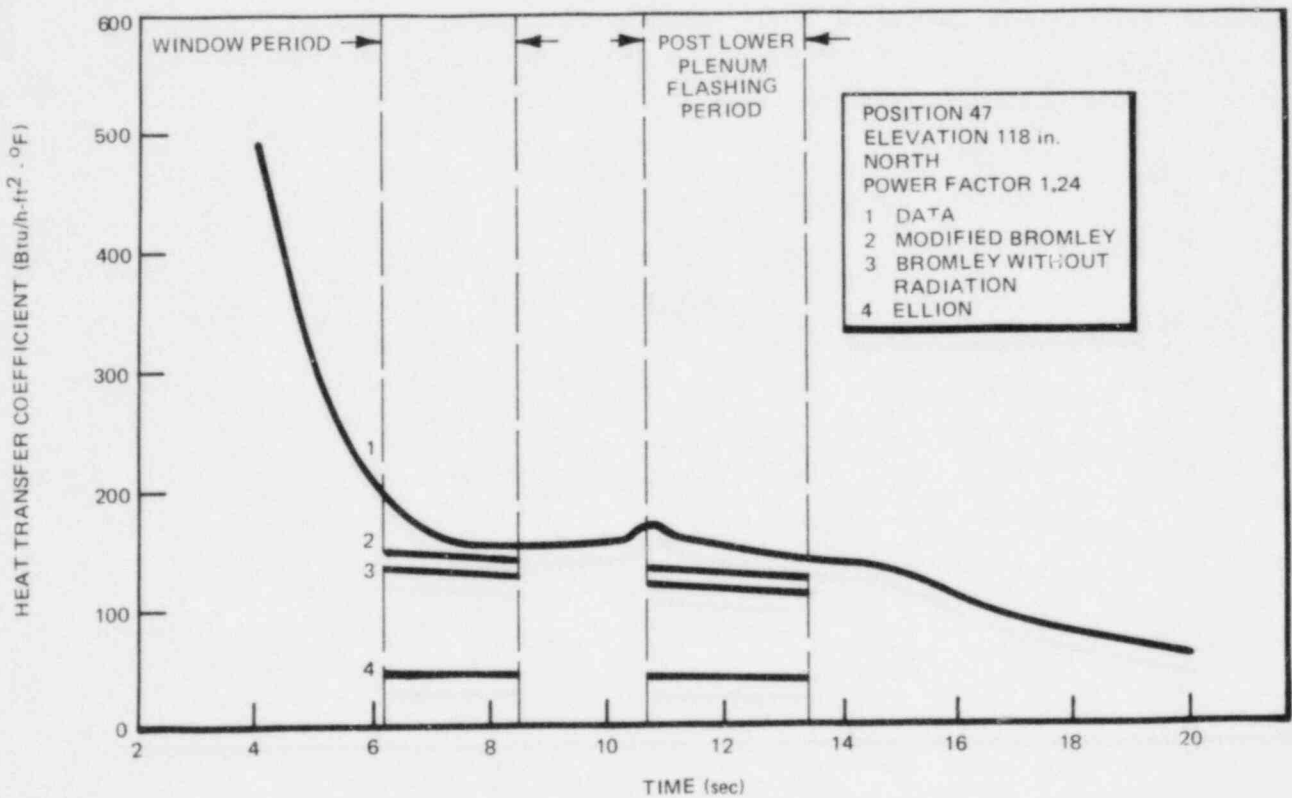


Figure 41. Comparison of Measured Heat Transfer Coefficients with Various Correlations for Test 4914, Run 8

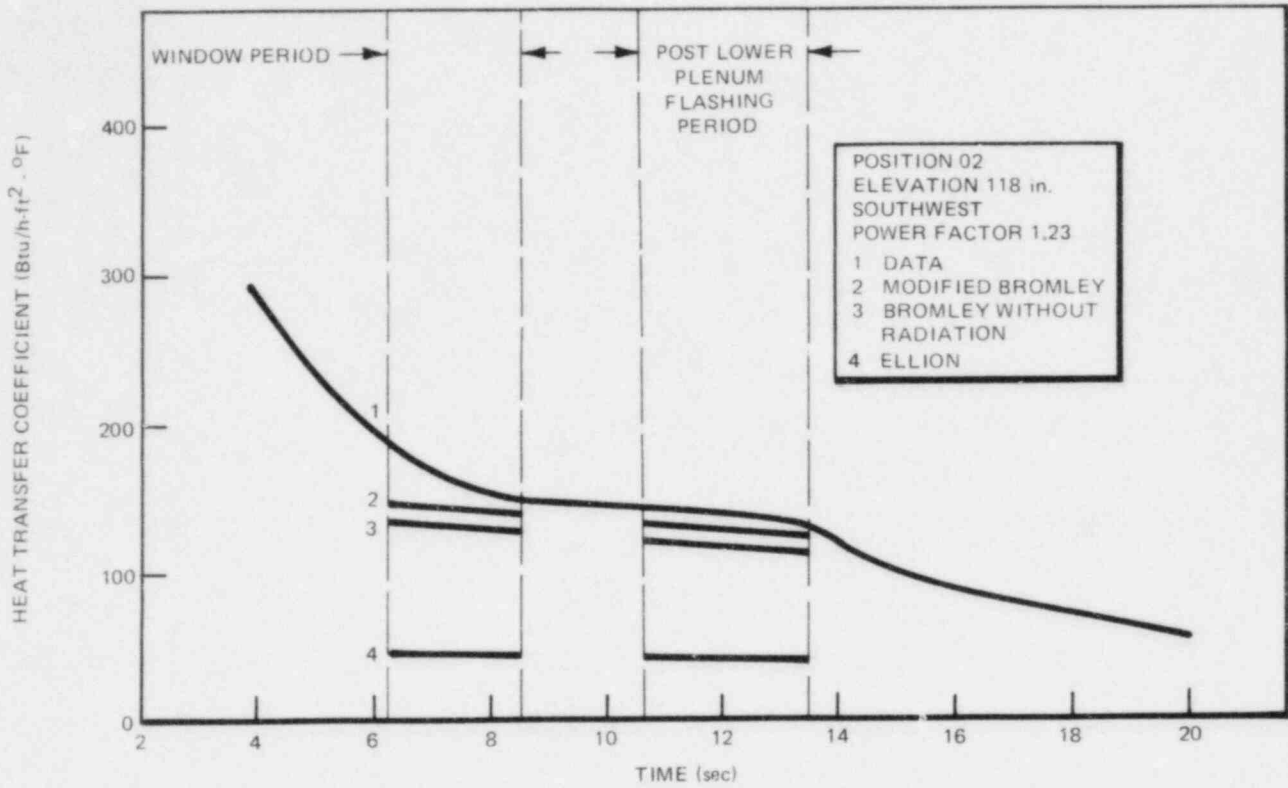


Figure 42. Comparison of Measured Heat Transfer Coefficients with Various Correlations for Test 4914, Run 8

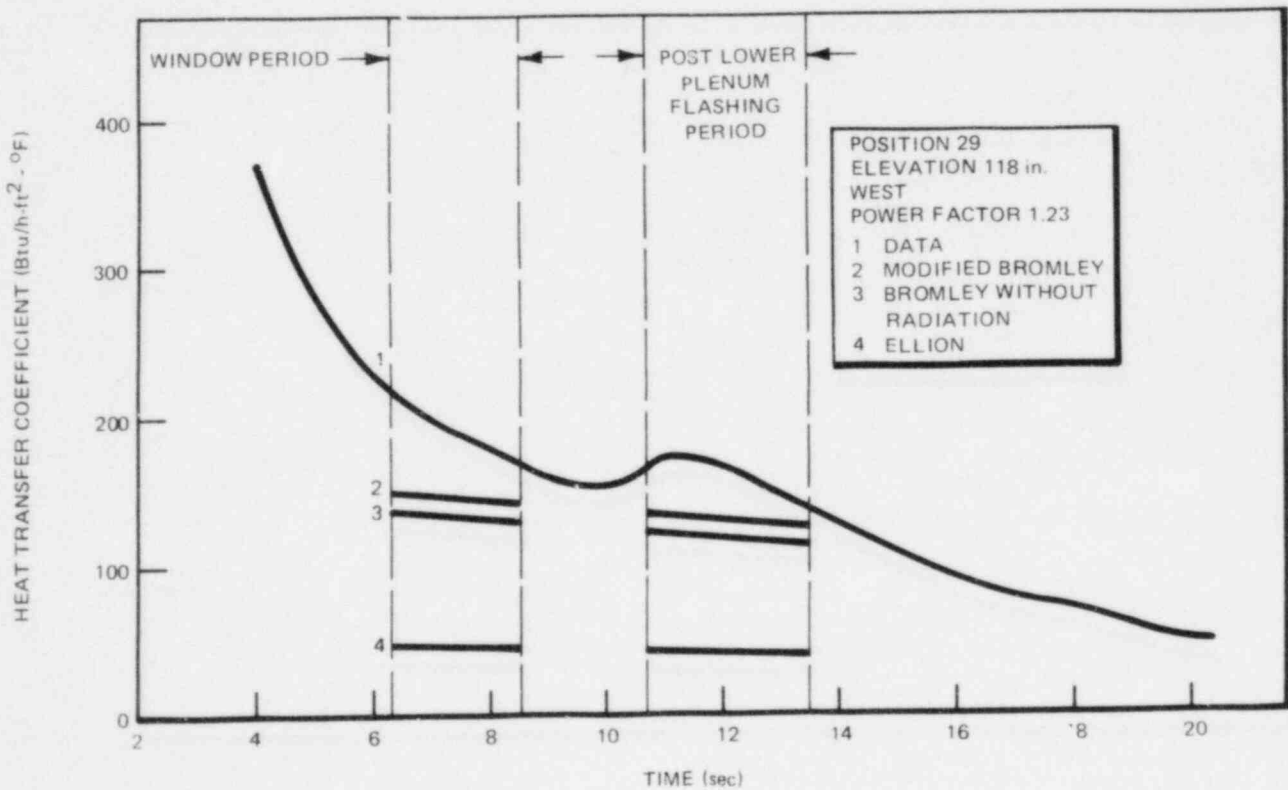


Figure 43. Comparison of Measured Heat Transfer Coefficients with Various Correlations for Test 4914, Run 8



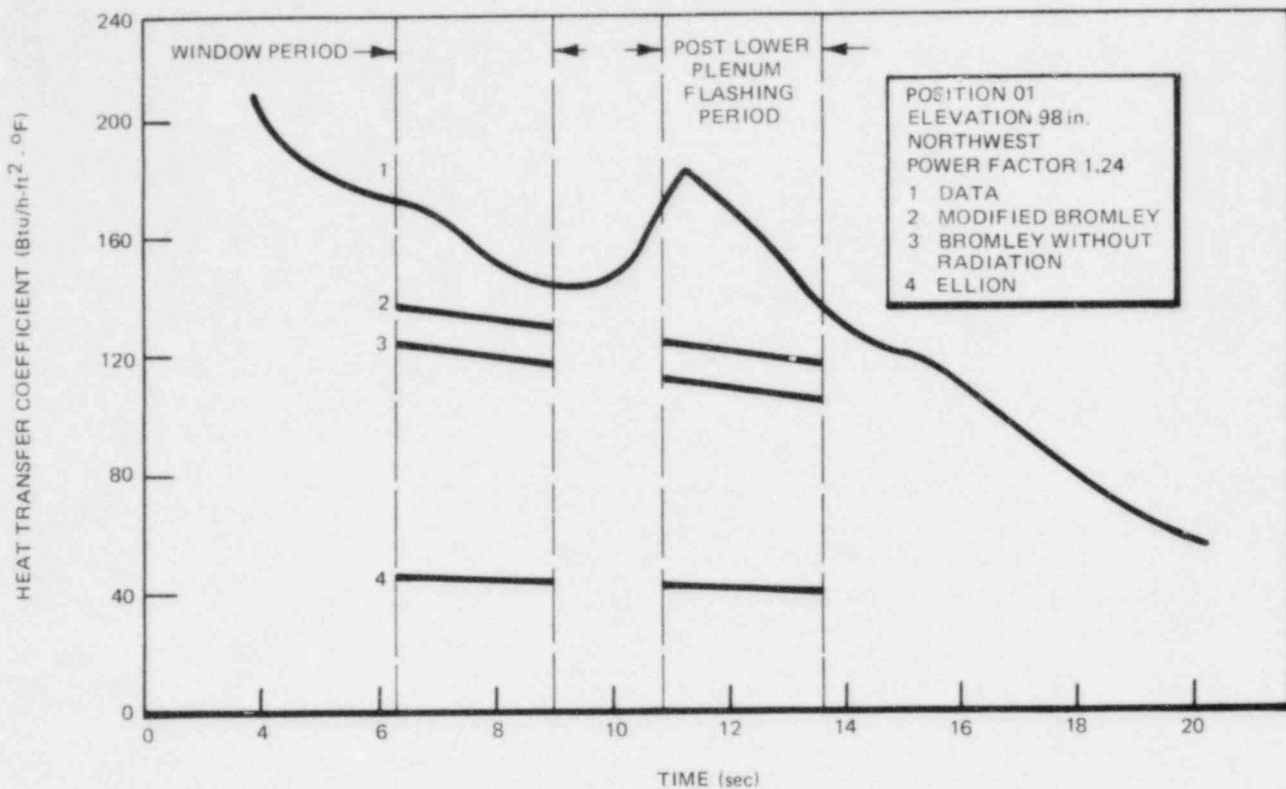


Figure 44. Comparison of Measured Heat Transfer Coefficients with Various Correlations for Test 4914, Run 8

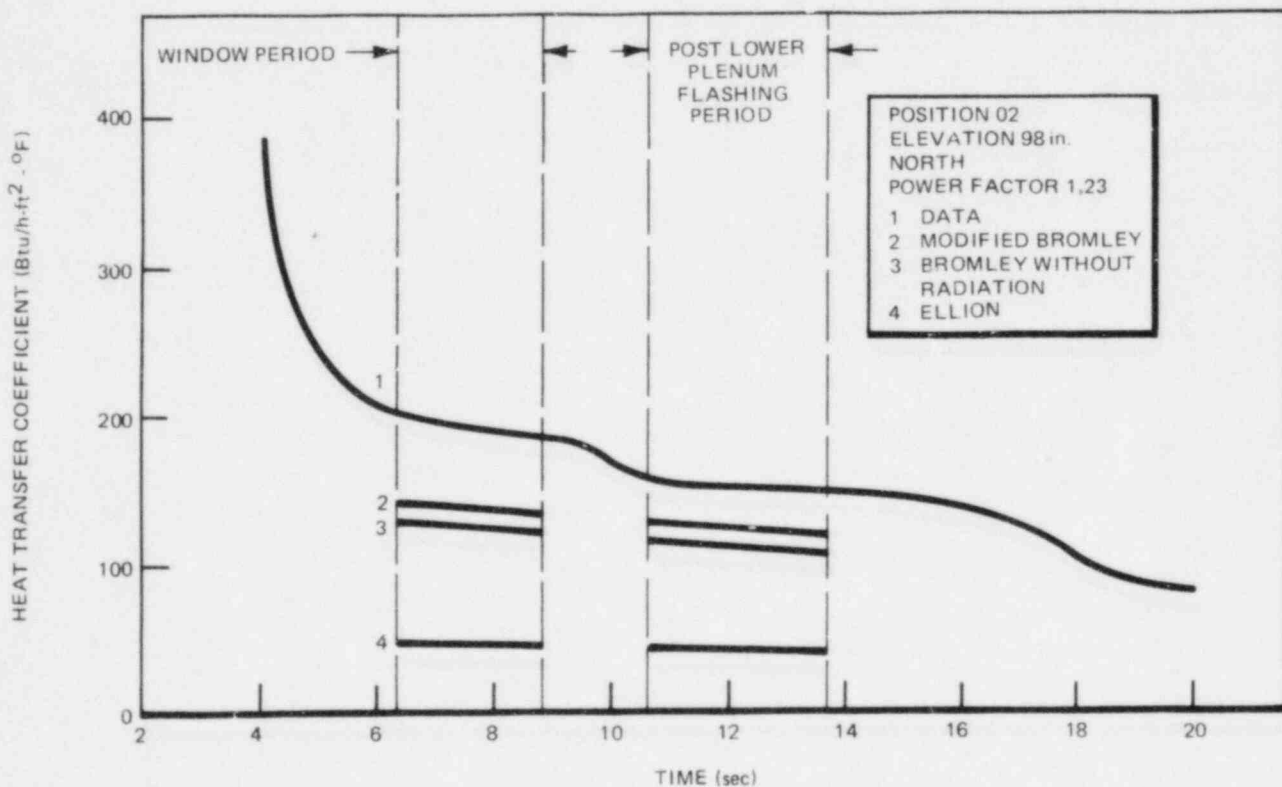


Figure 45. Comparison of Measured Heat Transfer Coefficients with Various Correlations for Test 4914, Run 8

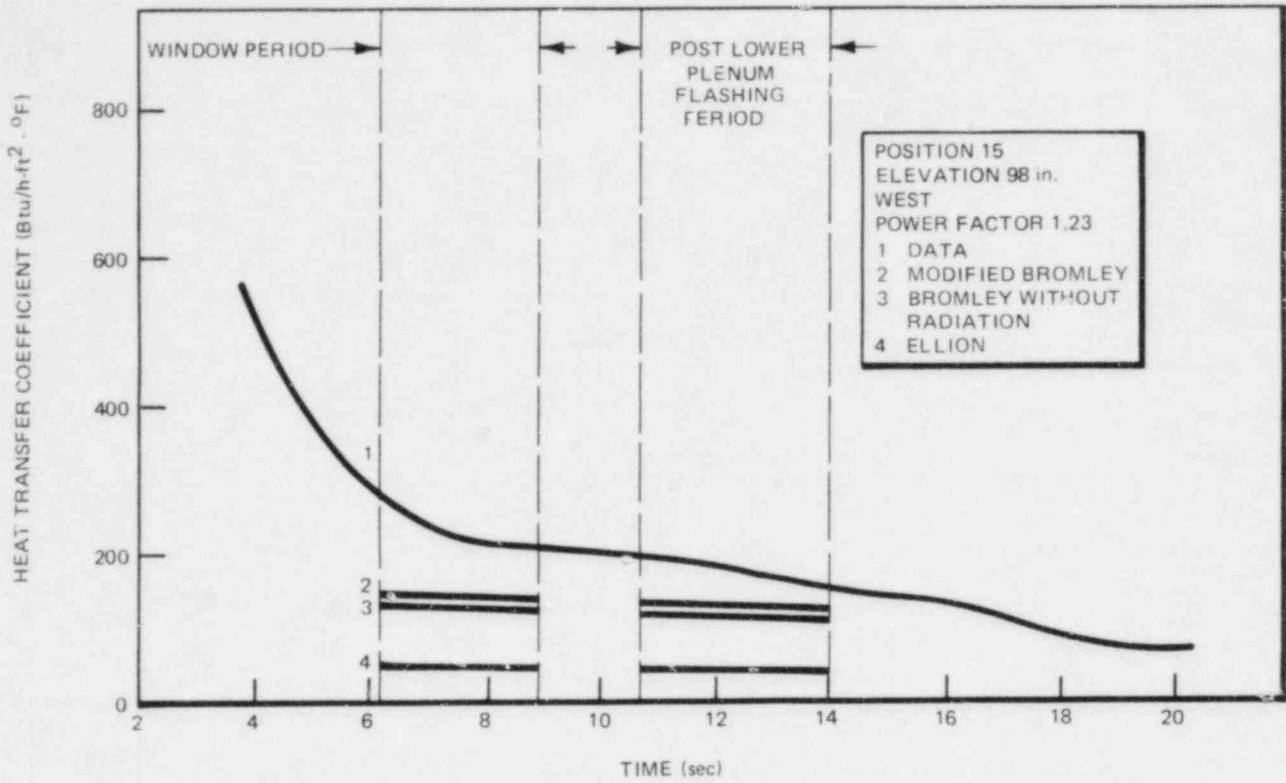


Figure 46. Comparison of Measured Heat Transfer Coefficients with Various Correlations for Test 4914, Run 8

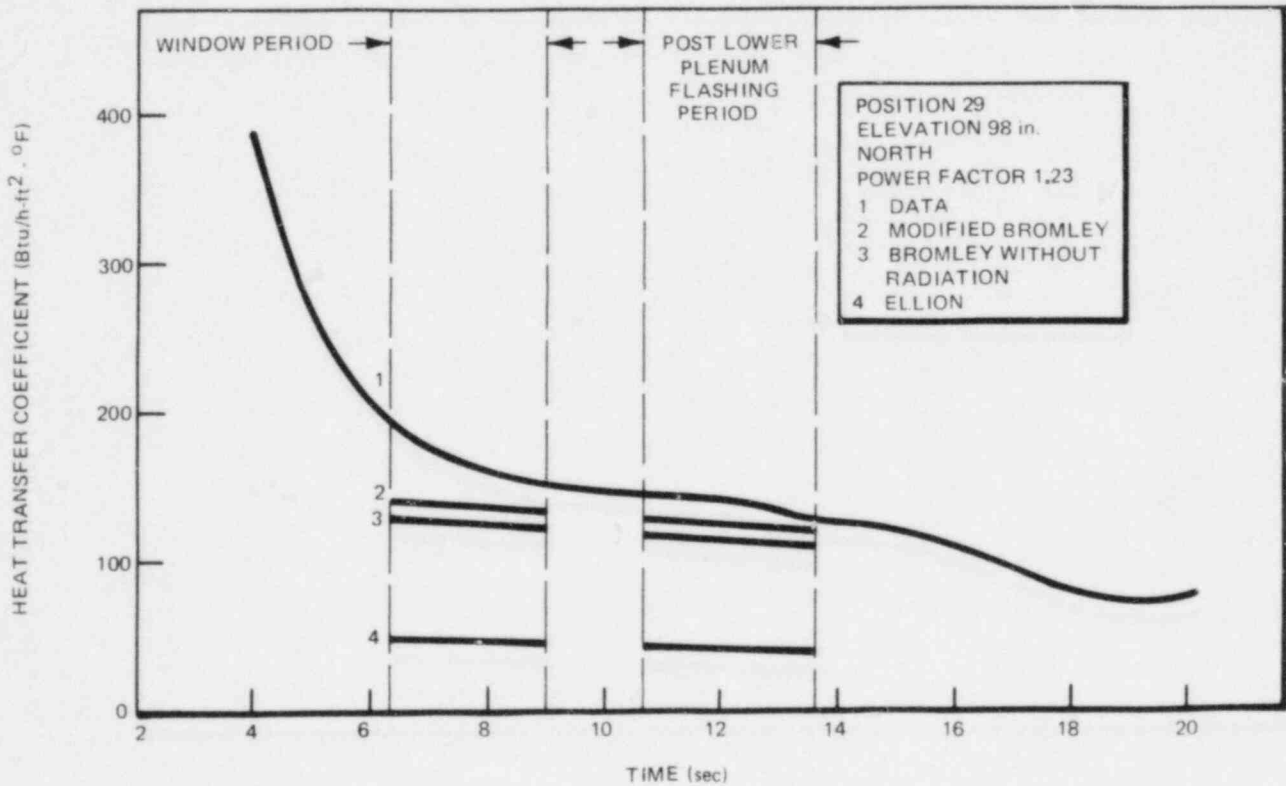


Figure 47. Comparison of Measured Heat Transfer Coefficients with Various Correlations for Test 4914, Run 8

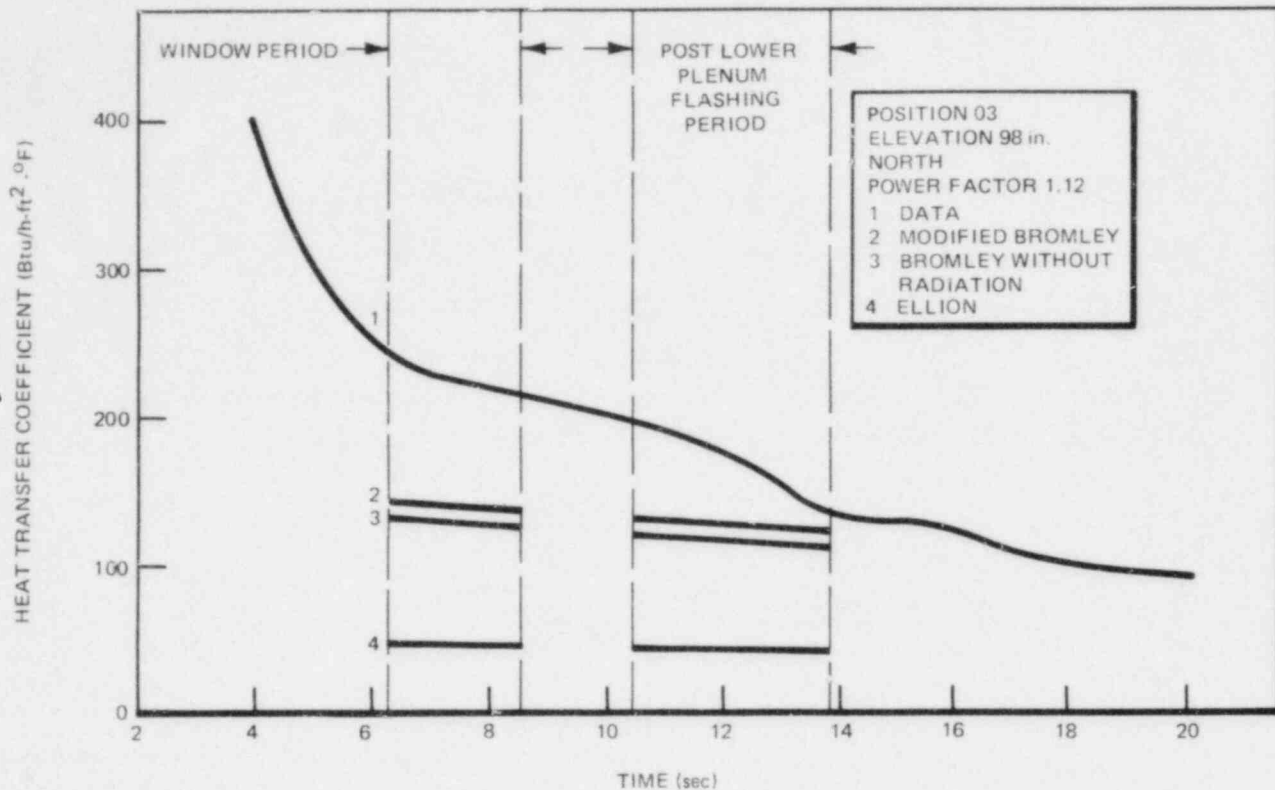


Figure 48. Comparison of Measured Heat Transfer Coefficients with Various Correlations for Test 4914, Run 8

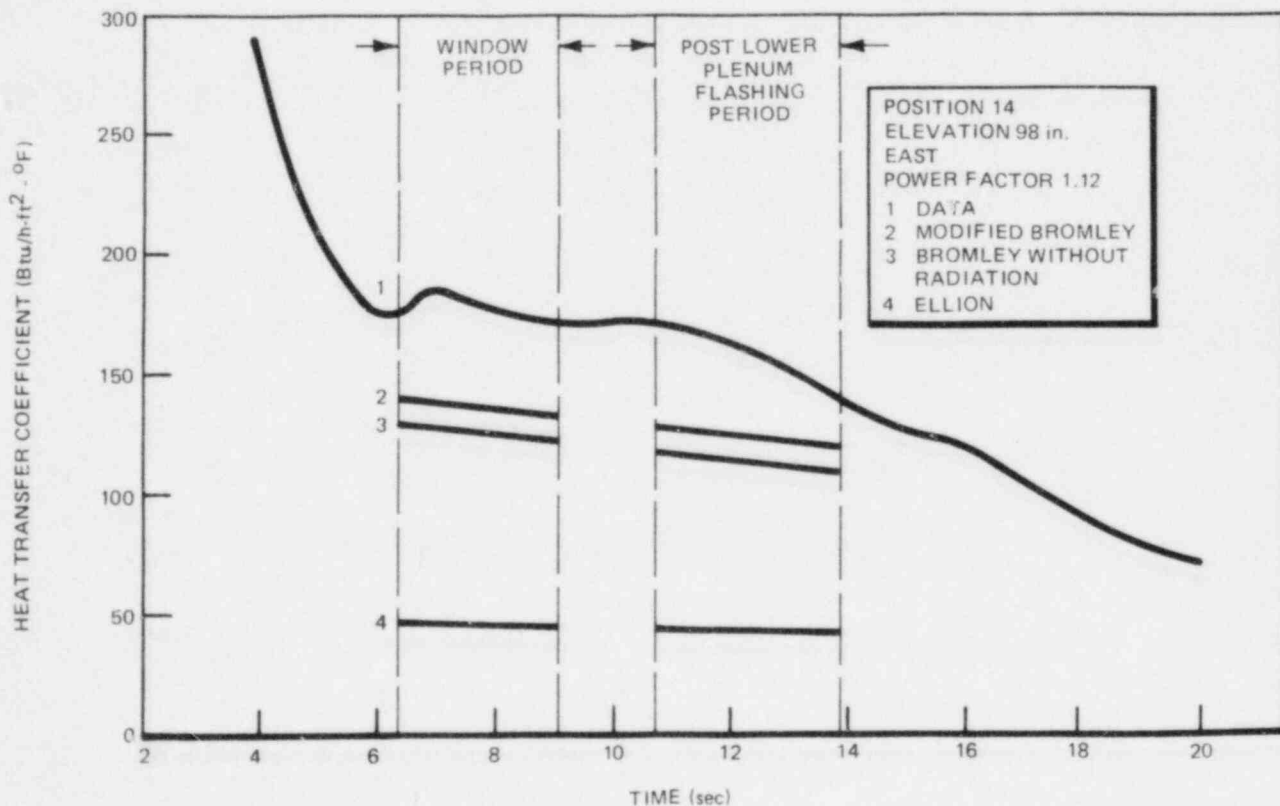


Figure 49. Comparison of Measured Heat Transfer Coefficients with Various Correlations for Test 4914, Run 8

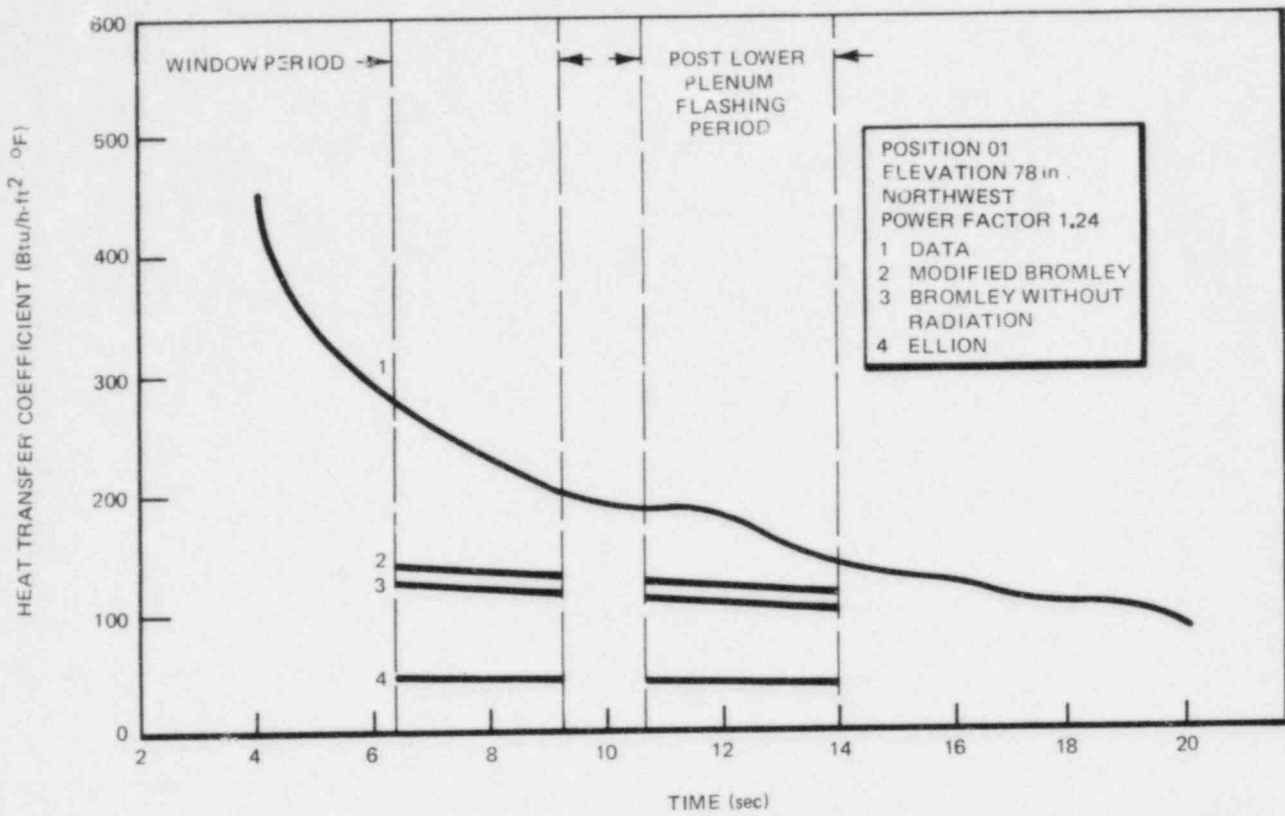


Figure 50. Comparison of Measured Heat Transfer Coefficients with Various Correlations for Test 4914, Run 8

Bromley correlation. The lowest data are 10% below the correlation. All the low data were obtained either at the very beginning or end of the PLPF period, i.e., when the two-phase level had just covered or uncovered the particular elevation, and could lie in a transition between the dispersed-flow and inverted-annular-flow regimes. It is interesting to note, however, that this does not result in a severe decrease in the heat transfer coefficient. Over the entire range of wall superheats, the modified Bromley correlation is thus a conservative representation of the heat transfer coefficient. The calculated void fractions at the three elevations of interest are shown in Figure 52.

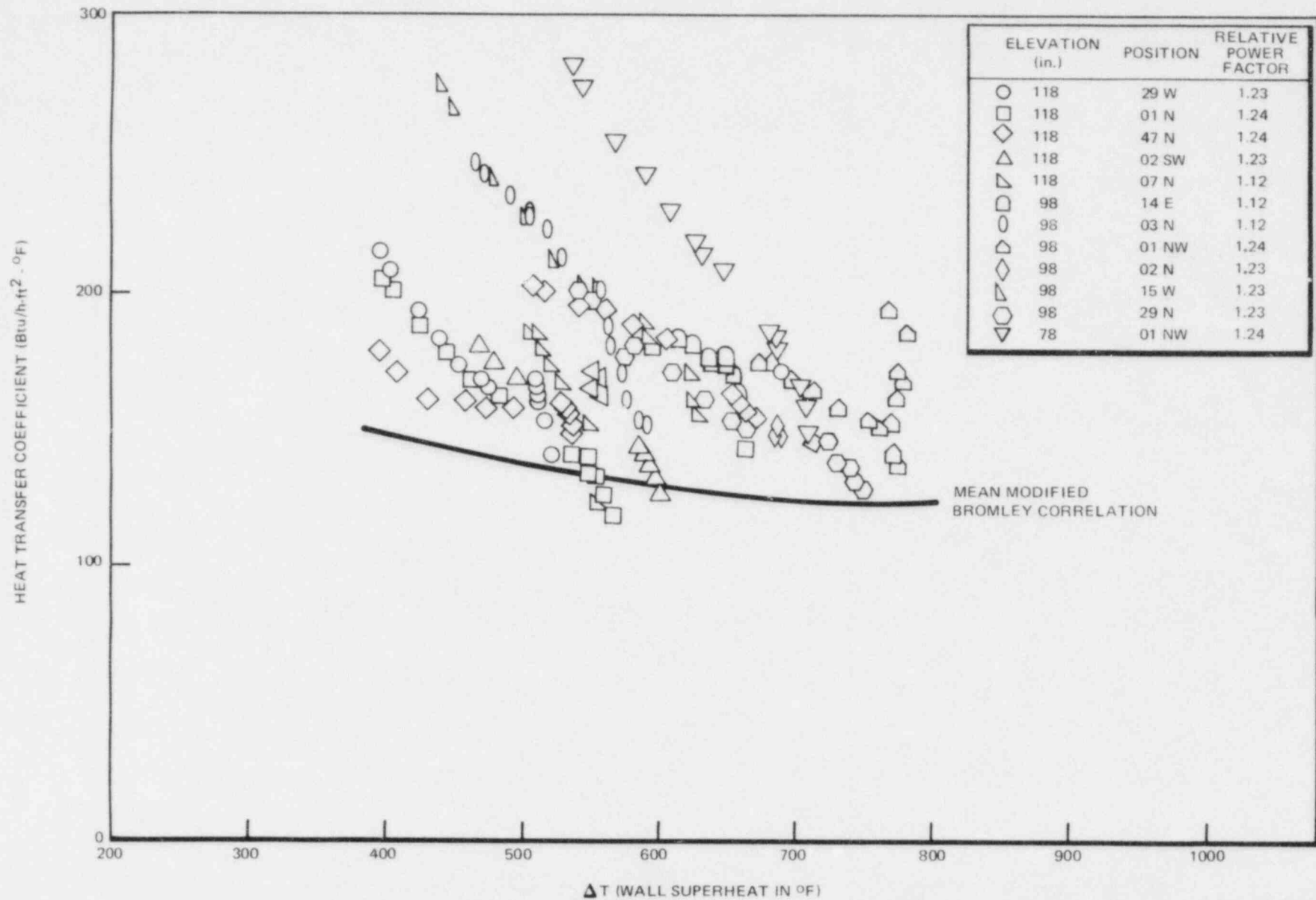


Figure 51. Comparison of Measured Heat Transfer Coefficients versus Modified Bromley Correlation as a Function of Wall Superheat, Test 4914, Run 8

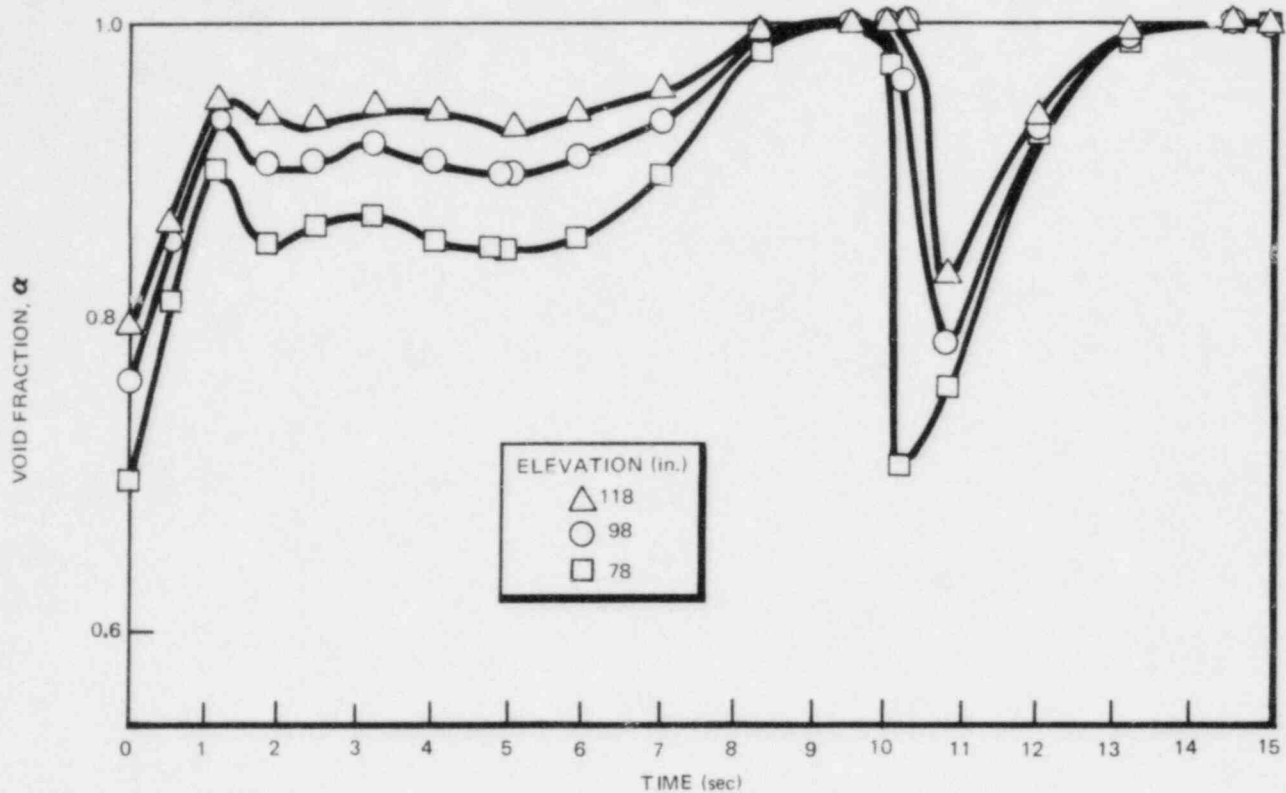


Figure 52. Calculated Void Fractions at Three Elevations, Test 4914, Run 8

d) TEST 4904

Figures 53 and 54 depict the inlet flow and two-phase level transients. Figures 55 through 62 show the heat transfer coefficients in the film boiling regime for this test at three different elevations. The modified Bromley correlation is also shown for the relevant periods of low flow and below-level conditions. The results are summarized in Figure 63 in the form of heat transfer coefficients as a function of wall superheat, again showing that the modified Bromley correlation is a reasonable lower bound to the data.

Figure 64 shows the calculated variation in the void fraction at the three relevant elevations.

The results from all these tests show conclusively that the modified Bromley correlation is applicable as a lower bound for the heat transfer coefficient during low flow portions of the blowdown transient.

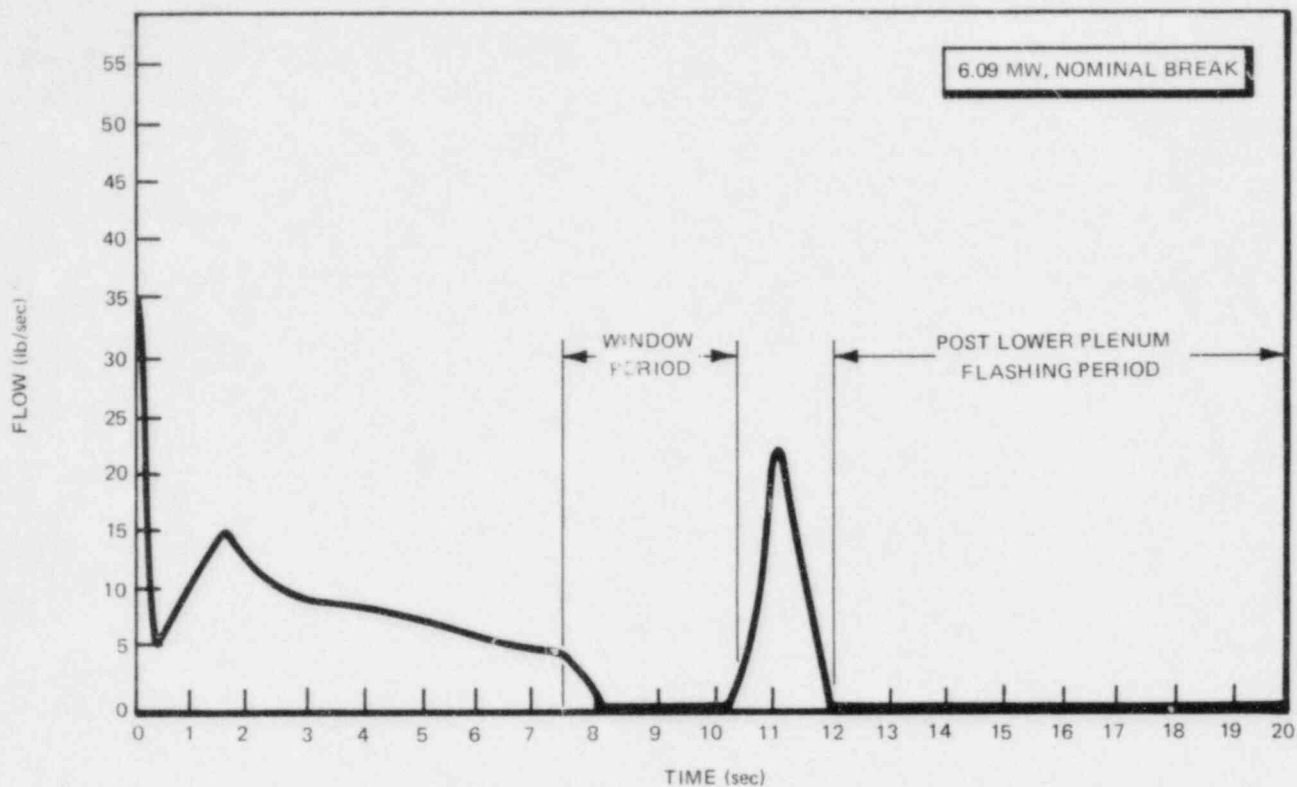


Figure 53. Inlet Flow Variation for Test 4904, Run 45

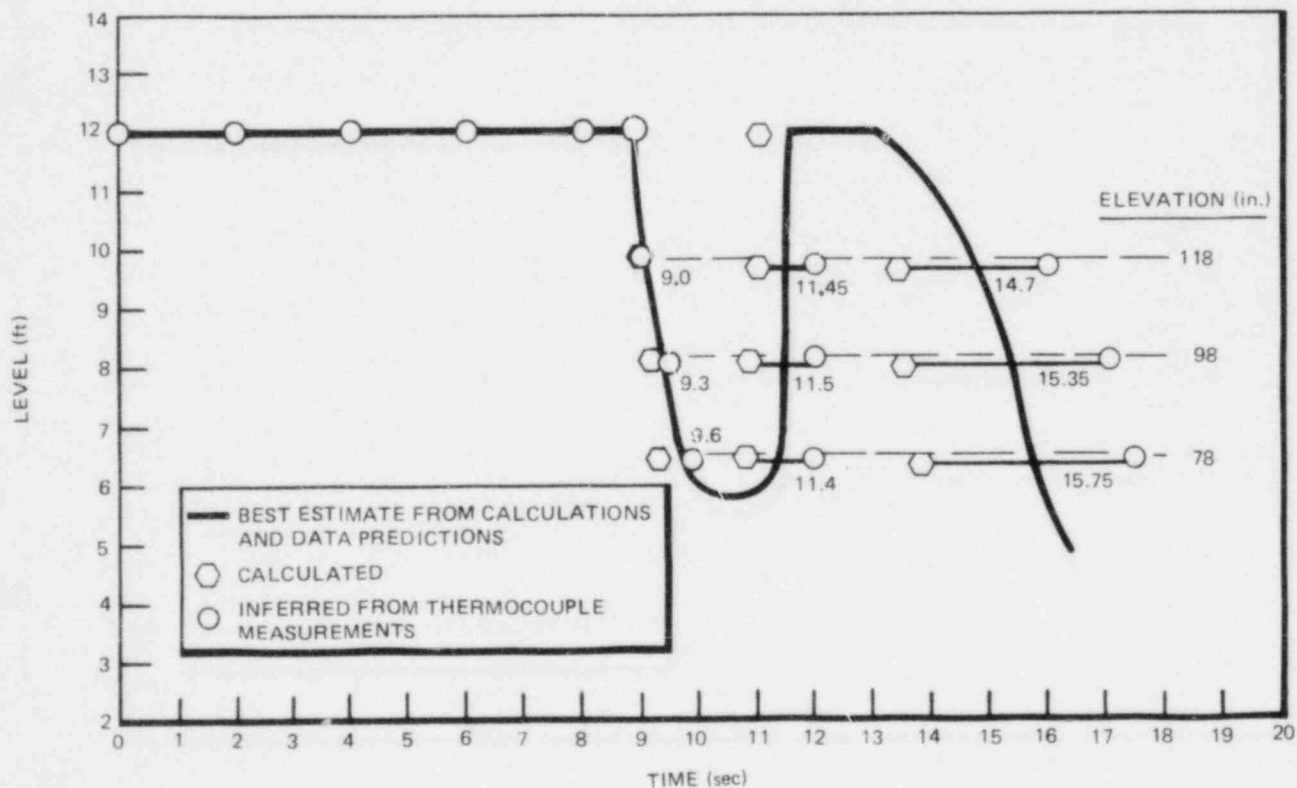


Figure 54. Two-Phase Level Measurements and Predictions in Bundle, Test 4904, Run 45

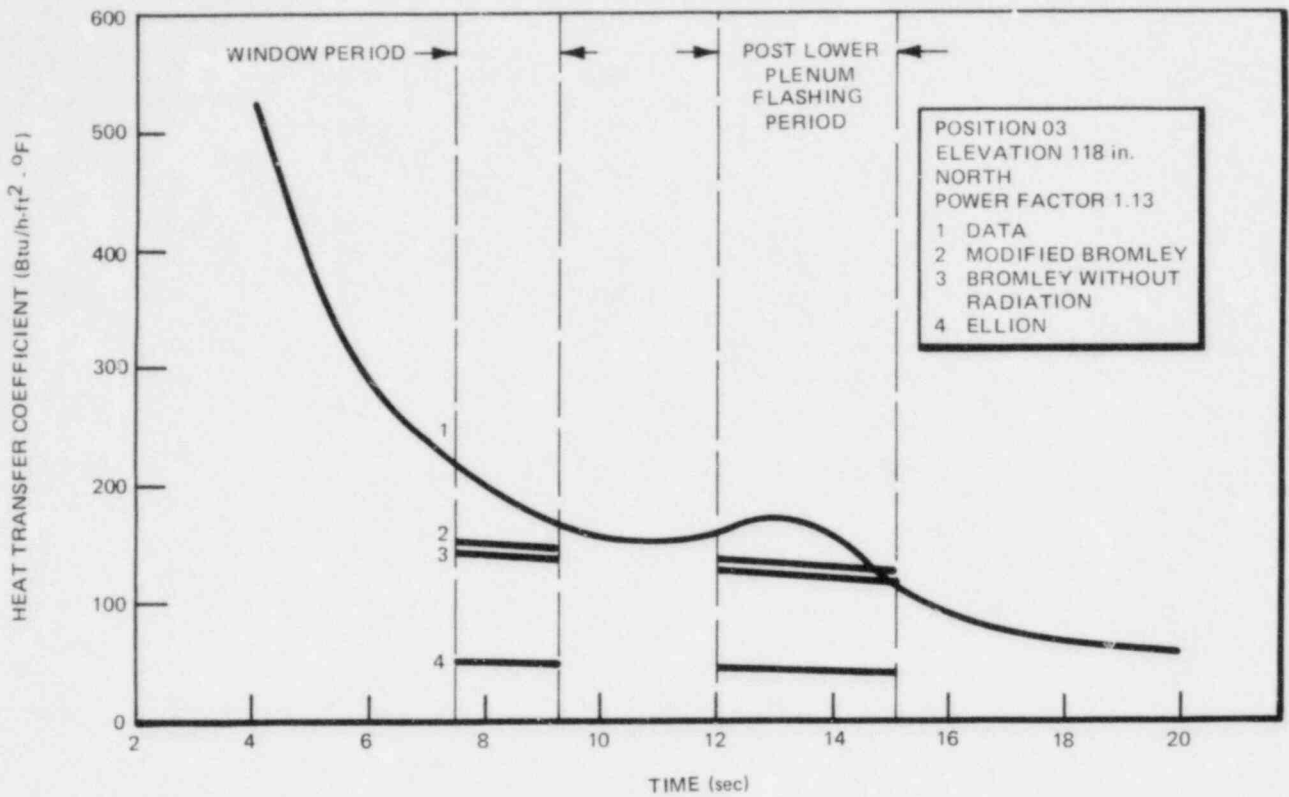


Figure 55. Comparison of Measured Heat Transfer Coefficients with Various Correlations for Test 4904, Run 45

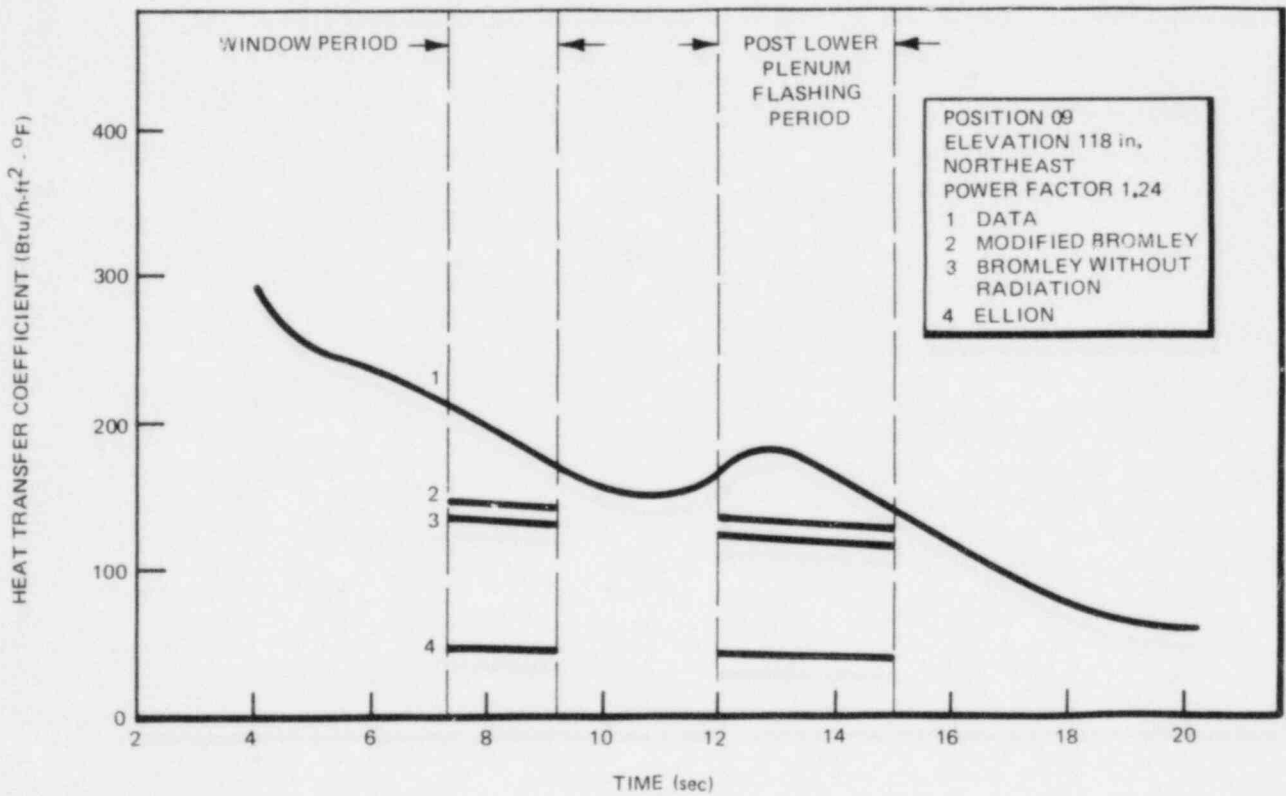


Figure 56. Comparison of Measured Heat Transfer Coefficients with Various Correlations for Test 4904, Run 45



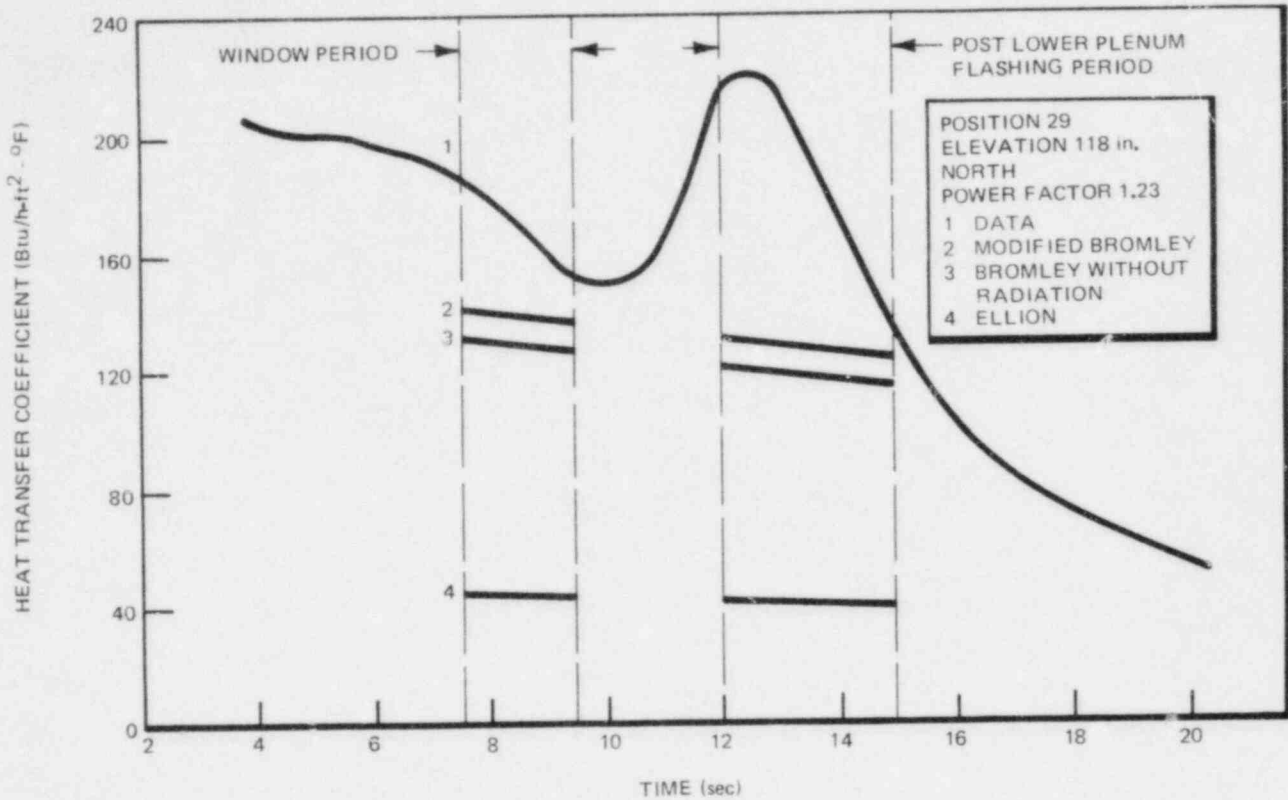


Figure 57. Comparison of Measured Heat Transfer Coefficients with Various Correlations for Test 4904, Run 45

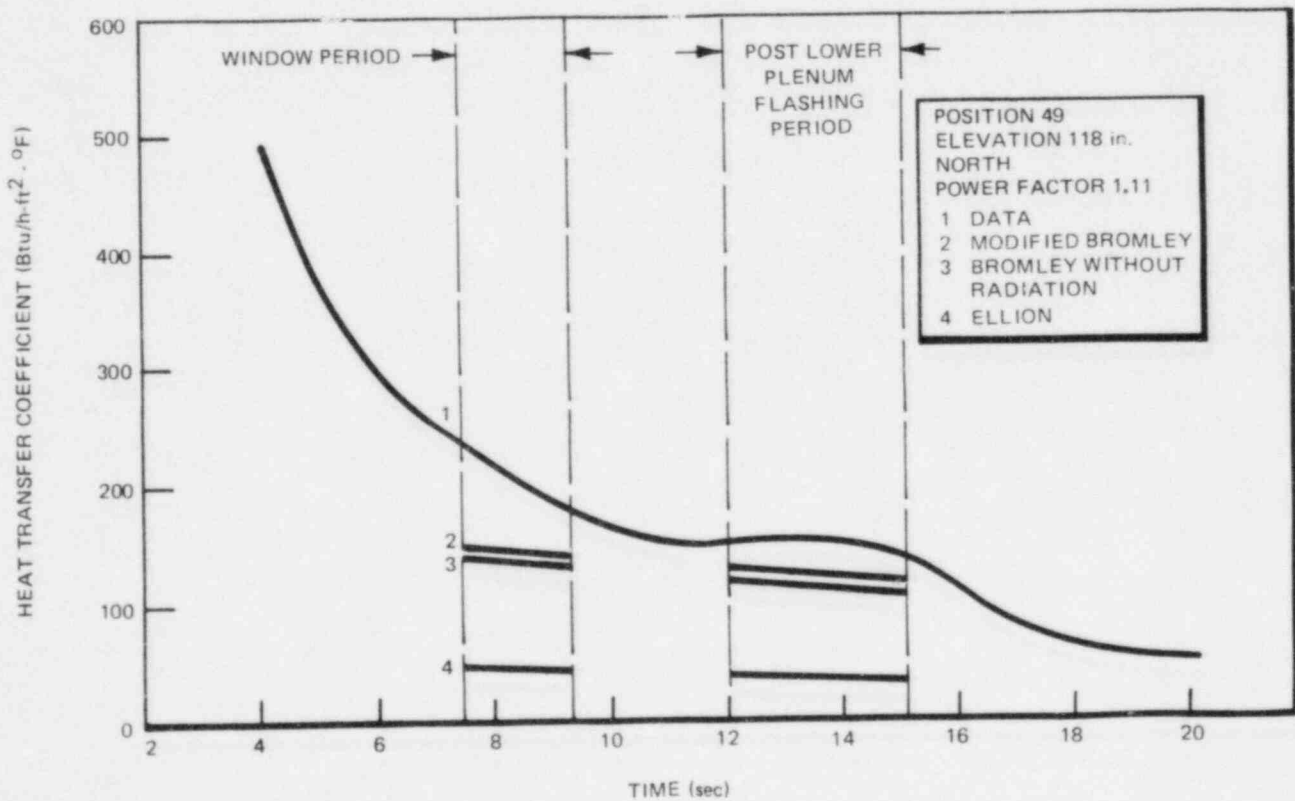


Figure 58. Comparison of Measured Heat Transfer Coefficients with Various Correlations for Test 4904, Run 45

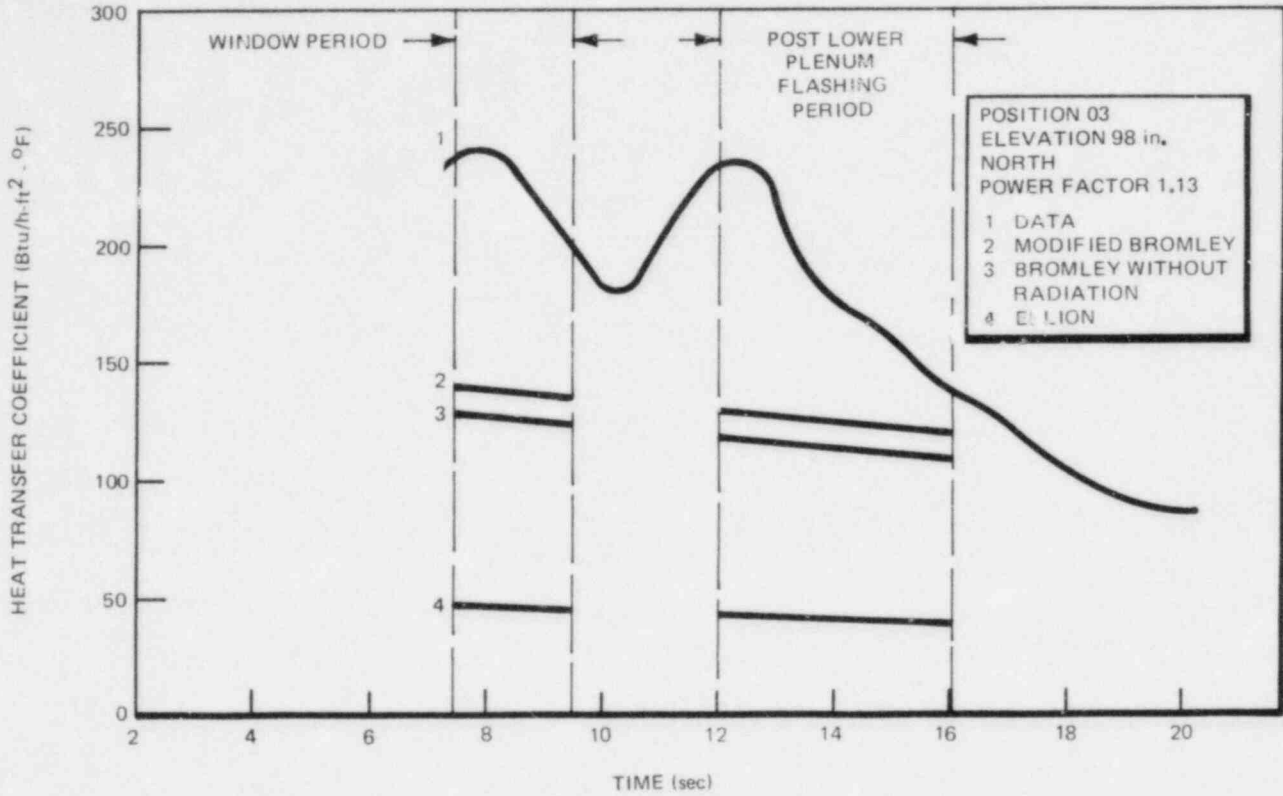


Figure 59. Comparison of Measured Heat Transfer Coefficients with Various Correlations for Test 4904, Run 45

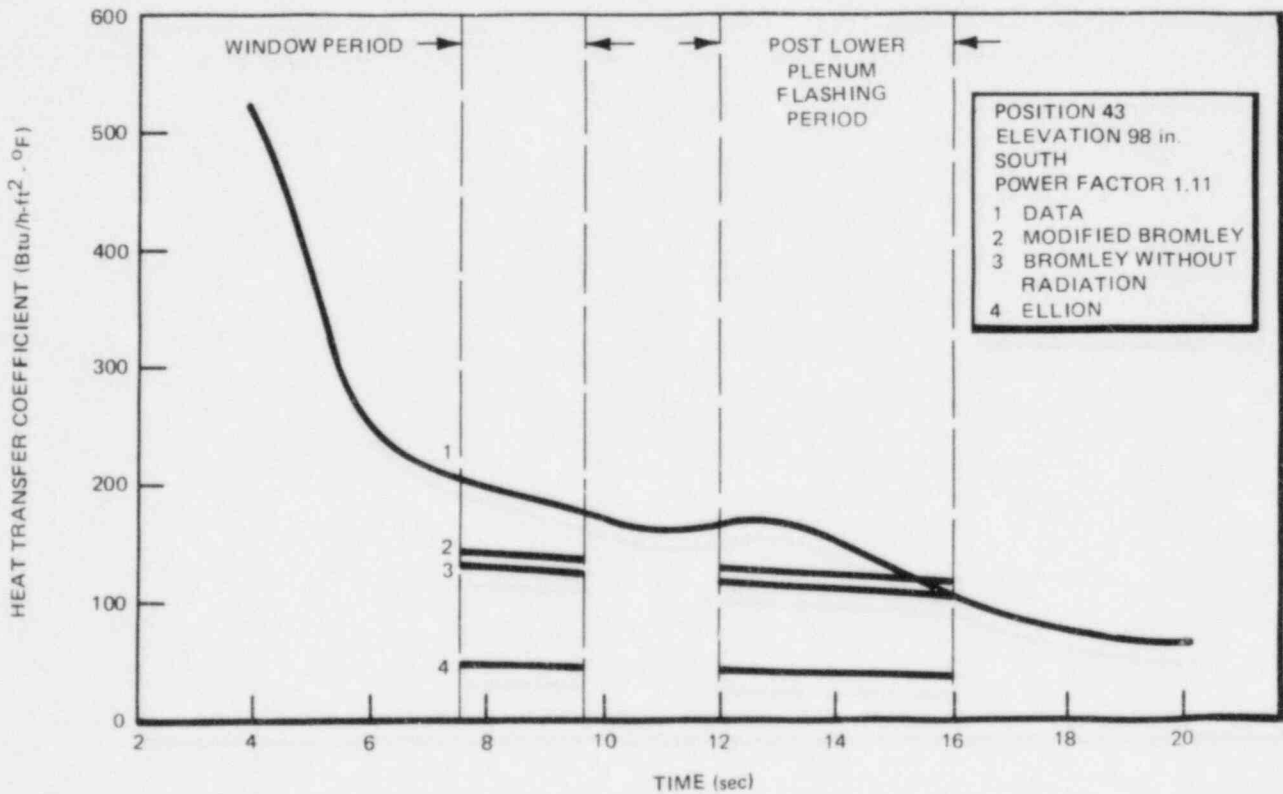


Figure 60. Comparison of Measured Heat Transfer Coefficients with Various Correlations for Test 4904, Run 45

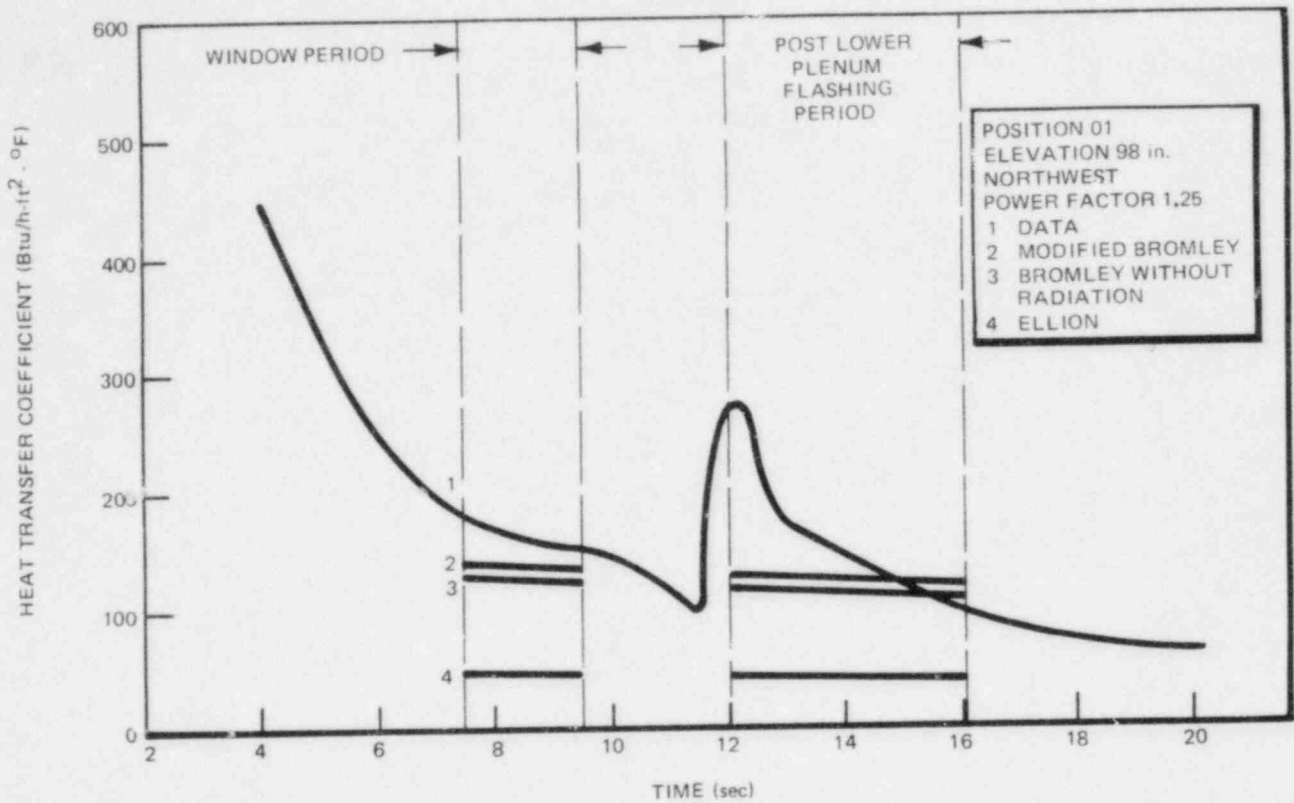


Figure 61. Comparison of Measured Heat Transfer Coefficients with Various Correlations for Test 4904, Run 45

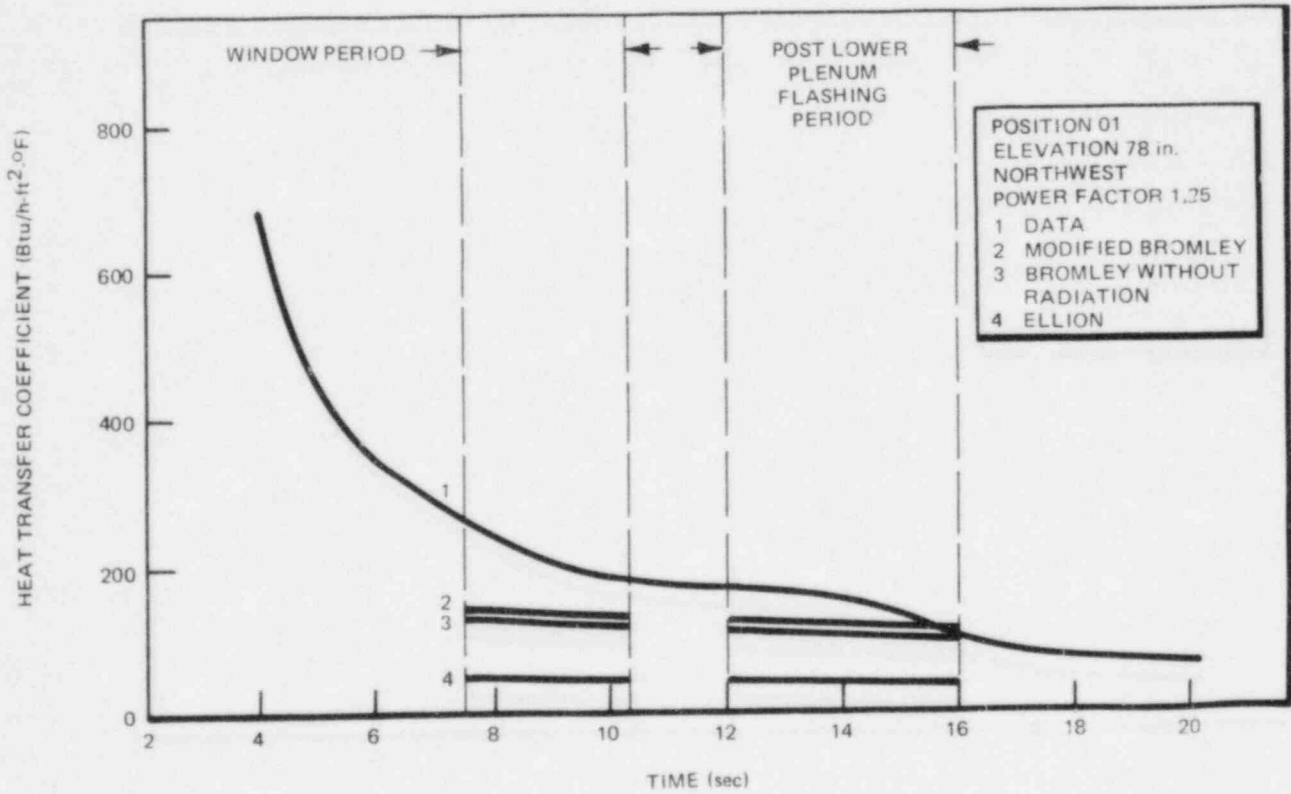


Figure 62. Comparison of Measured Heat Transfer Coefficients with Various Correlations for Test 4904, Run 45

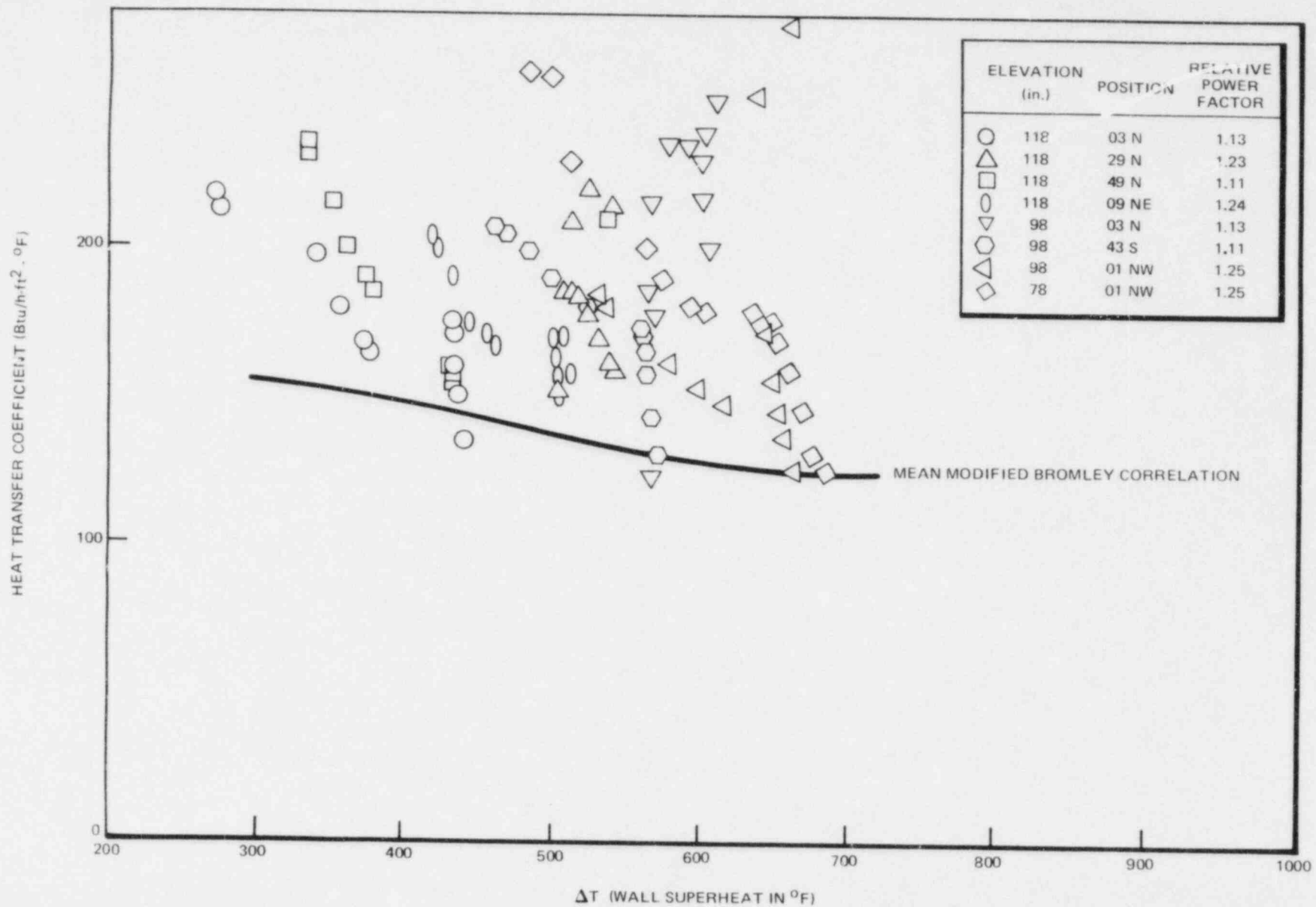


Figure 63. Comparison of Measured Heat Transfer Coefficients versus Modified Bromley Correlation as a Function of Wall Superheat, Test 4904, Run 45

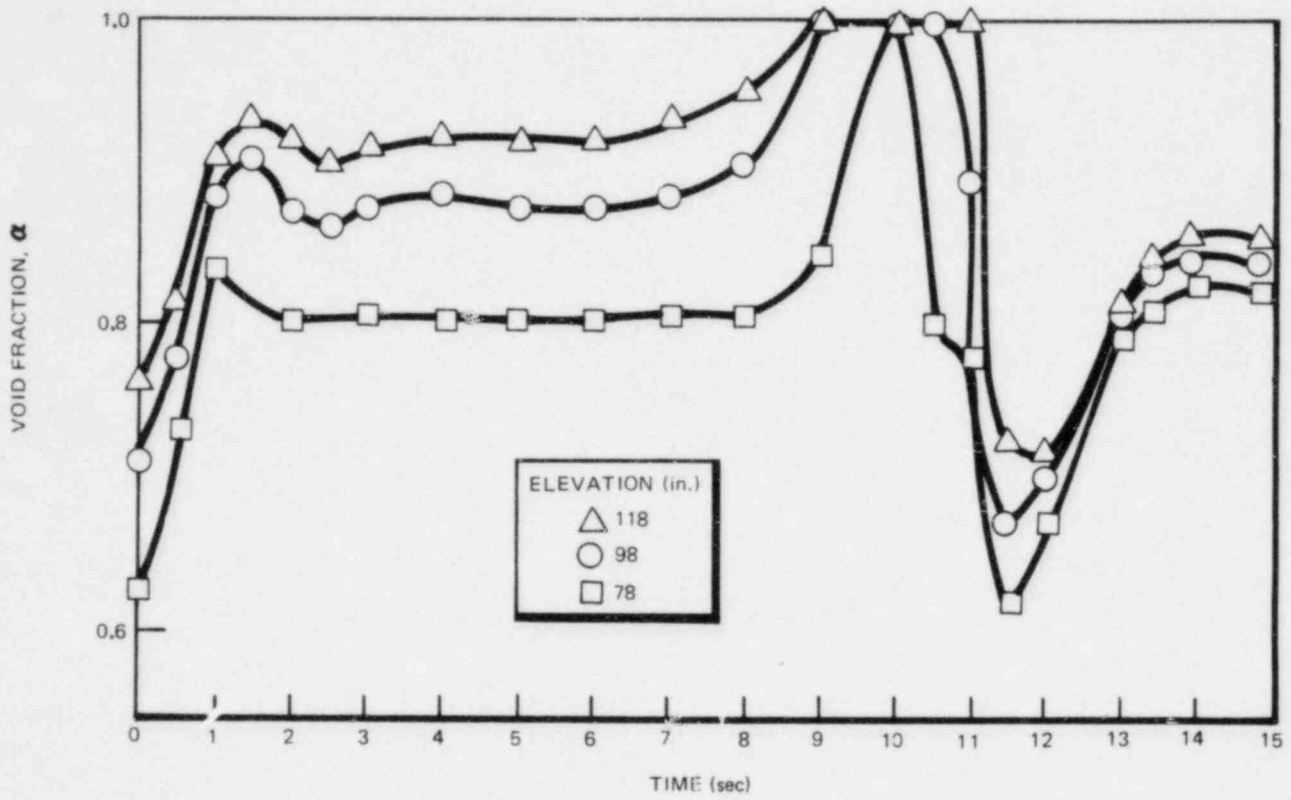


Figure 64. Calculated Void Fractions at Three Elevations, Test 4904, Run 45

4. CONCLUSION

For the conditions of low flow film boiling in the postulated BWR LOCA, the heat transfer can be conservatively approximated by the zero-flow film boiling relation

$$h = h_{FB} + h_R$$

where

$$h_{FB} = 0.62 \left[ \frac{K_g^3 (\rho_f - \rho_g) h_{fg} g}{\mu_g (T_{WALL} - T_{SAT}) L_H} \right]^{1/4}$$

with  $L_H$  obtained from Helmholtz instability considerations

$$L_H = 16.24 \left[ \frac{\sigma h_{fg}^4 \mu_g^5 g_c^4}{\rho_g (\rho_f - \rho_g)^5 K_g^3 (T_{WALL} - T_{SAT})^3} \right]^{1/11}$$

and

$$h_R = \epsilon_W \sigma R \frac{(T_W^4 - T_{SAT}^4)}{(T_W - T_{SAT})}$$

The applicability of this relation to four specific periods of the BWR LOCA shows that it does an excellent job of predicting or conservatively bounding the data. These periods include: (1) the "window" period immediately prior to lower plenum flashing, (2) the period following lower plenum flashing where a two-phase level exists in the bundle, (3) the period of channel bypass reflooding, and (4) the period of bundle reflooding. The recommended correlation is applicable as a lower bound (zero flow) for any similar conditions of low film boiling.

5. NOMENCLATURE

c	Constant
d	Film thickness, ft
g	Gravitational acceleration, ft/sec <sup>2</sup> or ft/h <sup>2</sup>
g <sub>c</sub>	Gravitational conversion factor, ft-lb <sub>m</sub> /lb <sub>f</sub> -h <sup>2</sup>
h	Heat transfer coefficient, Btu/h-ft <sup>2</sup> /°F
h <sub>FB</sub>	Film boiling heat transfer coefficient, Btu/h-ft <sup>2</sup> /°F
h <sub>fg</sub>	Latent heat of vaporization, Btu/lb
h <sub>R</sub>	Radiation heat transfer coefficient, Btu/h-ft <sup>2</sup> -°F
K, k	Thermal conductivity, Btu/h-ft-°F
k	Wave number
L	Characteristic film length, ft
L <sub>B</sub>	Bailey characteristic length, ft
L <sub>H</sub>	Helmholtz instability length, ft
L <sub>T</sub>	Taylor instability wavelength, ft
m	Vaporization, lb/h-ft
n	Parameter for interfacial shear
p	Pressure, psia
r	Radius of surface, ft
T <sub>L</sub>	Temperature of liquid, °F
T <sub>S</sub>	Saturation temperature, °R
T <sub>SAT</sub>	Saturation temperature, °F
T <sub>W</sub>	Wall temperature, °R
T <sub>WALL</sub>	Temperature of surface, °F
ΔT	Wall superheat = T <sub>w</sub> - T <sub>sat</sub> , °F
v	Velocity, ft/h

$V_o$	Maximum velocity in film, ft/h
$v_{in}$	Cold reflooding rate, in./sec
$w$	Film flow, lb/ft-h
$We$	Weber number of film
$x$	length, ft
$y$	length, ft
$z$	Length, ft

### Greek Symbols

$\epsilon$	Perturbation
$\epsilon_W$	Emissivity of the wall
$\lambda$	Wavelength, ft
$\sigma$	Surface tension, lb/ft
$\sigma_R$	Stefan-Boltzmann constant, Btu/h-ft <sup>2</sup> -°R <sup>4</sup>
$\rho$	Density, lb/ft <sup>3</sup>
$\mu$	Viscosity, lb/ft-h
$\omega$	Frequency, h <sup>-1</sup>
$\tau_d$	Shear stress on liquid film at liquid-vapor interface, lb/ft-h <sup>2</sup>

### Subscripts

f	Designates liquid phase
g	Designates vapor phase
H	Helmholtz
o	Reference value
S	Saturation
W	Wall
d	Liquid-vapor interface



6. REFERENCES

1. M. E. Ellion, *A Study of the Mechanism of Boiling Heat Transfer*, Jet Propulsion Laboratory, Memo 20-88, C.I.T. (1954).
2. *Analytical Model for Loss-of-Coolant Analysis in Accordance with LOCFR50 Appendix K*, General Electric Co., 1974 (NEDO-20566).
3. L. A. Bromley, "Heat Transfer in Stable Film Boiling," *Chem. Eng. Progr.*, B46, 221-227 (1950).
4. N. A. Bailey, *Film Boiling on Submerged Vertical Cylinders*, 1971 (AEEW-M1051).
5. Y. Y. Hsu and J. W. Westwater, "Approximate Theory for Film Boiling on Vertical Surfaces," *Chem. Eng. Prog. Symp. Series*, No. 30, Vol. 56 (1960).
6. Y.Y. Hsu, *Tentative Correlations of Reflood Heat Transfer*, LOCA Research Highlights, April 1 - June 30, 1975, July 1975.
7. R. J. Simoneau and F. F. Simon, *A Visual Study of Velocity and Buoyancy Effects on Boiling Nitrogen*, 1966 (NASA TN-D-3354).
8. S. Chandrasekhar, "Hydrodynamic and Hydromagnetic Stability," Oxford University Press, pp 434-484 (1961).
9. P. J. Berenson, "Film Boiling Heat Transfer from a Horizontal Surface," *J. of Heat Transfer*, B83, M pp. 351-358 (August 1961).
10. H. Amm and G. Uirych, "Comparison of Measured Heat Transfer Coefficients During Reflooding a 340-rod Bundle and Those Calculated from Current Heat Transfer Correlations," *European Two-Phase Flow Meeting*, Harwell (June 1974).
11. K. H. Sun and J. E. Leonard, *Experimental Study of Pool Film Boiling from a Vertical Surface*, General Electric Co. January 1977 (NEDE-21600).
12. *Forty-Sixth Monthly Report, BWR Blowdown Heat Transfer Program*, General Electric Co., Contract No. AT(04-3)-189, P.A. 58 (May 1975).
13. W. C. Panches, *MAYU04 - A Method to Evaluate Transient Thermal-Hydraulic Conditions in 49-Rod Bundles*, General Electric Co., June 1977 (GEAP-23517).

## APPENDIX A

THEORETICAL MODEL FOR FILM BOILING ON A VERTICAL SURFACE

In low flow film boiling, a thin film of superheated steam exists at the surface, and the heat is transferred by conduction across the film. This is justified by the low Reynolds number of the film. The laminar film is assumed to grow and break up, as shown in Figure A-1, at a critical wavelength. For purposes of analysis, the film is then assumed to start as zero and grow in a repetitive manner.<sup>A-1</sup> In reality a wavy film is probably maintained throughout the length; the important point is that the film will not grow indefinitely. Classical Nusselt-type analysis for growing films is then used to determine the growth rate of the film and the average heat transfer coefficient for one wavelength.

## A.1 LAMINAR FLOW MODEL

The velocity profiles in the developing film can be derived as below. (Refer to Figure A-2.)

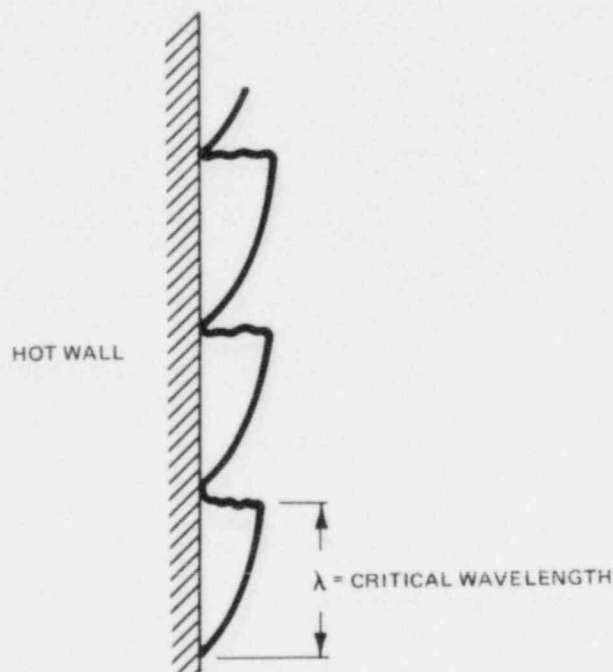


Figure A-1. Assumed Film Growth

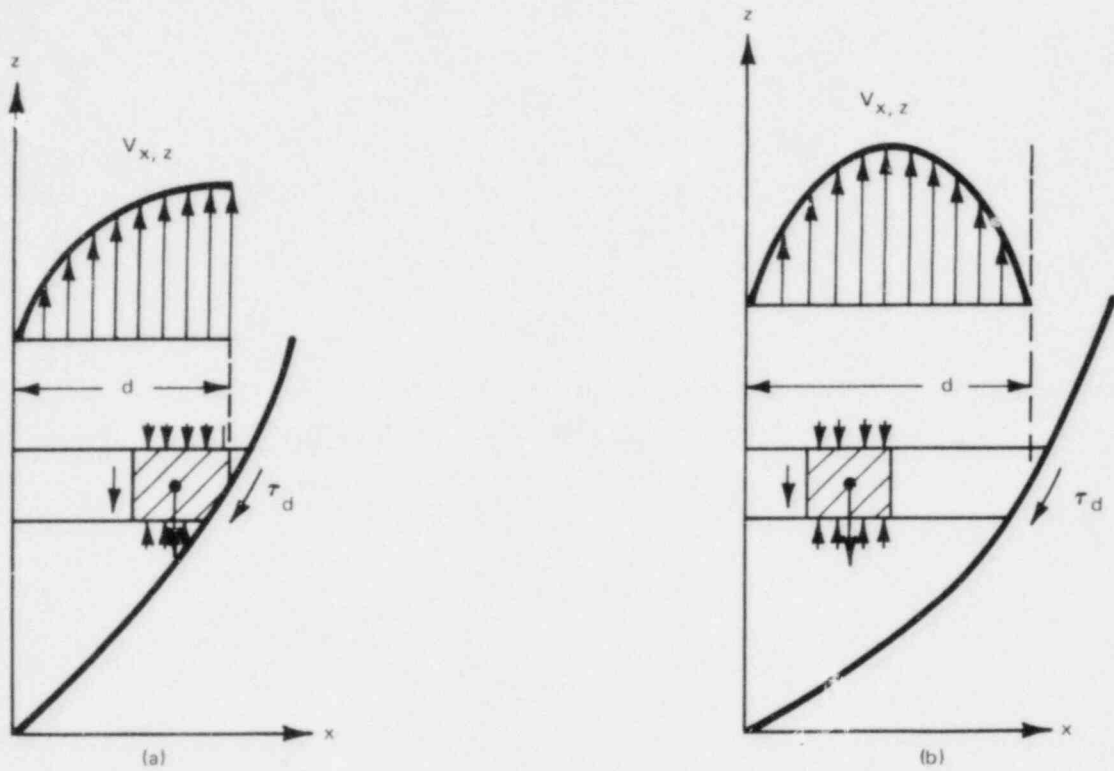


Figure A-2. Velocity Profiles and Control Volumes

A force balance on the shaded control volume gives:

$$-\mu_g \frac{dv}{dx} = g\rho_g (d - x) + \frac{dp}{dz} (d - x) + \tau_d \quad (\text{A-1})$$

Two boundary conditions representing the extreme situations can be represented by:

Figure A-2a:  $\tau_d = 0$       and      Figure A-2b:  $v_d = 0$

For the first case, setting  $\tau_d = 0$ , Equation A-1 can be integrated from the wall ( $x = 0, v = 0$ ) to yield:

$$v_{x,z} = - \frac{\left(g\rho_g + \frac{dp}{dz}\right)}{\mu_g} \left(dx - \frac{x^2}{2}\right) \quad (\text{A-2})$$

$$v_{o_z} = v_{d,z} = - \frac{\left(g\rho_g + \frac{dp}{dz}\right)}{\mu_g} \frac{d^2}{2} \quad (A-3)$$

$$v_{x,z} = v_{o_z} \left[ 1 - \left(\frac{x}{d} - 1\right)^2 \right] \quad (A-4)$$

For the second case,  $\tau_{d/2} = 0$  by symmetry. For the control volume shown in Figure A-2b:

$$-\mu_g \frac{dv}{dx} = g\rho_g \left(\frac{d}{2} - x\right) + \frac{dp}{dz} \left(\frac{d}{2} - x\right) \quad (A-5)$$

Integrating from the wall with  $v = 0$  at  $x = 0$ ,

$$v_{x,z} = - \frac{\left(g\rho_g + \frac{dp}{dz}\right)}{\mu_g} \left(\frac{dx}{2} - \frac{x^2}{2}\right) \quad (A-6)$$

$$v_{o_z} = v_{d/2,z} = - \frac{\left(g\rho_g + \frac{dp}{dz}\right)}{\mu_g} \left(\frac{d^2}{8}\right) \quad (A-7)$$

$$v_{x,z} = v_{o_z} \left[ 1 - \left(\frac{x}{d/2} - 1\right)^2 \right] \quad (A-8)$$

or, in general,

$$v = v_o \left[ 1 - \left(\frac{x}{nd} - 1\right)^2 \right], \quad 0 \leq x \leq d \quad (A-9)$$

where  $0.5 \leq n < 1$ , and  $n = 0.5$  correspond to zero velocity at the interface and  $n = 1.0$  to zero shear at the interface.

The mean velocity of the steam is given by

$$\bar{v} = \frac{1}{d} \int_c^d v(x) dx = v_o \left( \frac{1}{n} - \frac{1}{3n^2} \right) \quad (\text{A-10})$$

and the total steam flow by

$$W = d \rho_g \bar{v} = d \rho_g v_o \left( \frac{1}{n} - \frac{1}{3n^2} \right) \quad (\text{A-11})$$

The pressure gradient is determined by the shear stresses

$$\begin{aligned} \frac{dP}{dz} &= - \left. \frac{\mu_g}{nd} \frac{dv}{dx} \right|_{x=0} \\ &= - \frac{2\mu_g}{(nd)^2} v_o \end{aligned} \quad (\text{A-12})$$

With the assumption of low flow rates for the water, the pressure gradient is also given by

$$\frac{dP}{dz} = - g(\rho_f - \rho_g) \quad (\text{A-13})$$

Combining Equations A-12 and A-13 gives

$$v_o = (nd)^2 \frac{g(\rho_f - \rho_g)}{2\mu_g} \quad (\text{A-14})$$

and inserting this in Equation A-11 gives

$$W = d^3 \frac{g(\rho_f - \rho_g)\rho_g}{2\mu_g} n - \frac{1}{3} \quad (\text{A-15})$$

The steam generation is given by the conduction across the film

$$m = \frac{dW}{dz} = \frac{k_g (T_w - T_s)}{dh_{fg}} \quad (\text{A-16})$$

Combining Equations A-15 and A-16 we get\*

$$d = \frac{8}{3n - 1} \left[ \frac{k_g (T_w - T_s) \mu_g z}{h_{fg} g \rho_g (\rho_f - \rho_g)} \right]^{1/4} \quad (\text{A-17})$$

Defining the heat transfer coefficient by

$$h = \frac{k_g}{d}$$

we obtain

$$h = \left( \frac{3n - 1}{8} \right)^{1/4} \left[ \frac{k_g^3 h_{fg} g \rho_g (\rho_f - \rho_g)}{\mu_g (T_w - T_s) z} \right]^{1/4} \quad (\text{A-18})$$

\* Ellion<sup>A-2</sup> assumes  $m$  is independent of  $z$  and thereby of  $d$ , and for the case of zero interface velocity obtains  $c = 0.714$ . Bailey<sup>A-1</sup> sets  $(d^3) = (\bar{d})^3$  and obtains for the case of zero interface shear  $c = 0.759$ . For the case of zero interface shear Bromley's analysis<sup>A-3</sup> gives  $c = 0.943$ .

and the average heat transfer coefficient over one wavelength  $L$  is given by

$$\begin{aligned} \bar{h} &= \frac{1}{L} \int_0^L h \, dz \\ &= c \left[ \frac{k_g^3 h_f \rho_g (\rho_f - \rho_g) g}{\mu_g (T_w - T_s) L} \right]^{1/4} \end{aligned} \quad (\text{A-19})$$

where

$$c = \frac{4}{3} \left[ \frac{3n - 1}{8} \right]^{1/4} = \begin{cases} 0.667 & \text{for } n = 1/2 \\ 0.943 & \text{for } n = 1 \end{cases}$$

## A.2 FILM STABILITY MODEL

The film will not grow infinitely but it will break down due to the Helmholtz instability (see Figure A-3) caused by the velocity difference between flow in the vapor film and the stagnant liquid.

The following simplified analysis is presented to estimate the magnitude of the critical wavelength.

Let a small perturbation of the surface be given by

$$d = d_0 (1 + \epsilon \sin kz) \quad (\text{A-20})$$

The velocity distribution is then, to the first order approximation, given by

$$v = v_0 (1 - \epsilon \sin kz) \quad (\text{A-21})$$

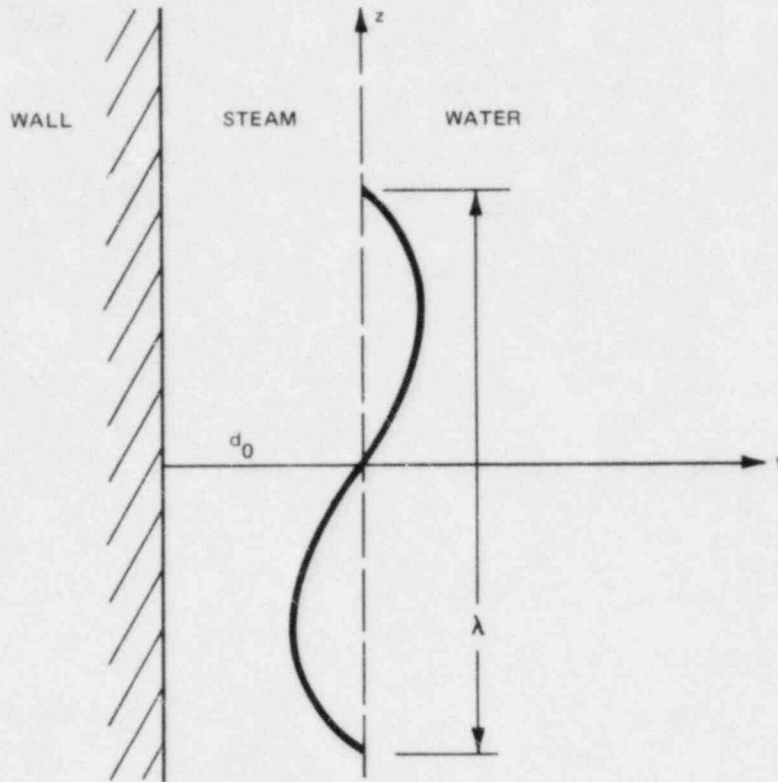


Figure A-3. Helmholtz Instability for a Film

Assuming constant pressure  $P_0$  in the water and using Bernoulli's equation, the pressure drop across the interface is given by

$$\Delta P = \left( \rho_g v_o^2 - \sigma d_o k^2 \right) \epsilon \sin kz \tag{A-22}$$

and it is seen that instability occurs for

$$k < \left[ \frac{\rho_g v_o^2}{\sigma d_o} \right] \tag{A-23}$$

or

$$\lambda > 2\pi \left[ \frac{\sigma d_o}{\rho_g v_o^2} \right]^{1/2} \tag{A-24}$$



Assuming an incompressible liquid and potential flow, i.e.,

$$\nabla \cdot \bar{v} = 0 \quad \text{and} \quad \nabla_x \bar{v} = 0 \quad (\text{A-25})$$

and that the perturbation grows exponentially, i.e.,

$$\varepsilon = \varepsilon_0 e \exp(\omega t) \quad (\text{A-26})$$

the velocity of the liquid, to the first order approximation, is given by

$$v_z = -d\varepsilon_0 \omega \cos kz e \exp(-ky + \omega t) \quad (\text{A-27})$$

$$v_y = d\varepsilon_0 \omega \sin kz e \exp(-ky + \omega t) \quad (\text{A-28})$$

Applying the momentum equation for the axial direction at the interface

$$\rho_f \frac{\partial v_z}{\partial t} = - \frac{\partial \Delta p}{\partial z} \quad (\text{A-29})$$

we get

$$\omega^2 = \frac{\sigma}{\rho_f d^3} kd \left[ We - (kd)^2 \right] \quad (\text{A-30})$$

The maximum growth for instabilities is then found to occur for

$$kd = \left[ \frac{We}{3} \right]^{1/2} \quad (\text{A-31})$$

or

$$\lambda = 2\pi \left[ \frac{3\sigma d}{\rho_g v^2} \right]^{1/2} \quad (\text{A-32})$$

A.3 AVERAGE HEAT TRANSFER COEFFICIENT

Instabilities with a wavelength given by Equation A-32 are the most likely to occur. They will cause the film to break up, and the steam will leave the surface as bubbles. A new film will then form and grow until it also becomes unstable. Accordingly the most unstable wavelength is a good approximation for the length L of the film, i.e.,

$$L = 2\pi \left[ \frac{3\sigma d}{\rho_g v_g^2} \right]^{1/2} \tag{A-33}$$

Several idealizations and simplifications have been made in this derivation and a correction factor could be introduced for the critical wavelength. Comparison with simple geometry data has shown, however, that this is not necessary.

Combining Equations A-15, A-17 and A-33 gives

$$L = \left[ \frac{\left( \frac{3\sqrt{3}}{2\pi} \right)^8}{\left( \frac{3n-1}{8} \right)^5} \frac{\sigma^4 h_f^3 \mu_g^5}{\rho_g (\rho_f - \rho_g)^5 k_g^3 (T_W - T_S)^3} \right]^{1/11} \tag{A-34}$$

which by insertion of Equation A-19 gives

$$\bar{h} = c_1 \left[ \frac{k_g^9 h_f^2 \rho_g^3 (\rho_f - \rho_g)^4 g^4}{\mu_g^4 (T_W - T_S)^2 \sigma} \right]^{1/11} \tag{A-35}$$

where

$$C_1 = \frac{4}{3} \left[ \frac{\left( \frac{3n-1}{8} \right)^4}{\left( \frac{3\sqrt{3}}{2} \pi \right)^2} \right]^{1/11} \quad \begin{array}{l} 0.3321 \text{ for } n = 0.5 \\ 0.5498 \text{ for } n = 1.0 \end{array}$$

The Reynolds number of the film is given by

$$\begin{aligned} Re = \frac{W}{\mu_g} &= \frac{2}{3} (2(3n-1))^{1/4} \\ &= \frac{2}{3} (2(3n-1))^{1/4} \left[ \frac{k_g^3 (T_w - T_s)^3 z^3 \rho_g (\rho_f - \rho_g) g}{\mu_g^5 h_{fg}^3} \right]^{1/4} \end{aligned} \quad (A-36)$$

The plot of the maximum stable film length is given in Figure A-4, the maximum Reynolds number for the film in Figure A-5, and the average heat transfer coefficient in Figure A-6. All of these figures are for atmospheric pressure. The fluid properties can be calculated at the saturation temperature or at the average film temperature,  $1/2(T_w + T_s)$ . The steam is produced at the saturation temperature, but since the heat capacity of the steam is small compared to the latent heat of vaporization, the temperature profile of the steam across the film will be linear. Accordingly, the average film temperature is the most reasonable value to use for the evaluation of the material properties. The saturation temperature properties yield more conservative results. (From Figure A-5 it is seen that the assumption of laminar flow is justified (i.e.,  $Re \leq 100$ ).

Calculation of the steam velocity from Equations A-15 and A-17 indicates that the typical velocity is on the order of 4 to 5 ft/sec. A bounding relation for zero liquid velocity gives a conservative result for BWR application. Since

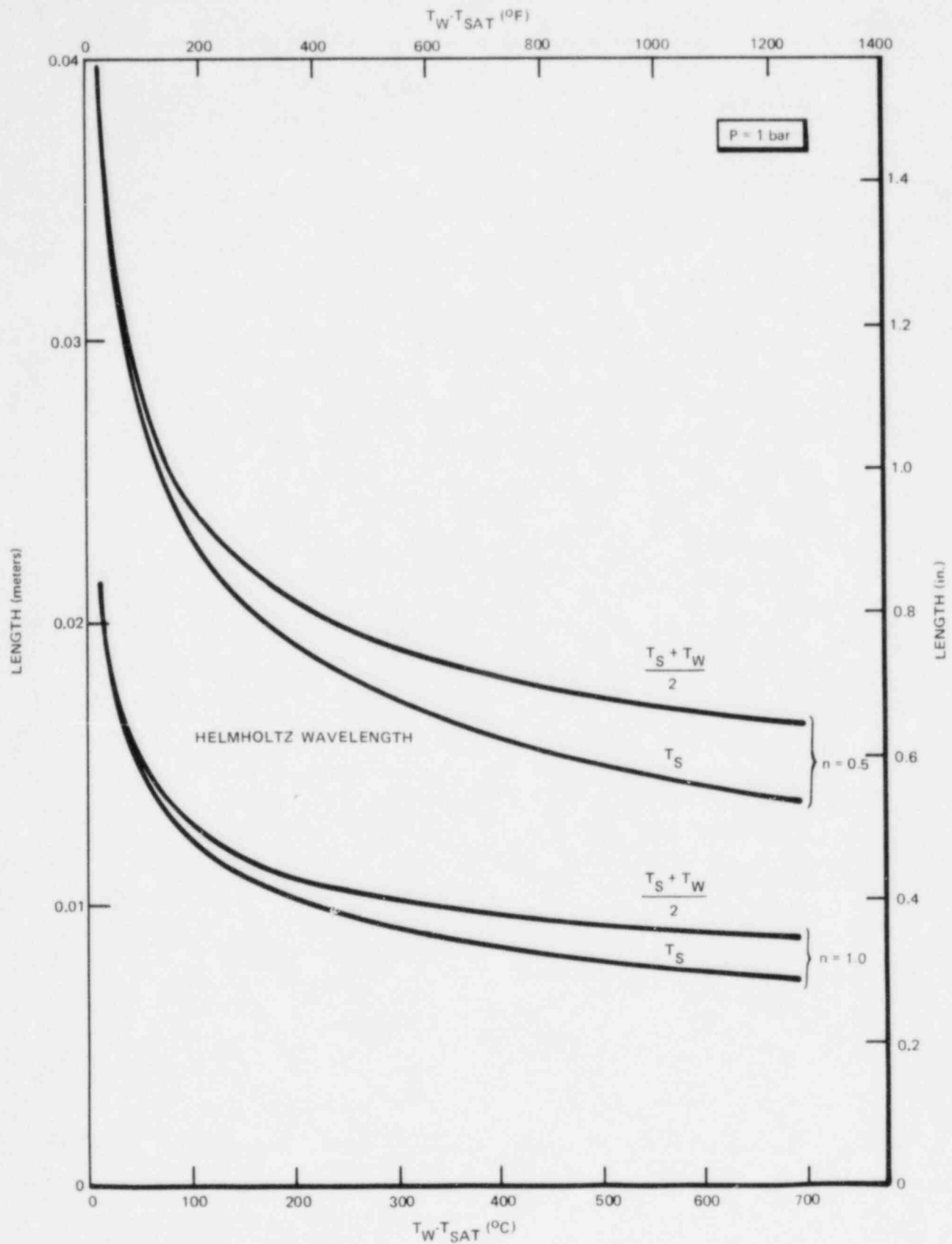


Figure A-4. Maximum Length of Film

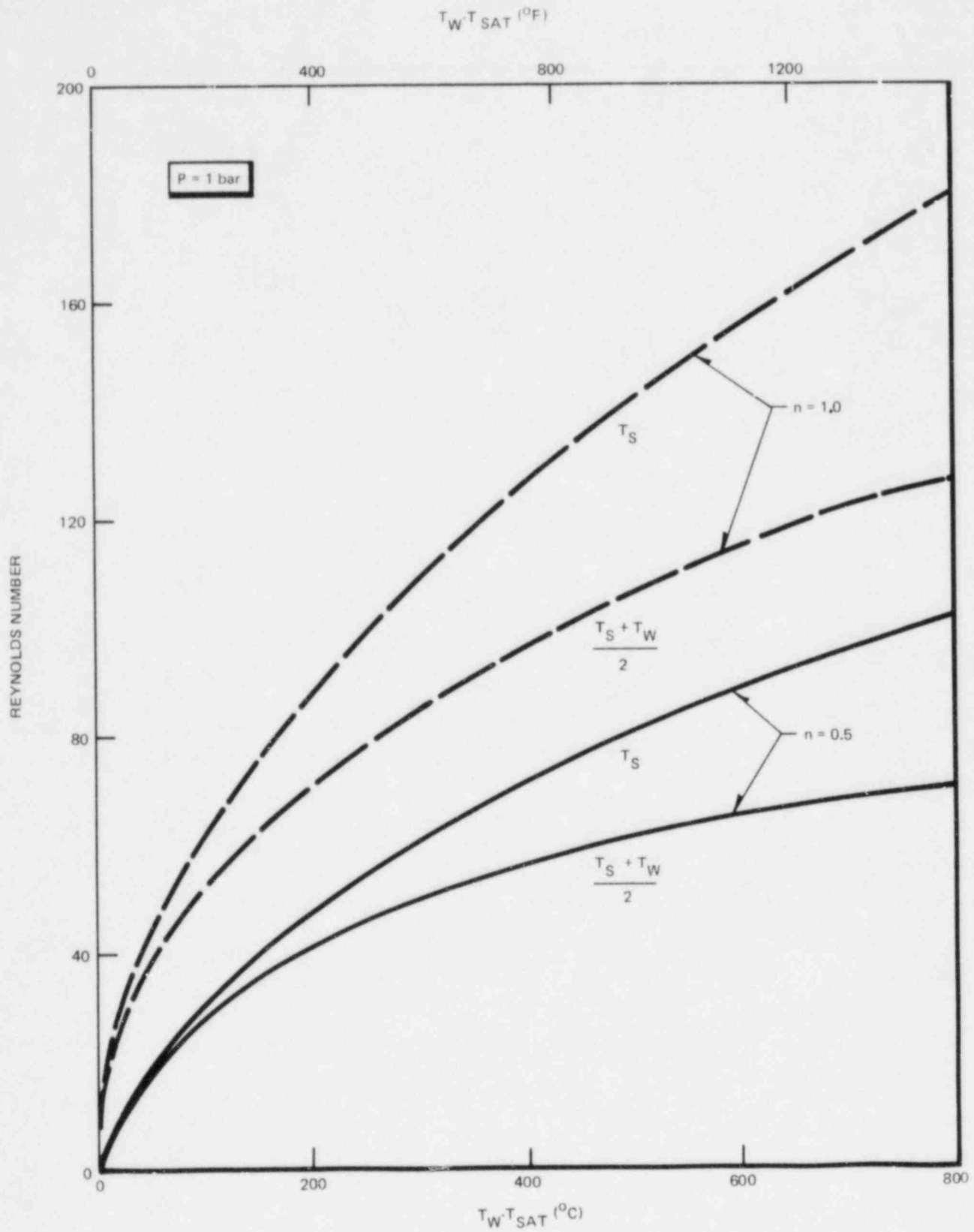


Figure A-5. Maximum Reynolds Number for Film

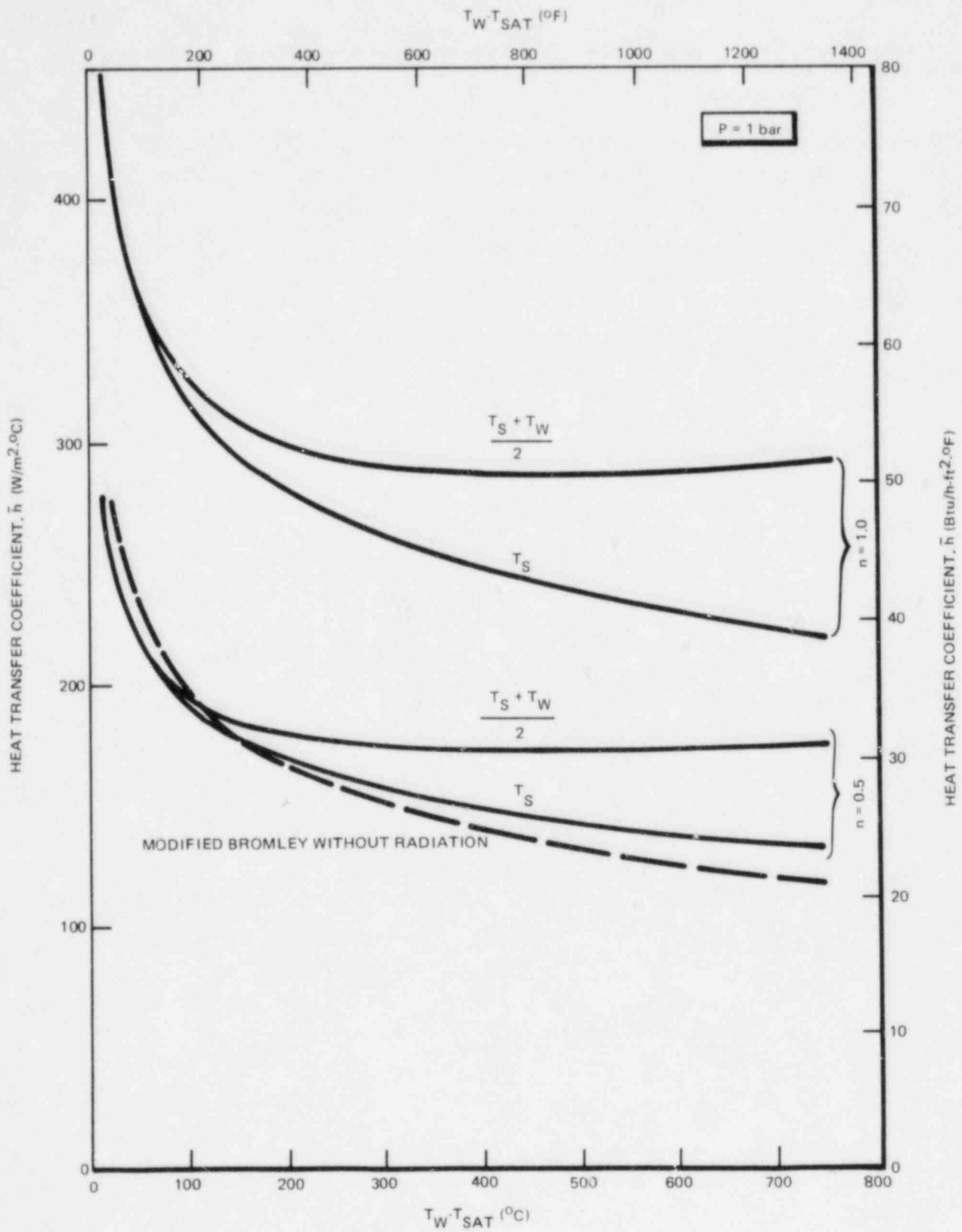


Figure A-6. Average Heat Transfer Coefficient

the viscosity of the water is much larger than the viscosity of the steam, in the limiting case of zero liquid flow the interface would be a zero velocity interface (i.e.,  $n = 0.5$ ).

On Figure A-6 the modified Bromley correlation is compared with the heat transfer coefficient calculated using the Helmholtz instability wavelength as the film length. The empirical modified Bromley correlation is seen to give slightly conservative heat transfer coefficients as compared to this theoretical model.

A.4 REFERENCES

- A-1. N. A. Bailey, *Film Boiling on Submerged Vertical Cylinders*, 1971 (AEEW-M1051).
- A-2. M. E. Ellion, *A Study of the Mechanism of Boiling Heat Transfer*, Jet Propulsion Laboratory, Memo 20-88, C.I.T. (1954).
- A-3. L. A. Bromley, *Heat Transfer in Stable Film Boiling*, Chem. Eng. Progr., 46, 221-227 (1950).



## APPENDIX B

APPLICABLE RANGE OF THE MODIFIED BROMLEY CORRELATION

The modified Bromley correlation as described is

$$h = h_{FB} + h_R$$

where

$$h_{FB} = 0.62 \left[ \frac{K_g^3 (\rho_f - \rho_g) h_{fg} g}{\mu_g (T_{WALL} - T_{SAT}) L_H} \right]^{1/4}$$

with  $L_H$  obtained from Helmholtz instability considerations.

$$L_H = 16.24 \left[ \frac{\sigma^4 h_{fg}^3 \mu_g^5 g^5 \epsilon_c^4}{\rho_g (\rho_f - \rho_g)^5 K_g^3 (T_{WALL} - T_{SAT})^3} \right]^{1/11}$$

and

$$h_R = \epsilon_W \sigma \frac{(T_W^4 - T_S^4)}{(T_{WALL} - T_{SAT})}$$

All of the thermodynamic properties,  $K_g$ ,  $\rho_f$ ,  $\rho_g$ ,  $h_{fg}$ ,  $\mu_g$ , and  $T_{SAT}$  are functions of the system pressure,  $P$ , only. Therefore, the modified Bromley correlation can be written in functional form as

$$h = f \left[ P, T_{WALL} \right]$$

That is, the modified Bromley correlation is a function only of the system pressure,  $P$ , and the wall temperature,  $T_{WALL}$ . The modified Bromley correlation is derived from theoretical considerations and compared to experimental data over a sufficiently wide range to verify the correlation. The data base covers a wide range of wall superheats,  $T_{WALL} - T_{SAT}$ , from about 100 to about 1300°F, or a range of wall temperature,  $T_{WALL}$ , of about 300 to about 1600°F. The system pressures in the data base also cover a wide range. The Westinghouse data (PWR-FLECHT Program) shown on Figures 10 through 12 covers a range of pressures from 1 atmosphere to 90 psia. The KWU data shown on Figure 13 were taken at a pressure of 50 psia. The GE single-rod data shown on Figures 6-9 were taken at a pressure of 1 atmosphere. The GE Blowdown Heat Transfer (BDHT) data shown on Figures 23, 35, 51, and 63 were taken with time-varying pressures having values comparable to those predicted for design basis accidents (values between about 700 and 1000 psia). These BDHT runs were chosen for the correlation comparison because they had the lowest measured heat transfer coefficients of all of the BDHT tests and therefore provide a conservative measure of the degree of underprediction of the heat transfer coefficients with the modified Bromley correlation.

Based on the above verification of the modified Bromley correlation the range of its applicability is

$$T_{WALL} < 2300^{\circ}\text{F}$$

$$P < 1200 \text{ psig}$$

This range covers the entire range of wall temperatures and system pressure that would occur following the initiation of a LOCA. This range is an extrapolation beyond the data base used to verify the correlation. Since the correlation is based upon theoretical considerations and is verified by data over a wide range of wall temperatures and pressure it is appropriate to extend the correlation to the full range of wall temperatures and pressure calculated following a LOCA.

## APPENDIX C

RESPONSES TO NRC QUESTIONS TRANSMITTED BY LETTER FROM OLAN D. PARR  
TO G. G. SHERWOOD DATED 5/30/79

Question 1: Figures 14, 25, 37 and 53 of NEDO-20566-1, Rev. 1 show the inlet flow variation for several tests from the BDHT program. These figures show that low flow exists in the "window" period and in the "post lower plerum flashing" period and thus support the contention that the Modified Bromley correlation is applicable to these periods. However, the same data are given in quarterly reports from the BDHT program and the results are quite different. The curves equivalent to those listed above are GEAP-13317-10, Figure D5.3; GEAP-13317-10, Figure D4.3; GEAP-13317-14, Figure D-2; and GEAP-13317-10, Figure 4-3. The flow data were presumably verified before inclusion in the quarterly reports. Please explain the differences in the data plots and explain why the data are supportive of the use of Modified Bromley.

Response

The bundle inlet flow measurement methodology in the TLTA has undergone several evolutionary stages of improvement from the original configuration, TLTA 1 in 1974, to the present configuration, TLTA 5A. During the early 7x7 BDHT test series in TLTA 1, several techniques were evaluated utilizing a combination of pressure drop measurements across the bundle inlet orifice. The bundle inlet design itself was based on an *in situ* flow calibration of the inlet orifice in a low-pressure, low-temperature mockup vessel (GEAP-13317-06). The TLTA 1 with the selected orifice was subsequently assembled and further steady-state and transient flow calibrations were conducted *in situ* in TLTA 1 (GEAP-13317-07, -08, -09) to confirm the design over the expected test procedure range of 1000 psia to 14.7 psia. The steady-state calibration extended over a flow range of 50 lbm/sec to 8 lbm/sec with the minimum orifice pressure drop around 0.2 psi (GEAP-13317-06). Transient shakedown testing (GEAP-13317-09) indicated that this range of flow measurements could be extended down to lower flow, but at these lower flow rates there was a much higher uncertainty in the flow coefficient.

The original TLTA configuration also included drag discs at the bundle inlet for an alternate measurement of the core flow as measured by the pressure drop across the inlet orifice. These instruments, however, failed to operate in the high-pressure and high-temperature environment of the TLTA.

Subsequently, during the actual BDHT testing, a need for better evaluation of the core inlet flow during the early coastdown and window period (GEAP-13317-10) of the blowdown transient was identified. Special tests (GEAP-13317-10, -11, and -12) were conducted to establish the resolution and the dynamic response of the bundle inlet orifice pressure drop measurement. These tests led to several modifications in the pressure drop measurement arrangements and their installation.

During the course of this entire development period, the data from the 7x7 BDHT test were reported continuously using the calibration data and methodology mentioned earlier (GEAP-13317-09). The core inlet flow reported in GEAP-13317-10 and -14 were based on the measured flow inlet pressure drop, unadjusted or uncorrected for any bias or resolution uncertainty in the measurement.

Subsequently, detailed data analyses utilizing the bundle inlet flow measurements were performed with the MAYU-04 (GEAP-23517) code. From these studies it was clear that the indicated bundle inlet flow, as well as the pressure drop measurement from which it was derived, was not reliable during the extremely low flow periods when the measured inlet pressure drop was less than about 0.1 psi. Hence, an alternate method was developed wherein a flow balance in the lower plenum was utilized to provide a better indication of the bundle inlet flow during the window period. Each of the flow components in such a flow balance is large and of higher accuracy than the core inlet. This led to a more reliable evaluation of the core inlet flow than originally reported. The flow balance is derived from the mass balance in the lower plenum, which includes the inlet and outlet flow rates of subcooled water through the jet pumps and bypass region. Such mass balance evaluations for the core inlet flow are compared with those derived from the pressure drop measurement across the inlet orifice in Figures C-1, C-2, and C-3. In each instance the core flows determined for both evaluations agree well except during the window period. For that very low flow period the flow balance method is more reliable. Therefore, the flow evaluations using the flow balance method were utilized in the studies reported in NEDO-20566-1.

During these low flow periods, i.e., window and post-lower-plenum-flashing periods, the low bundle inlet flow rates lead to local mass velocities within

the bundle that are less than  $0.1 \times 10^6$  lbm/h-ft<sup>2</sup>. These low mass velocities are typical of gravity-controlled flow, as opposed to forced flow, and provided the locations are in liquid continuum, the corresponding heat transfer rates are characterized by pool boiling or pool film boiling, i.e., Modified Bromley.

Figures C-4 and C-5 show the core flow rates measurements for the 8x8 BDHT test series, derived from the combination of methods as described above. These are used in conjunction with the response to Question 2.

Question 2: Compare the Modified Bromley correlation to appropriate portions of data from the BDHI program with 8x8 fuel bundles; include tests from the BD/ECC program in the comparison. The purpose of this request is to extend the data base supporting Modified Bromley to 8x8 fuel design and to the early portion of the reflood transient.

### Response

#### Basis for Selection of Heat Transfer Data

The Modified Bromley correlation should only be compared with the thermocouple data which are in the liquid continuum region (below the two phase level) and indicate sustained dryout during the low flow period. The thermocouples above the mixture level are cooled by steam updraft cooling and are not relevant for the comparisons. Only tests that were initiated from peak bundle power conditions produced such sustained dryout in the liquid continuum region during the coastdown period. From these tests, the highest reading (minimum heat transfer) thermocouple data meeting the above conditions were evaluated for comparison with the Modified Bromley correlation.

#### Comparison of 8x8 Data with Modified Bromley Correlation

Figures C-6 and C-7 show comparisons of reduction test data with the correlation at two elevations, 199 and 200 inches above the bottom of the heated length (BHL), for Test 6006 Run 3. The corresponding two-phase mixture level and coastdown core flow are shown in Figure C-7. Figures C-5, C-8, and C-9 present comparisons for Test 6005 Run 6 at elevations 120 and 100 inches above the BHL.

The periods of interest for low flow comparisons are indicated on the figures. This comparison of Modified Bromley and experimental heat transfer coefficients from the 8x8 bundle shows the same results as previously reported for the 7x7 bundle in NEDO-20566-1. Therefore, the Modified Bromley provides a low-bound estimate of the heat transfer for both the 7x7 and 8x8 bundles.

Question 3: Currently, the GE ECCS evaluation model applies the maximum of ELLION or transition boiling heat transfer to the flooded portion of the rods after lower plenum flashing. It is not clear how GE proposes to change this with Modified Bromley. Will the logic be the maximum of Modified Bromley or transition boiling for this period or will Modified Bromley be used exclusively?

Response

GE proposes to use the Modified Bromley correlation for four applications described below in the CHASTE code:

1. Flow "window" period prior to lower plenum flashing and following boiling transition

The higher of the Modified Bromley correlation and the "pool film/transition boiling" heat transfer coefficient lower bound value of  $30 \text{ Btu/h-ft}^2\text{-}^\circ\text{F}$  will be used.

2. Post-lower-plenum-flashing period

The higher of the Modified Bromley correlation and the Dougall-Rohsenow correlation will be used before uncovering.

3. Channel wall during reflooding of bypass and core regions

The Modified Bromley correlation will replace the currently used value of  $5 \text{ Btu/h-ft}^2\text{-}^\circ\text{F}$  on the outside surface during bypass flooding and inside surface during core reflooding.

4. Rod bundle during reflooding

The Modified Bromley correlation will replace the currently used value of  $25 \text{ Btu/h-ft}^2\text{-}^\circ\text{F}$ .

Question 4: Figure IC.5.11 of NEDE-20566, p.I-356, shows that the Ellion correlation does a reasonable job of predicting the minimum heat transfer coefficient from RUN 159 in the single loop test apparatus. Modified Bromley would probably predict a higher heat transfer coefficient than was measured. Unless the data can be shown to not be applicable, compare Modified Bromley to RUN 159 and other appropriate runs from the single loop test apparatus program.

#### Response

During the early testing phases of the BWR BDHT program, some heat transfer data were obtained in a full-length, 16-rod bundle (GEAP-13317-06). These tests were conducted in a single loop test apparatus (SLTA) which was readily available at that time. The primary purpose of these tests was to check out the heater design and measurement techniques in support of the BWR BDHT program and TLTA design. While this test facility (SLTA) permitted the simulation of typical pressure and temperature conditions, the exact BWR LOCA phenomena were not necessarily replicated. However, some limited blowdown heat transfer information was obtained. Independently, a methodology was developed to evaluate the local heat transfer coefficient from the measured heater rod temperatures. The method is entitled HCODE (GEAP-21731).

Data from the SLTA tests were utilized to demonstrate the capabilities of the methodology in evaluating heat transfer coefficients. The results were compared with typical heat transfer correlations used to demonstrate the reasonableness of the results (NEDE-20566). One such comparison was shown in Figure IC.5.11 (NEDE-20566, PI-356) for Test 2105 Run 159. Evaluation of the bundle pressure drop and cladding temperature indicates that the post-dryout bundle heatup was due to transition from a liquid continuum pool boiling to steam cooling following the drop in mixture level in the bundle. The post-dryout heat transfer coefficients were therefore typical of the transition from nucleate boiling to steam cooling and not representative of the pool film boiling regime. The comparison merely served to demonstrate that the Ellion pool film boiling correlation formed a lower bound to the steam cooling heat transfer rates observed during the tests. A more realistic comparison of the deduced heat transfer coefficients would have been with the prediction by the Dittus-Boelter Correlation for single-phase (steam) forced convection. Such a comparison was not made at that time since local flow conditions were not measured during the tests.



To conclude, the test data presented in NEDE-20566 is not phenomenologically related to the flow conditions for which either Ellion or Modified Bromley correlation is applicable, but rather is due to single-phase steam cooling.

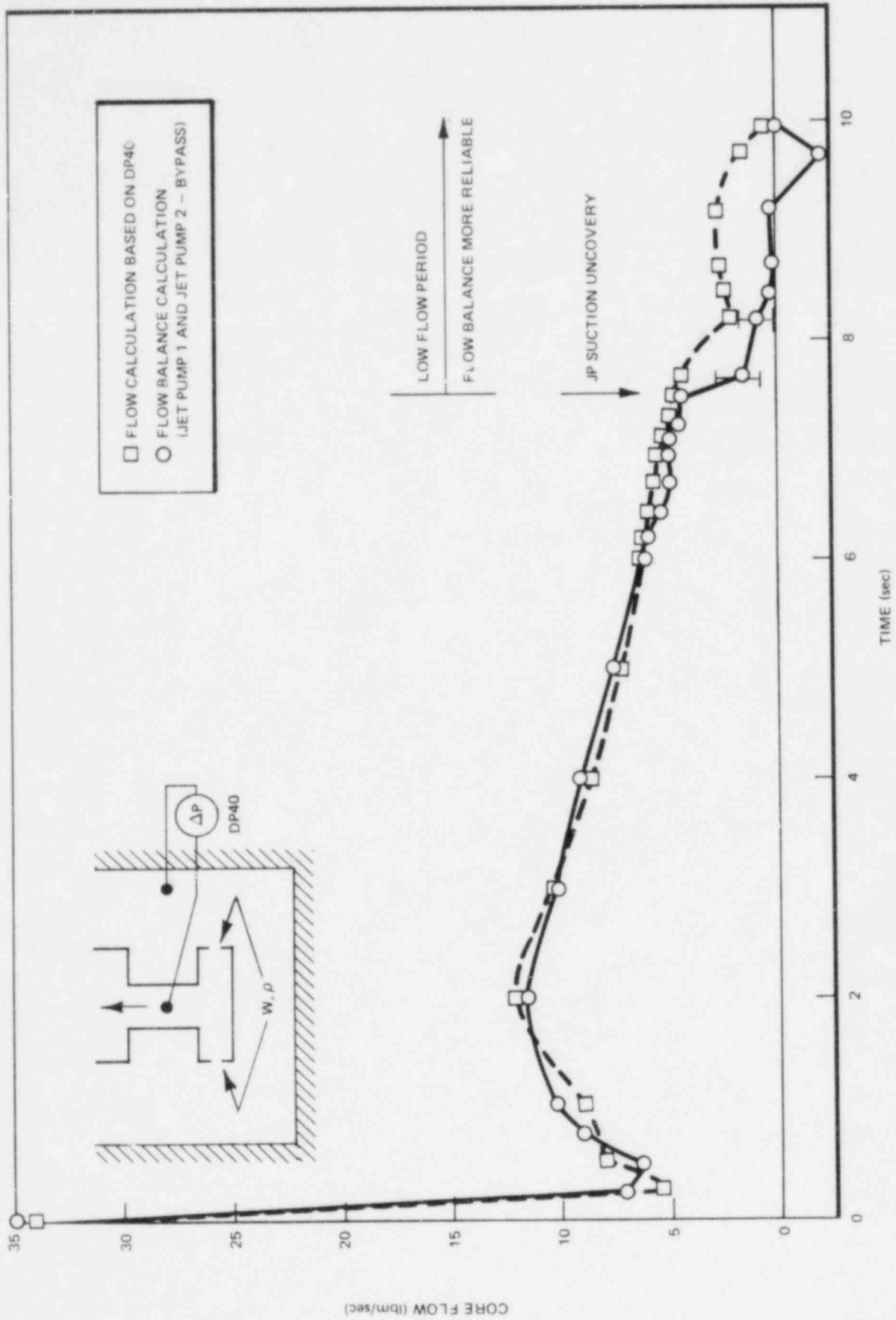


Figure C-1. Bundle Inlet Flow (Test 4907, Run 10)

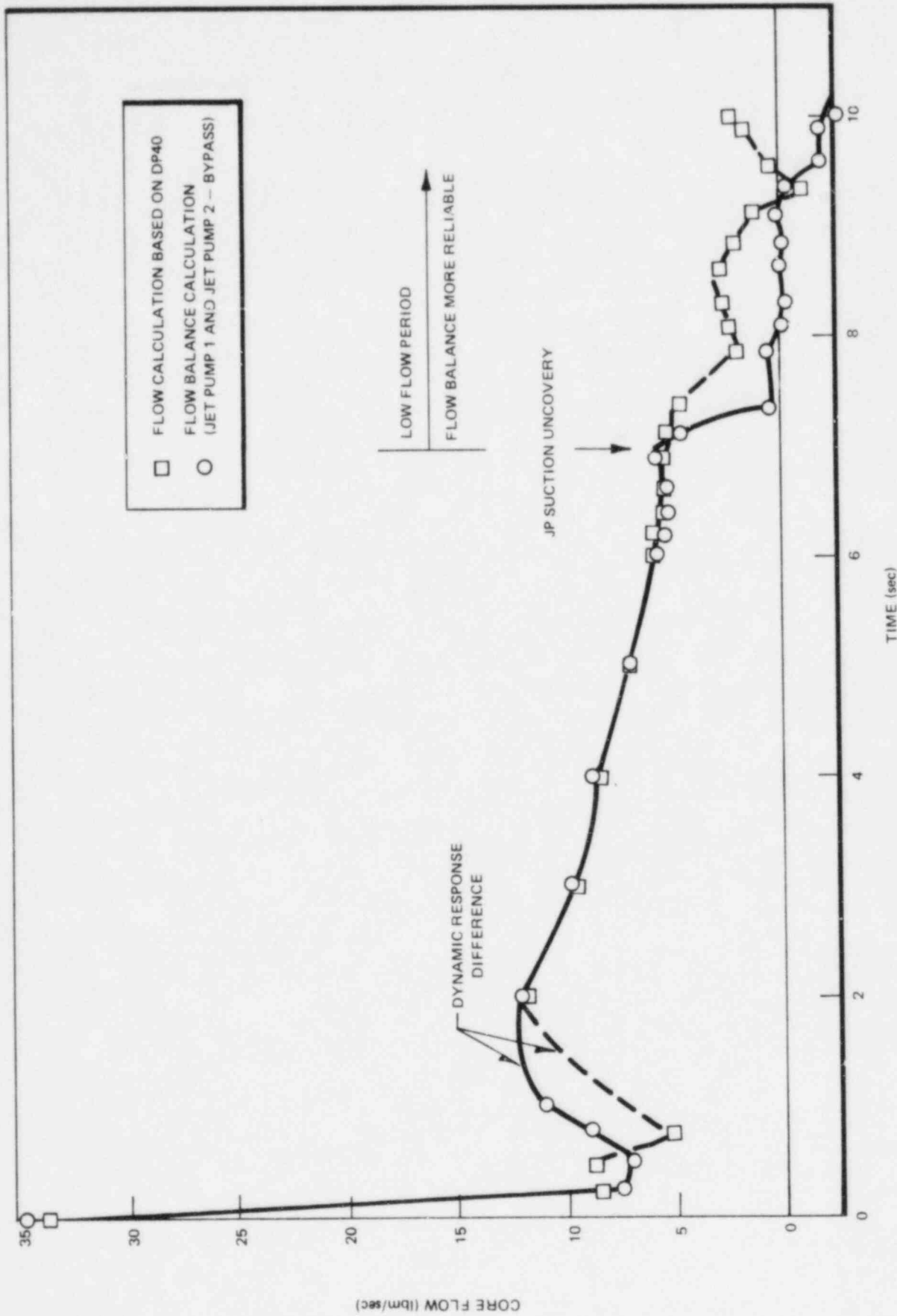


Figure C-2. Bundle Inlet Flow (Test 4904, Run 45)

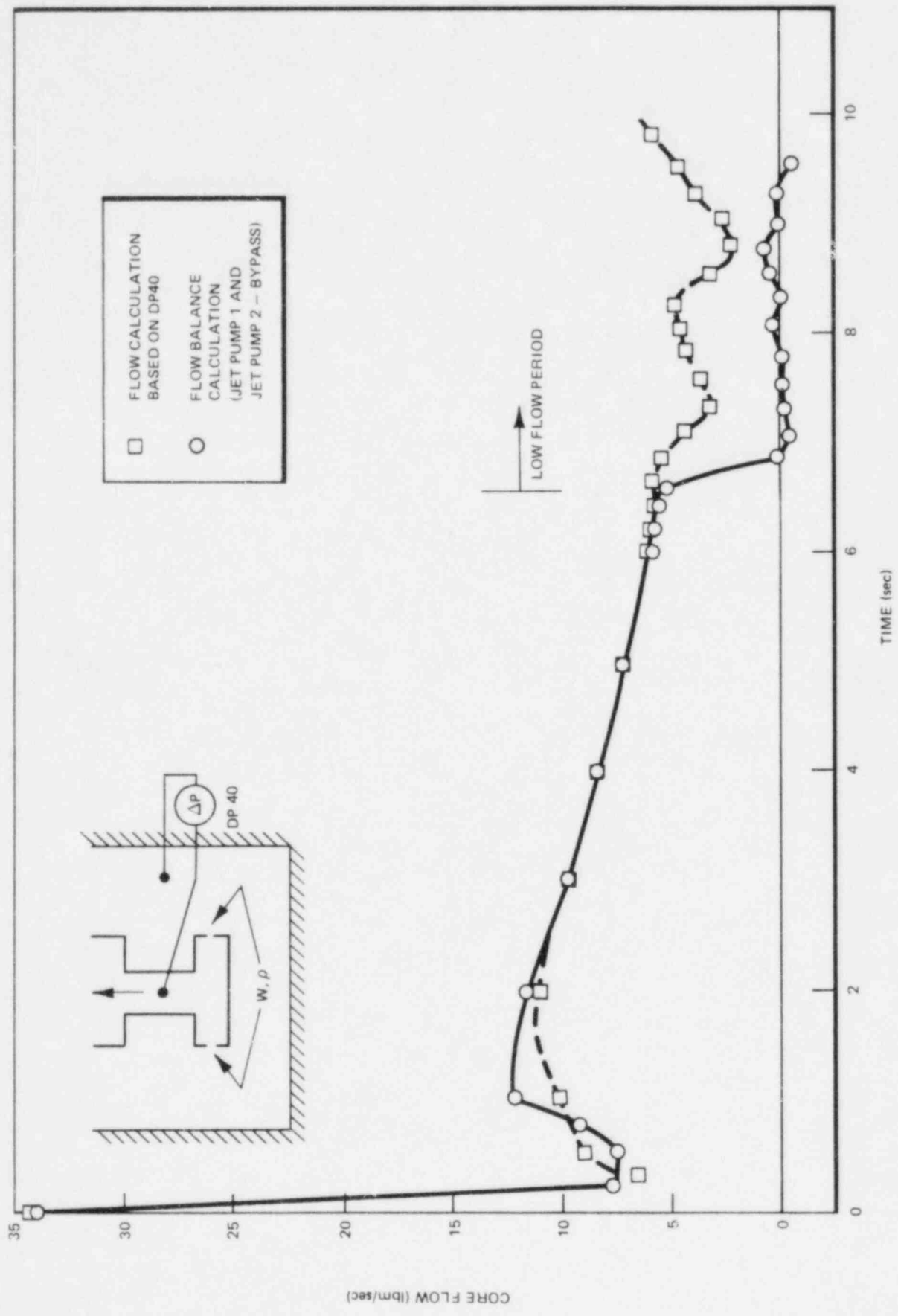


Figure C-3. Bundle Inlet Flow (Test 4910, Run 13)

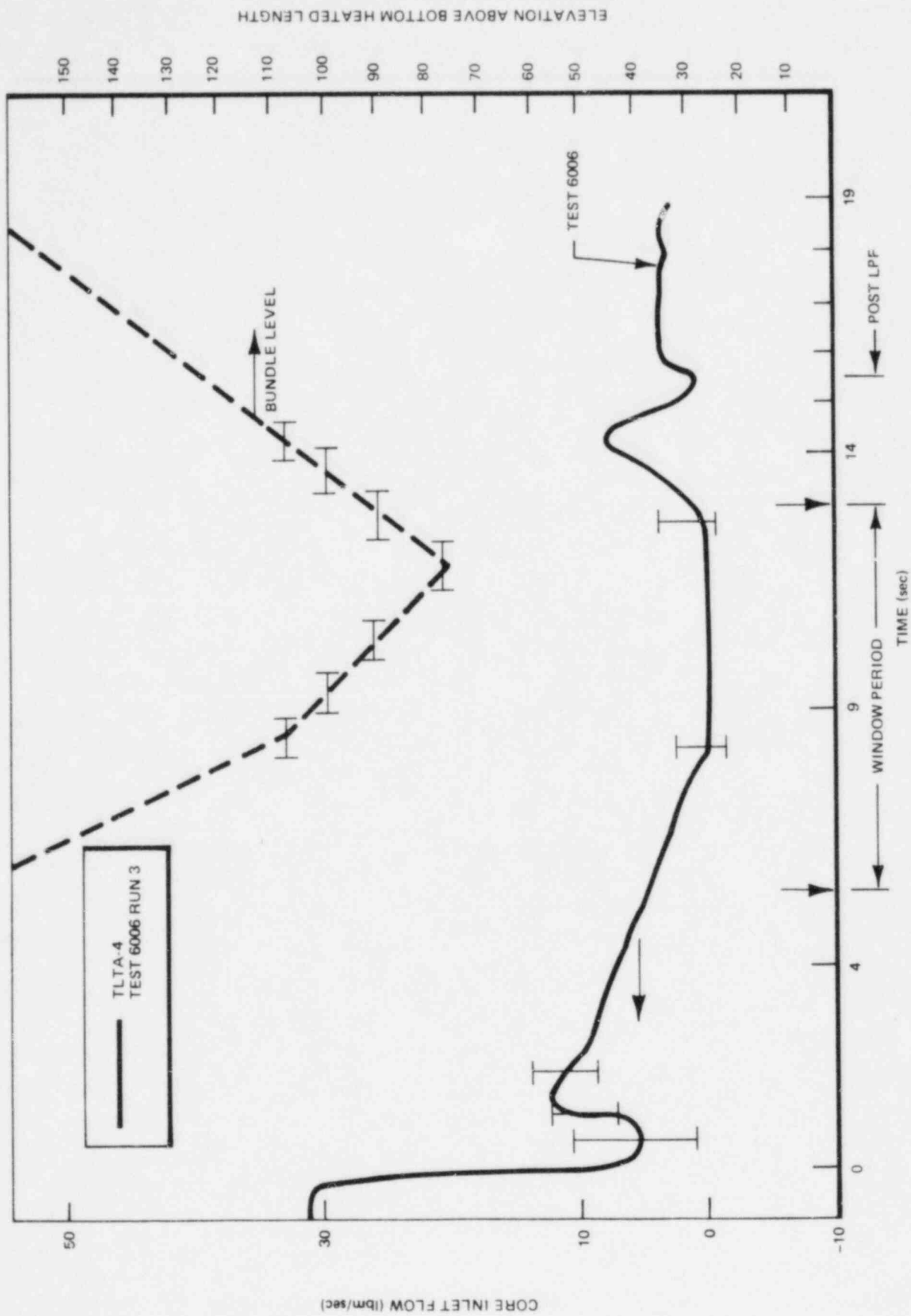


Figure C-4. Comparison of Core Inlet Flow and Bundle Level

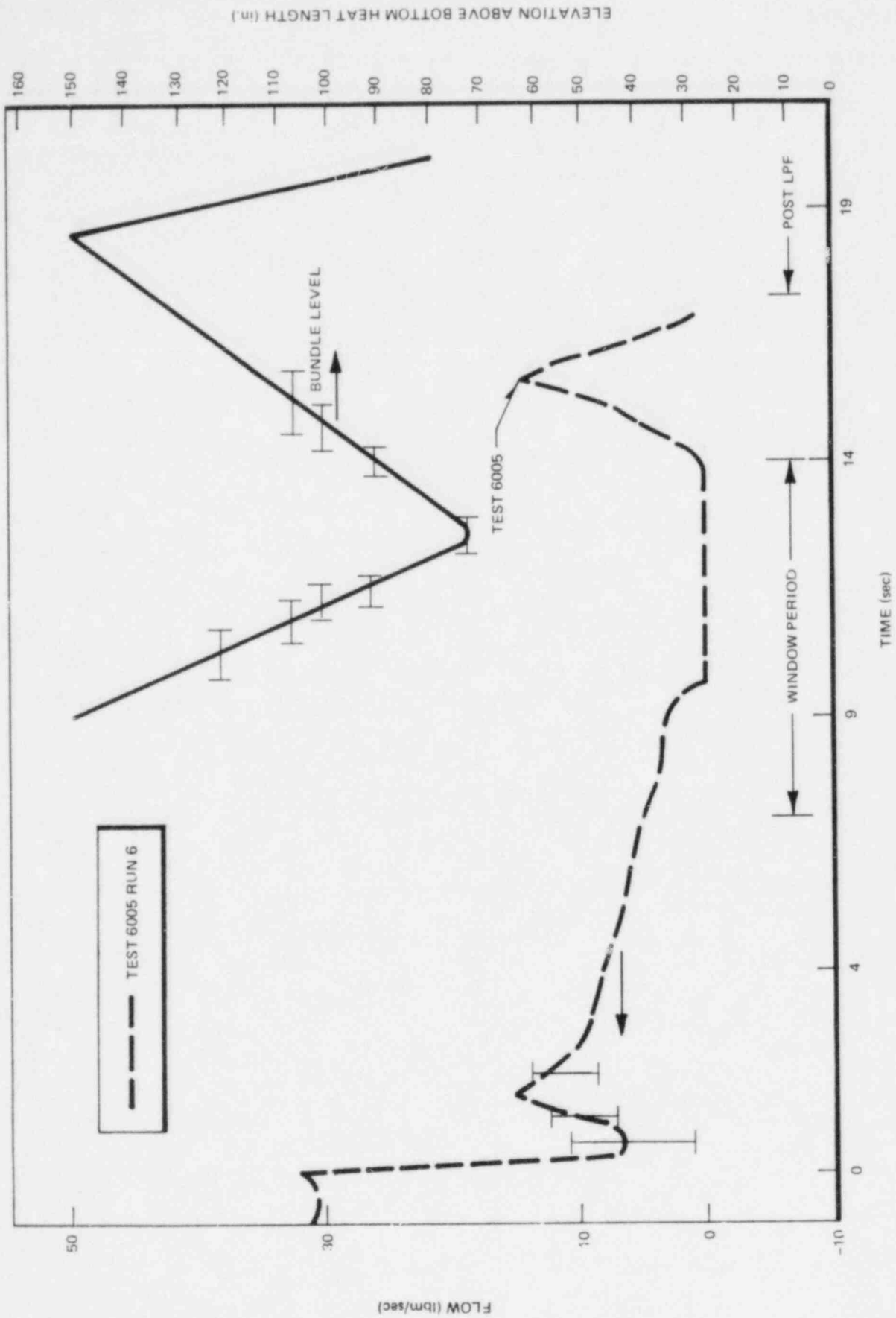


Figure C-5. Comparison of Core Inlet Flow and Bundle Level

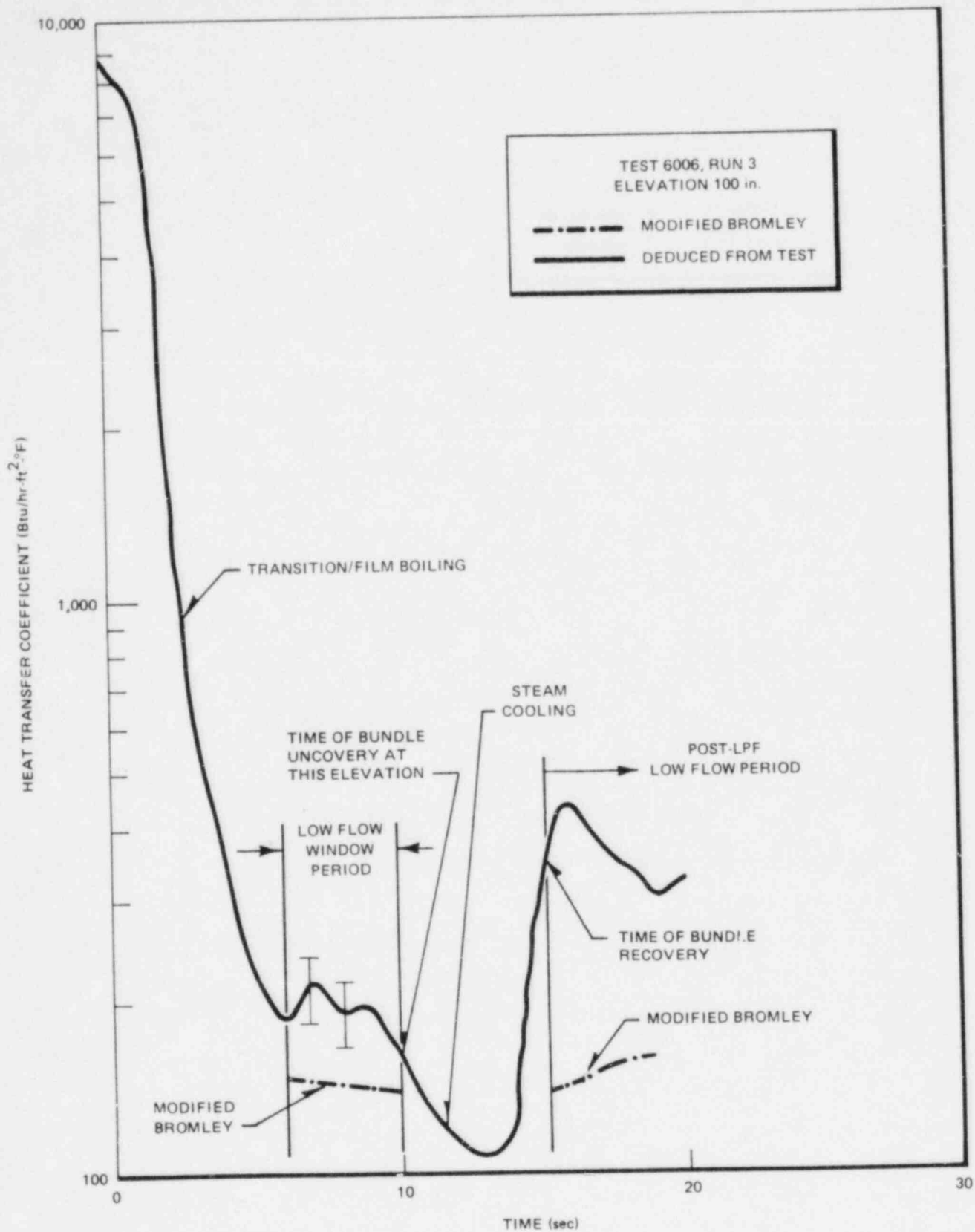


Figure C-6. Deduced Heat Transfer Coefficient vs Modified Bromley Correlation

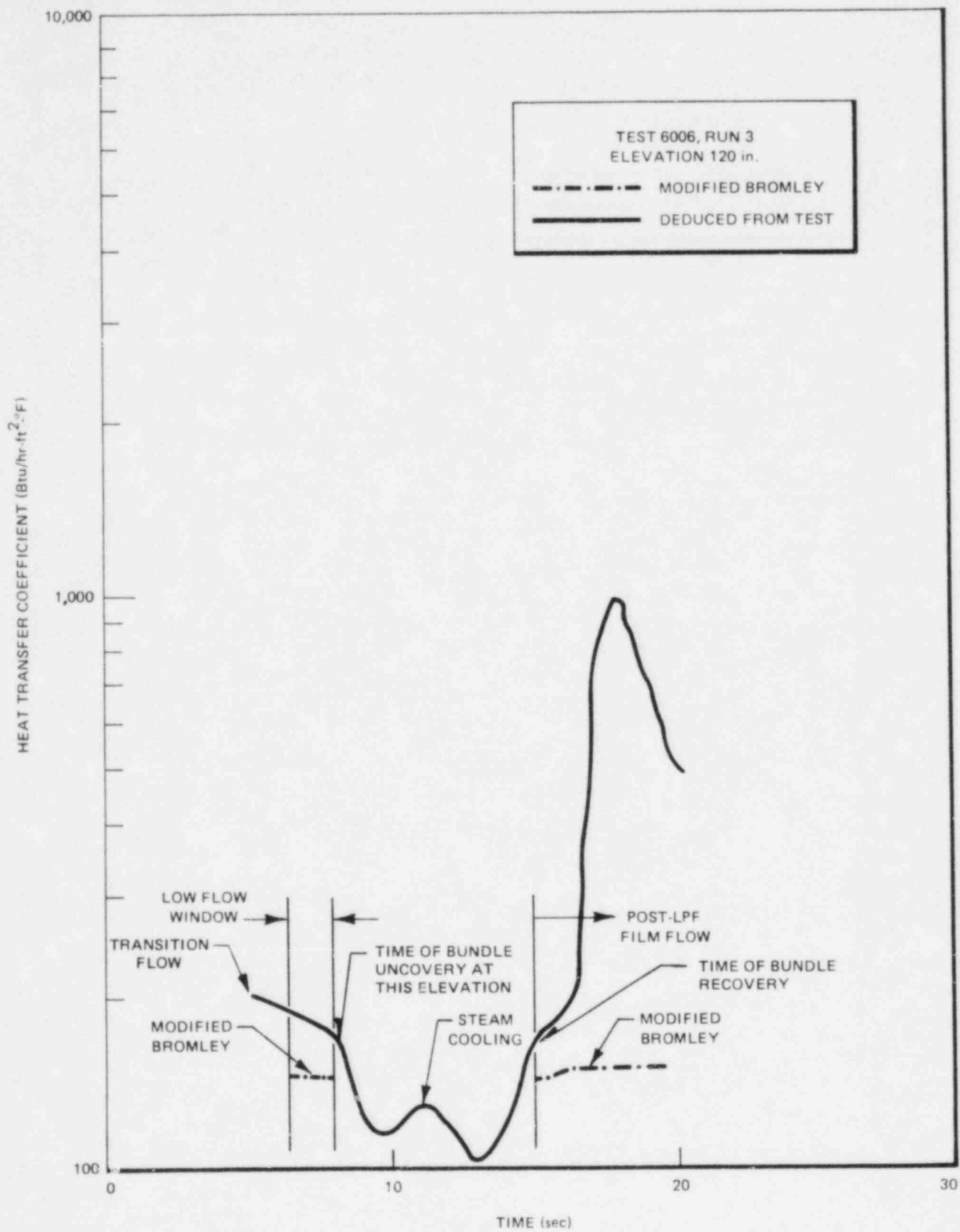


Figure C-7. Deduced Heat Transfer Coefficient vs Modified Bromley Correlation



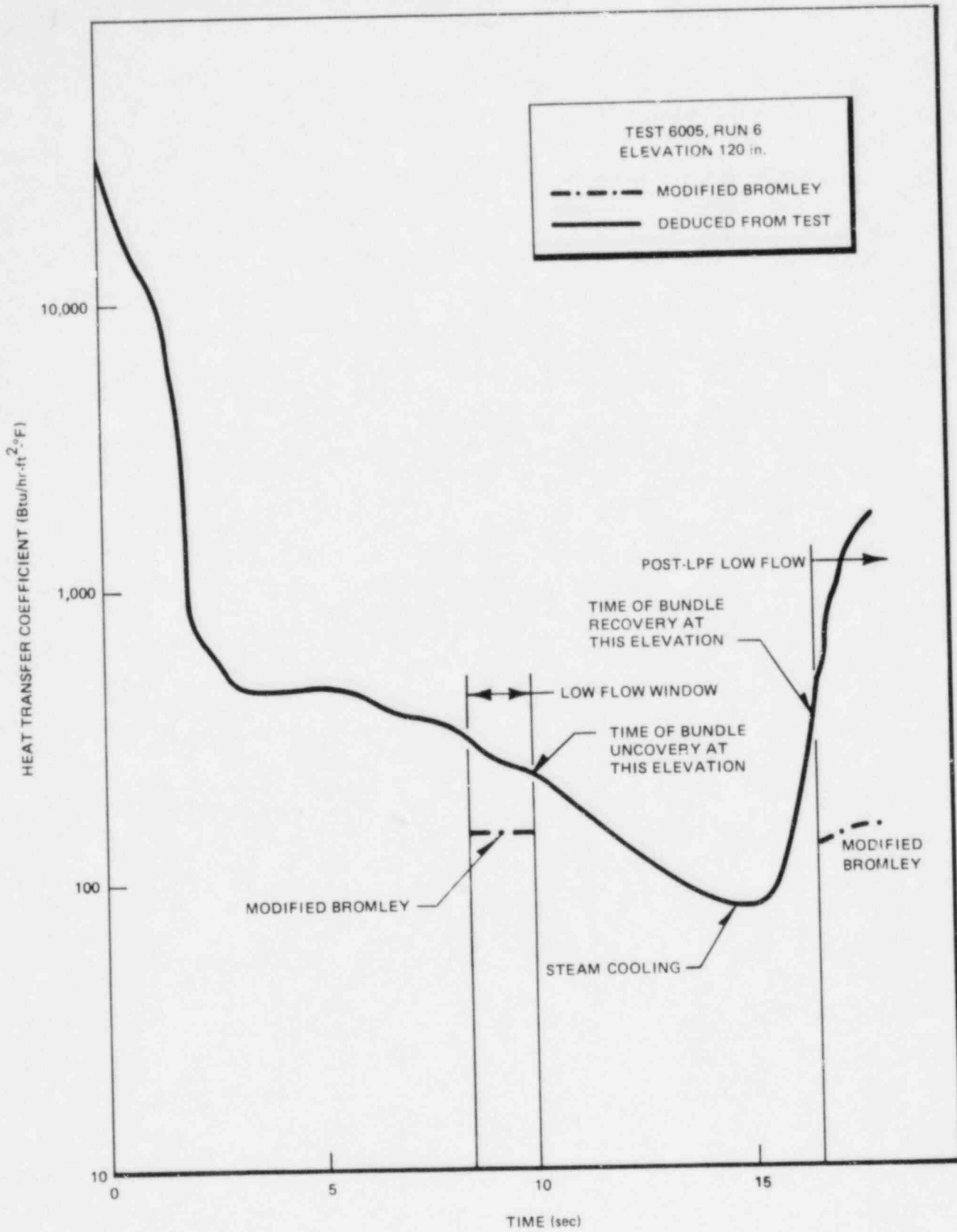


Figure C-8. Deduced Heat Transfer Coefficient vs Modified Bromley Correlation

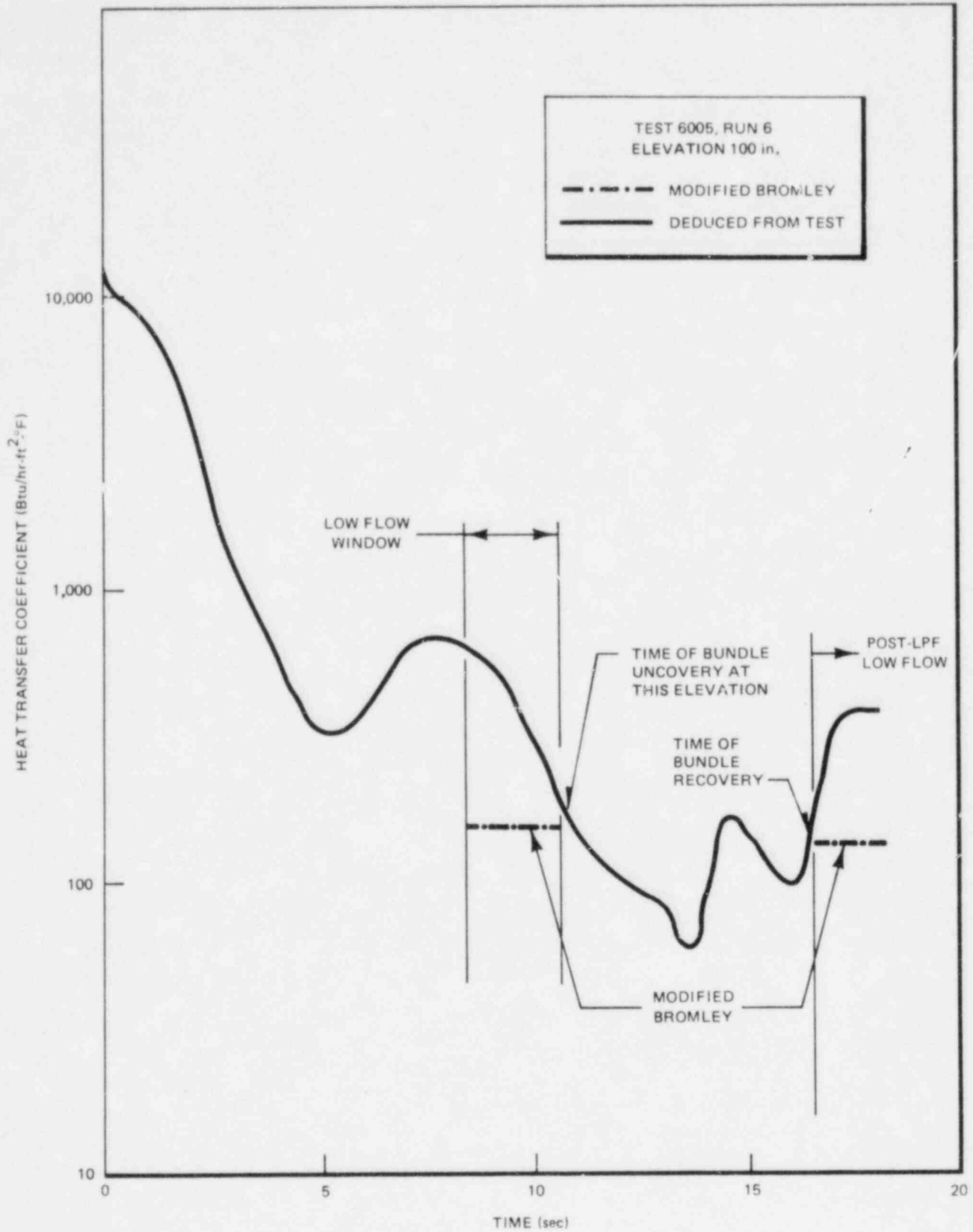


Figure C-9. Deduced Heat Transfer Coefficient vs Modified Bromley Correlation

## DISTRIBUTION

<u>Name</u>	<u>M/C</u>
J. A. Alai	150
J. G. Munthe Andersen	186
D. K. Dennison	682
G. E. Dix	588
S. S. Dua	766
D. A. Hamon	767
J. E. Leonard	889
D. Matzner	583
J. F. Quirk	682
B. S. Shiralkar	186
B. Stevens (5 + 1 fiche)	126
H. E. Townsend	186
W. A. Sutherland	583
J. E. Wood	148
NEBO Library (2)	528
VNC Library (2)	V01
SLO Files (2)	682
TIE (5)	Bldg 81, RM A133 SCH



TECHNICAL INFORMATION EXCHANGE

TITLE PAGE

AUTHOR J.E. LEONARD et al	SUBJECT 730, 740	TIE NUMBER 77NED304
		DATE October 1982
TITLE CALCULATION OF LOW FLOW FILM BOILING HEAT TRANSFER FOR BWR LOCA ANALYSIS		GE CLASS I
		GOVERNMENT CLASS
REPRODUCIBLE COPY FILED AT TECHNICAL SUPPORT SERVICES, R&UO, SAN JOSE, CALIFORNIA 95125 (Mail Code 211)		NUMBER OF PAGES 107
SUMMARY <p>A model has been developed to calculate the heat transfer coefficient under low flow film or pool boiling conditions in the BWR geometry. The model includes the heat transferred by convection due to the vapor boundary layer and that transferred by radiation between the high-temperature surface and the liquid.</p> <p>The model is verified against a range of single-rod and full-scale rod bundle data. These data confirm the applicability of the model for a range of conditions postulated to occur during the BWR loss-of-coolant accident.</p>		

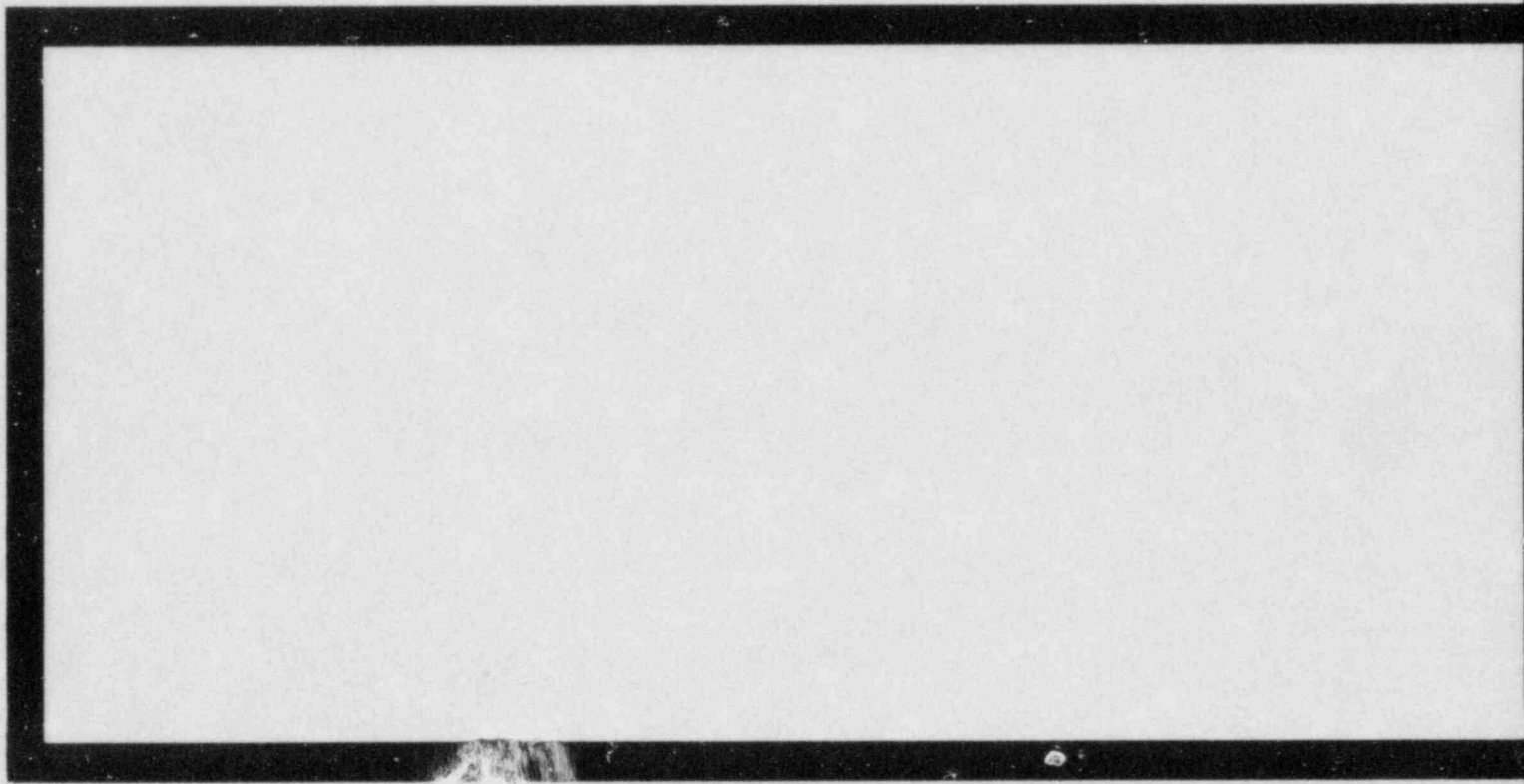
By cutting out this rectangle and folding in half, the above information can be fitted into a standard card file.

DOCUMENT NUMBER NEDO-20566-1-A

INFORMATION PREPARED FOR BOILING WATER REACTOR SYSTEMS DEPARTMENT

SECTION TECHNOLOGY AND DEVELOPMENT

BUILDING AND ROOM NUMBER 1900-146 MAIL CODE 150



**GENERAL  ELECTRIC**